



# PACIFIC EARTHQUAKE ENGINEERING RESEARCH CENTER

## **Performance Evaluation Database for Concrete Bridge Components and Systems under Simulated Seismic Loads**

**Yael D. Hose  
Frieder Seible**

Department of Structural Engineering  
University of California, San Diego

# **Performance Evaluation Database for Concrete Bridge Components and Systems under Simulated Seismic Loads**

**Yael D. Hose and Frieder Seible**  
Department of Structural Engineering  
University of California, San Diego

This work was supported in part by the Pacific Earthquake Engineering Research Center  
through the Earthquake Engineering Research Centers Program  
of the National Science Foundation under Award number SA2016

PEER Report 1999/11  
Pacific Earthquake Engineering Research Center  
College of Engineering  
University of California, Berkeley

November 1999

## **ABSTRACT**

Through lessons learned in recent earthquakes, the need for new seismic bridge design methodologies that consider structural performance explicitly and address the inelastic response of bridge structures more directly is recognized. Efforts are in progress to define and quantify limit states and associated performance goals to develop a multi-level bridge design methodology. A multi-level design approach can be implemented, however, only when structural behavior or limit states can accurately be characterized and assessed for the wide range of probable input or demands. The outlined capacity assessment database addresses the response determination and parameterization of bridge components, sub-assemblages, and systems in direct support of the development of multi-level performance design and evaluation procedures for bridges. Through the use of a standardized template, a performance library for bridge structures, which is open for access and expansion to the entire practicing bridge engineering community, has been initiated.

## **ACKNOWLEDGMENTS**

This work was supported in part by the Pacific Earthquake Engineering Research Center through the Earthquake Engineering Research Centers Program of the National Science Foundation under Award number EEC-5121999. The opinions, findings, conclusions, and recommendations expressed herein are those of the authors and do not necessarily reflect the views of PEER. The authors gratefully acknowledge the many researchers that have contributed their time and test results to this project. We would also like to thank University of California, San Diego, post-doctoral research scientist Pedro Silva and undergraduate researcher Karen Wilson for their assistance in the formulation of the bridge performance database.

# CONTENTS

ABSTRACT .....	iii
ACKNOWLEDGMENTS.....	iv
TABLE OF CONTENTS .....	v
LIST OF FIGURES.....	vii
LIST OF TABLES .....	ix
NOMENCLATURE.....	xi
<b>1 INTRODUCTION.....</b>	<b>1</b>
<b>2 FIVE-LEVEL PERFORMANCE EVALUATION APPROACH .....</b>	<b>5</b>
2.1 Background .....	5
2.2 Calculation of Parameters .....	9
<b>3 CASE STUDIES AND PERFORMANCE EVALUATION SUMMARIES .....</b>	<b>17</b>
3.1 Evaluation Template .....	17
<b>4 PERFORMANCE ASSESSMENT AND DESIGN METHODOLOGIES .....</b>	<b>23</b>
<b>5 CONCLUSIONS .....</b>	<b>27</b>
<b>CASE STUDY APPENDIXES .....</b>	<b>29</b>
APPENDIX A: Components.....	31
Sun, Rectangular Column, R-1 .....	33
Sun, Rectangular Column, R-5 .....	37
Hose, Circular Flexural Reference Column, SRPH-1.....	41
Hose, Circular Flexural Column with Relocated Plastic Hinge, SRPH-2 .....	45
Hose, Circular Flexural Column with Relocated Plastic Hinge, SRPH-3 .....	49
Hose, Circular Flexural Column with Relocated Plastic Hinge, SRPH-4 .....	53
Hose, Circular Shear Column with Relocated Plastic Hinge, SRPH-6.....	57
Hose, Circular Flexure-Shear Column with Relocated Plastic Hinge, SRPH-7 .....	61
Hose, Circular Flexural Column Subjected to Large Static Velocity Pulse, VP2 .....	65
Sanchez, Rectangular Double Spiral Reference Column, RDS-1.....	69
Sanchez, Rectangular Double Spiral Flared Column, RDS-2.....	73
Sanchez, Rectangular Double Spiral Flared Column, RDS-6.....	77
APPENDIX B: Sub-Assemblages.....	81

Silva, Standard Caltrans Pile Design, STD1 .....	83
Silva, Standard Caltrans Pile Design, STD2 .....	87
Silva, Standard Caltrans Pile Design, STD3 .....	91
APPENDIX C: Systems.....	95
Silva, Full-scale Test of Alaska Multiple Column Bridge Bent, MCBA.....	97
Innamorato, Santa Monica Viaduct Multiple Column Bridge Bent Phase I, SMV-I....	101
Innamorato, Santa Monica Viaduct Multiple Column Bridge Bent Phase II, SMV-II .....	107
<b>REFERENCES .....</b>	<b>113</b>

## LIST OF FIGURES

Fig. 2.1. Bilinear approximation for displacement ductility parameter .....	12
Fig. 2.2. Residual deformation index (RDI), equivalent viscous damping ratio ( $\xi_{eq}$ ), and effective stiffness ( $K_{eff}$ ) for symmetric hysteresis loops.....	13
Fig. 2.3. Residual deformation index (RDI), equivalent viscous damping ratio ( $\xi_{eq}$ ), and effective stiffness ( $K_{eff}$ ) for asymmetric hysteresis loops .....	15
Fig. 4.1. Identification curve for <i>brittle</i> behavior mode.....	25
Fig. 4.2. Identification curve for <i>strength degrading</i> behavior mode. ....	25
Fig. 4.3. Identification curve for <i>ductile</i> behavior mode.....	25

## LIST OF TABLES

Table 2.1 Bridge damage assessment.....	6
Table 2.2 Bridge performance assessment.....	7
Table 2.3 Bridge performance/design parameters.....	8
Table 3.1 Evaluation template.....	19
Table 3.2 Damage observations during testing .....	21

## NOMENCLATURE

$A_g$	Gross area of critical column cross section
$b_b$	Beam width perpendicular to axis
$b_c$	Column width perpendicular to axis
$b_{je}$	Effective width of joint
$E_d$	Energy dissipation per cycle
$E_{d1}$	Energy dissipation per push half cycle
$E_{d2}$	Energy dissipation per pull half cycle
$E_s$	Elastic strain energy per cycle
$E_{s1}$	Elastic strain energy per push half cycle
$E_{s2}$	Elastic strain energy per pull half cycle
<i>Drift</i>	Drift ratio
$F$	Force at given experimental level
$F_1$	Force at given experimental level during push half cycle
$F_2$	Force at given experimental level during pull half cycle
$F_n$	Ideal yield force
$F_y$	Theoretical yield force
$f_c'$	Concrete compression strength
$f_h$	Average axial stress in horizontal direction of joint
$f_u$	Ultimate strength of steel reinforcement
$f_v$	Average axial stress in vertical direction of joint
$f_y$	Yield strength of steel reinforcement
$h_b$	Cap beam section depth
$h_c$	Column section depth perpendicular to axis
$K_{eff}$	Effective stiffness at given experimental level
$K_{eff1}$	Effective stiffness at given experimental level during push half cycle

$K_{eff 2}$	Effective stiffness at given experimental level during pull half cycle
$K_o$	Initial stiffness at ideal yield
$K_{o1}$	Initial stiffness at ideal yield during push half cycle
$K_{o2}$	Initial stiffness at ideal yield during pull half cycle
$L$	Distance between critical section of plastic hinge and point of contraflexure
$M^o$	Overstrength moment of plastic hinge in column
$M_n$	Ideal yield moment
$M_y$	Theoretical first yield moment
$n_k$	Normalized effective stiffness
$P$	Axial load of column
$P_b$	Axial compression force in beam
$P_c$	Column axial force
$p_c$	Principal compression stress in joint
$p_t$	Principal tension stress in joint
$RDI$	Residual deformation index
$V_{col}^o$	Overstrength applied shear in column
$V_{jh}$	Horizontal joint shear force
$V_{jv}$	Vertical joint shear force
$v_{jh}$	Horizontal joint shear stress
$v_{jv}$	Vertical joint shear stress
$w$	Crack width
$\Delta$	Total displacement at given experimental level
$\Delta_1$	Total displacement at given experimental level during push half cycle
$\Delta_2$	Total displacement at given experimental level during pull half cycle
$\Delta_p$	Plastic displacement at given experimental level
$\Delta_r$	Permanent residual deformation
$\Delta_{r1}$	Permanent residual deformation during push half cycle

$\Delta_{r2}$	Permanent residual deformation during pull half cycle
$\Delta_y$	Ideal yield displacement
$\Delta_y^t$	Theoretical first yield displacement
$\Delta_{y1}$	Ideal yield displacement during push half cycle
$\Delta_{y2}$	Ideal yield displacement during pull half cycle
$\varepsilon_c$	Concrete strain
$\varepsilon_s$	Steel strain
$\mu_\Delta$	Displacement ductility factor
$\mu_\phi$	Curvature ductility factor
$\phi$	Curvature at given experimental level
$\phi_y$	Curvature at ideal yield
$\theta_p$	Plastic rotation
$\xi_{eq}$	Equivalent viscous damping ratio

# 1 Introduction

Current seismic design methods are largely based on elastic design principles, which are understood by the profession and easy to implement. To account for inelastic structural response, these design procedures rely on simplified physical models and empirical coefficients that make the design process inconsistent. Capacities and demands are not considered explicitly, and actual inelastic actions are unexplored (Krawinkler 1995).

Through lessons learned in recent earthquakes, the bridge engineering community recognizes the need for new seismic design methods and approaches. Although the current design methodology expects that a structure will not collapse at a maximum level design earthquake, the amount of damage in a structure after small and moderate earthquakes is unknown. Observed damage has demonstrated that performance goals, which go beyond the life safety concern expressed in most codes, are necessary to ensure different levels of functionality and to protect against large socio-economic losses. Recent seismic codes contain performance objectives that are descriptive but are not quantified, making it difficult for engineers to explain to owners the type of protection they are paying for (Krawinkler 1995). Efforts are in progress to define and quantify various limit states and associated performance goals in order to develop a consistent performance-based design methodology. These performance-based considerations may be addressed better with deformation-based design and analysis approaches that assess the inelastic response of structures more directly (SEAOC 1996) or by new design approaches based on the most probable response of the structure to different seismic inputs.

Performance-based design attempts to embrace a broader scope of design that yields more predictable seismic performance over the full range of earthquake demands. Although the framework of performance-based design has not yet been finalized, it focuses on establishing and meeting certain performance objectives. A performance objective is a combination of a performance level, which is defined by a particular damage state, and a seismic hazard specification, which can be defined in terms of ground shaking for a given return period.

Therefore, the relationship between ground motions (demand) and structural performance (capacity) is important.

Although past discussions on Performance-Based Earthquake Engineering (PBEE) have focused largely on the design of buildings, the philosophies can also be applied to the design of bridges. Following the 1995 Kobe earthquake, damage to highway bridges was evaluated and a preliminary performance-based design method was implemented into the seismic design specifications of highway bridges in Japan (Kawashima et al. 1997). However, the Japanese seismic design code is still based on safety factors and has not been fully verified.

In California, seismic design for important bridges already considers a multi-level design methodology for safety evaluation earthquakes (SEE), function evaluation earthquakes (FEE), and, where applicable, fault rupture (FR) events. The American Association of State Highway and Transportation Officials (AASHTO) is currently revising the load and resistance factor design (LRFD) specification for the seismic design of bridges (NCHRP 12-49 1999). Seismic performance is assured by verifying that displacements are limited depending on the desired performance level of the bridge. Although damage, performance, and serviceability levels are well defined, many design approaches have been proposed to achieve the desired range of performance objectives.

A design approach with multi-level performance criteria can be implemented only when structural behavior is accurately characterized and predicted. Recent research at the University of California, San Diego, has focused on describing the structural behavior of concrete bridges as it pertains to various performance response levels. It is essential to evaluate the characteristics of bridge components and systems at various stages of descriptive damage to determine if a consistent hierarchy of performance levels can be established.

In addition to the development of performance specifications and expectations, a consistent performance-based seismic design approach for bridges requires a detailed probabilistic demand assessment and capacity/response determination. Seismic hazard analysis is necessary for demand determination but is beyond the scope of this research. The following report addresses the capacity/response determination and parameterization of the behavior of bridge components, sub-assemblages, and systems. This is in direct support of the development of a multi-level performance design and evaluation procedure for bridges. The primary objective of the report is to promote a consistent and thorough method of reporting and evaluating the capacity and performance of our bridge structures. The main section of the report describes a

detailed evaluation procedure under development and outlines the proposed evaluation template, which is used for the bridge performance library. The appendixes provide case studies that document and demonstrate the assessment procedure.

## 2 Five-Level Performance Evaluation Approach

### 2.1 BACKGROUND

The evaluation of results from bridge components and systems tested at UCSD over the past 15 years has led to a preliminary determination of performance levels and corresponding qualitative and quantitative assessment parameters (Hose et al. 1999). The assessment procedure is closely related to previous work in buildings (SEAOC 1996), where performance, which is defined by a particular damage state, is classified into five levels. Although performance-based bridge design strategies are heading towards a two or three level approach, the capacity assessment needs to be subdivided to ensure that performance levels for different behavior modes can be differentiated. The selection of five levels was based on significant performance/damage states observed during large-scale experimental research.

The five-level assessment approach for the development of the bridge performance database consists of three stages of evaluation. The initial stage of evaluation, *Bridge Damage Assessment*, relates classifications of structural damage to socio-economic descriptions (SEAOC 1996) at the five designated performance levels. Seismic performance levels are also defined in terms of required repair effort. This bridge damage assessment stage, presented in Table 2.1, lists the classifications of damage for each of the five levels as well as corresponding damage, repair, and socio-economic descriptions. The five levels of damage range from NO visible damage to LOCAL FAILURE/COLLAPSE of components or the entire system. The NO damage level is described as barely visible hairline cracks that close after a seismic event and require no repair. The second category, MINOR damage, consists of visible cracking that does not likely require repair. The MODERATE damage level is characterized by the onset of concrete spalling, which is typically a good indicator of local damage, and would require minimum repair. However, in some cases like squat columns or steel-jacketed components, this level may be reached without the occurrence of spalling. Therefore, the level must be described by other damage indicators

such as wide-open cracks for squat columns, or damage in adjacent members for steel-jacketed components. The fourth category, MAJOR damage, is defined by large crack widths and extensive spalling which will require significant repair. Finally, the LOCAL FAILURE/COLLAPSE level can be classified by permanent visible deformation such as buckling and rupture of reinforcement and crushing of the concrete core. This Level V category of damage usually requires replacement of the component or structure.

**Table 2.1 Bridge damage assessment**

<b>Level</b>	<b>Damage Classification</b>	<b>Damage Description</b>	<b>Repair Description</b>	<b>Socio-economic Description</b>
<b>I</b>	NO	Barely visible cracking	NO REPAIR	FULLY OPERATIONAL
<b>II</b>	MINOR	Cracking	POSSIBLE REPAIR	OPERATIONAL
<b>III</b>	MODERATE	Open cracks Onset of spalling	MINIMUM REPAIR	LIFE SAFETY
<b>IV</b>	MAJOR	Very wide cracks Extended concrete spalling	REPAIR	NEAR COLLAPSE
<b>V</b>	LOCAL FAILURE /COLLAPSE	Visible permanent deformation Buckling/rupture of reinforcement	REPLACEMENT	COLLAPSE

The second stage of the database evaluation, *Bridge Performance Assessment*, is shown in Table 2.2, and can be determined from field investigations following a seismic event, detailed assessment of laboratory experiments, and/or detailed analyses. This stage incorporates the same five categories used in the *Bridge Damage Assessment* stage of evaluation to describe performance levels. To explicitly relate damage to capacity, engineering terms were selected for the performance levels rather than the socio-economic expressions taken from other documents and found in the last column of Table 2.1. The performance levels range from CRACKING to STRENGTH DEGRADATION. Qualitative and quantitative performance descriptions corresponding to these five performance levels are also given in Table 2.2. They represent simple descriptions of the performance levels that can be observed visually. The database attempts to explicitly define criteria at each level by providing quantitative guidelines such as crack widths, crack angles, and regions of spalling. The criteria for the classification of damage and

performance are based on the current state of knowledge, which will be adapted to reflect new information.

**Table 2.2 Bridge performance assessment**

<b>Level</b>	<b>Performance Level</b>	<b>Qualitative Performance Description</b>	<b>Quantitative Performance Description</b>
<b>I</b>	CRACKING	Onset of hairline cracks.	Cracks barely visible.
<b>II</b>	YIELDING	Theoretical first yield of longitudinal reinforcement.	Crack widths < 1mm.
<b>III</b>	INITIATION OF LOCAL MECHANISM	Initiation of inelastic deformation. Onset of concrete spalling. Development of diagonal cracks.	Crack widths 1-2mm. Length of spalled region > 1/10 cross-section depth.
<b>IV</b>	FULL DEVELOPMENT OF LOCAL MECHANISM	Wide crack widths/spalling over full local mechanism region.	Crack widths > 2mm. Diagonal cracks extend over 2/3 cross-section depth. Length of spalled region > 1/2 cross-section depth.
<b>V</b>	STRENGTH DEGRADATION	Buckling of main reinforcement. Rupture of transverse reinforcement. Crushing of core concrete.	Crack widths > 2mm in concrete core. Measurable dilation > 5% of original member dimension.

The first performance level in Table 2.2, CRACKING, which corresponds to the NO damage level, is again described as the onset of barely visible cracks. The second category in the performance table, YIELDING, is associated with the MINOR damage level. It is defined when reinforcement has yielded, and can be quantified by cracks that are clearly visible after the seismic event but are less than 1mm in width. The yielding of the reinforcement can be measured experimentally by strain gauges, and can also be analytically evaluated by cross-sectional moment curvature analyses.

The third performance level, INITIATION OF LOCAL MECHANISM, correlates to the MODERATE damage level in Table 2.1. It is qualitatively described as the onset of inelastic deformation, and depending on the prevalent failure mechanism, consists of the development of significant diagonal cracks or spalling of the cover concrete. This performance level can be quantified visually when crack widths between 1-2mm and/or lengths of spalled regions greater than 1/10 the cross-section depth develop. The MAJOR damage level correlates with the FULL DEVELOPMENT OF LOCAL MECHANISM performance level. Qualitatively, this level can

be described when cracks and spalling extend over the full region of the local mechanism. Cracks greater than 2mm in width and lengths of spalled regions that extend significantly beyond 25mm (for typical members this is roughly half the section depth in the loading direction) are commonly observed. The final performance level, STRENGTH DEGRADATION, occurs when the structural component or system experiences a significant reduction in observed or calculated strength, such that the load-carrying capacity of the component can no longer be relied upon. This performance level is reached when buckling of the main reinforcement is initiated, and hoop or tie reinforcement fails due to anchorage or rupture. It can also be defined by crushing of the concrete core. For field investigations following a seismic event, this level can be characterized by crack widths greater than 2mm within the concrete core, or when the measurable concrete dilation of the member is greater than 5% of the original member dimension. For laboratory experiments, Level V can be identified when the lateral capacity of the component drops below 85% of the maximum. However, in some instances a large reduction in strength of a component may not necessarily lead to overall failure of the system, but large residual deformations may impair the serviceability of these components, sub-assemblages, and systems.

The final stage of the capacity evaluation database consists of *Bridge Performance/Design Parameters* that correlate with the five qualitative performance levels. The quantitative parameters investigated are presented in Table 2.3. Since there is no fixed framework for performance-based design, this database attempts to evaluate as many different parameters as possible. Once the parameterization at each performance level is assessed for many case studies, the right combination of parameters can eventually be chosen for design.

**Table 2.3 Bridge performance/design parameters**

Parameter	Definition
$\epsilon_s$	Steel strain
$\epsilon_c$	Concrete strain
$\mu_\phi$	Curvature ductility factor
$\theta_p$	Plastic rotation
$p_c, p_t$	Principal compression and tension stresses
<b>Drift</b>	Drift ratio
$\mu_\Delta$	Displacement ductility factor
<b>RDI</b>	Residual deformation index
$\xi_{eq}$	Equivalent viscous damping ratio
$n_k$	Normalized effective stiffness

Contrary to the quantitative descriptions given in column four of Table 2.2, the numerical determination of these parameters requires instrumentation and/or analyses. Numerical derivations of these performance parameters will be performed and related to all five identified engineering limit states in Table 2.2.

## 2.2 CALCULATION OF PARAMETERS

The parameters in Table 2.3 include steel and concrete strains,  $\epsilon_s$  and  $\epsilon_c$ , that are obtained from experimental strain gauges placed on the extreme longitudinal reinforcement at the critical cross section. The curvature ductility,  $\mu_\phi$ , as well as local steel and concrete strains, relate to the response of an individual section and depend on reinforcement details, material properties, and axial load. Curvatures are determined from experimental test data and curvature ductility is calculated by Equation 2.1 as the ratio of curvature at a given force level divided by experimental curvature at ideal yield. Alternatively, sectional strains, curvature, and curvature ductility levels can be analytically determined from simple section analyses when experimental data is unavailable. These analytically determined parameters are denoted with an asterisk when reported in the database.

$$\mu_\phi = \frac{\phi}{\phi_y} \quad (2.1)$$

In support of the development of the new seismic provisions for AASHTO (NCHRP 12-49 1999), it was requested that the plastic rotation be reported at each level in the performance database. The plastic rotation is a function of the plastic curvature,  $\phi_p$ , which is assumed to be constant over an equivalent plastic hinge length. Assumptions for plastic hinge length vary depending on the type of application. Existing equations for plastic hinge length are defined as ultimate when the full plastic hinge region has formed. Since the calculation of plastic rotation is desired at all five performance levels, the use of current equations for plastic hinge length will yield inaccurate results. Also, cases that exhibit brittle behavior often do not form conventional plastic hinge regions. Therefore, it is difficult to define a general equation for plastic hinge length that applies to all cases. To avoid these inconsistencies, the plastic rotation in this assessment approach is calculated by Equation 2.2.

$$\theta_p = \frac{\Delta_p}{L} \quad (2.2)$$

where,

$\Delta_p = \Delta - \Delta_y =$  Plastic displacement at given experimental level

$\Delta_y = \frac{M_n}{M_y} \Delta'_y =$  Calculated ideal yield displacement

$\Delta'_y =$  Displacement at theoretical first yield

$\Delta =$  Displacement at given experimental force level

$M_n =$  Ideal yield moment from critical cross-section analysis at  $\epsilon_c = 0.004$

$M_y =$  Moment at theoretical first yield

For conventional designs, the critical section of the plastic hinge is assumed to occur at the interface of the connections. Thus the full member height is typically used for  $L$  in Equation 2.2. For retrofitted members with specified gap widths or members with relocated plastic hinges the full height is not appropriate. In these cases, the center of the plastic hinge region is clearly identified in design. Therefore,  $L$  in Equation 2.2 is taken as the distance between the critical section of the plastic hinge and the point of contraflexure in the member. This length is multiplied by two for the cases of double bending.

Some components such as cap-beam/column joint regions in sub-assemblages and systems are designed based on nominal principal compression and tension stress limitations which provide more relevant information regarding force transfer mechanisms and possible damage states in the joints. Therefore, the nominal **Principal Stress-State**, which consists of the principal compression and tension stresses ( $\mathbf{p}_c, \mathbf{p}_t$ ), is one of the parameters evaluated in Table 2.3. From a Mohr's circle analysis for stress, the nominal principal stresses in the joint region can be found by Equation 2.3 (Priestley et al. 1996). Typically, the principal stress-state parameter is not relevant for the design of columns. Therefore, it is not calculated in the column test examples in Appendix A. For the pile sub-assemblage and system examples presented in Appendices B and C, only the principal tension stress was considered relevant in the response assessment.

$$p_c, p_t = \frac{f_v + f_h}{2} \pm \sqrt{\left(\frac{f_v - f_h}{2}\right)^2 + v_j^2} \quad (2.3)$$

where,

$p_c, p_t =$  Nominal principal compression and tension stresses

$$f_v = \frac{P_c}{b_{je}(h_c + 0.5h_b)} = \text{Average axial vertical stress}$$

$$f_h = \frac{P_b}{b_b h_b} = \text{Average axial horizontal stress}$$

$$b_{je} = \sqrt{2}D = \text{Effective width of joint for circular columns}$$

$$b_{je} = h_c + h_b = \text{Effective width of joint for rectangular columns}$$

$$P_c = \text{Column axial force}$$

$$P_b = \text{Axial compression force in beam}$$

$$h_c = \text{Column section depth perpendicular to axis}$$

$$h_b = \text{Cap beam section depth}$$

$$b_c = \text{Column width perpendicular to axis}$$

$$b_b = \text{Beam width perpendicular to axis}$$

$$v_{jh} = \frac{V_{jh}}{b_{je} h_c} = v_{jv} = \frac{V_{jv}}{b_{je} h_b} = \text{Normal horizontal and vertical shear stresses in joint}$$

$$V_{jh} = \frac{V_{col}^o}{h_b} = \frac{M^o}{h_b} = \text{Horizontal joint shear force}$$

$$V_{jv} = \frac{V_{jh} h_b}{h_c} = \text{Vertical joint shear force}$$

$$M^o = \text{Overstrength moment of plastic hinge in column}$$

$$V_{col}^o = \text{Overstrength applied shear force in column}$$

Drift is calculated as the ratio between the lateral displacement experienced at each loading level divided by the effective height of the test unit. Displacement ductility,  $\mu_{\Delta}$  is a commonly used parameter to determine overall structural lateral response. It is obtained experimentally from the idealized bilinear approximation to the monotonic spine or cyclic peak envelope of the load-displacement curve shown in Fig. 2.1. Displacement ductility is defined by Equation 2.4 as the ratio of deformation at a given response level to the deformation at ideal

yield (Priestley et al. 1996).

$$\mu_{\Delta} = \frac{\Delta}{\Delta_y} \quad (2.4)$$

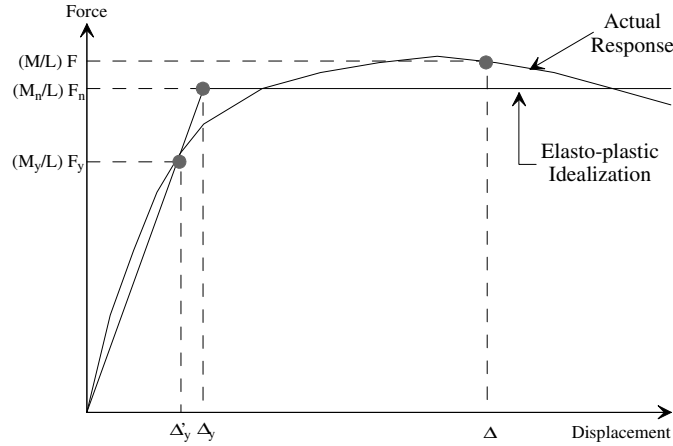


**Fig. 2.1. Bilinear approximation for displacement ductility parameter**

The residual deformation index, **RDI**, is a function of the inelastic behavior of the structure and can be used as an index to estimate damage or reparability following a seismic event. A cyclically loaded inelastic structural component or system incurs a residual displacement that remains when the lateral load is removed. The RDI is a non-dimensional index that is obtained by dividing the permanent residual displacement observed at each performance level by the ideal yield displacement. This calculation is shown in Equation 2.5. Note that for nonlinear elastic structural response or low-level inelastic response, the RDI can be less than one. The parameters necessary for the calculation of the RDI for test units with symmetric hysteresis loops are depicted in Fig. 2.2.

$$RDI = \frac{\Delta_r}{\Delta_y} \quad (2.5)$$

Another quantitative parameter that can be evaluated at each performance level is the equivalent viscous damping ratio,  $\xi_{eq}$ , which describes the equivalent viscous hysteretic damping. It is based on an equal area approach that represents the same amount of energy loss per cycle as seen in the real experiment (Priestley et al. 1996). The calculation of  $\xi_{eq}$  for cases with symmetric hysteresis loops is shown in Fig. 2.2. The area within the inelastic force-displacement response curve,  $E_d$  in the figure, is a measure of the hysteretic damping or energy-dissipating capacity of

the structure. The hatched region in Fig. 2.2 depicts the elastic strain energy stored in an equivalent linear elastic system,  $E_s$ . The equivalent viscous damping ratio,  $\xi_{eq}$ , is represented by Equation 2.6.

$$\xi_{eq} = \frac{1}{4\pi} \left( \frac{E_d}{E_s} \right) \quad (2.6)$$

The effective stiffness,  $K_{eff}$ , defines the slope of the equivalent linear elastic system represented by  $E_s$ , and is also depicted in Fig. 2.2. It is the ratio of the force at a given response level to the deformation at that level and is calculated by Equation 2.7. The initial stiffness at ideal yield,  $K_o$ , is calculated by Equation 2.8. For non-dimensional representation, the effective stiffness parameter in this document is normalized by the initial stiffness as shown in Equation 2.9. The equivalent viscous damping ratio and effective stiffness of an inelastic bridge system are important design parameters in some of the recent displacement-based bridge design methodologies and procedures (Kowalsky 1997).

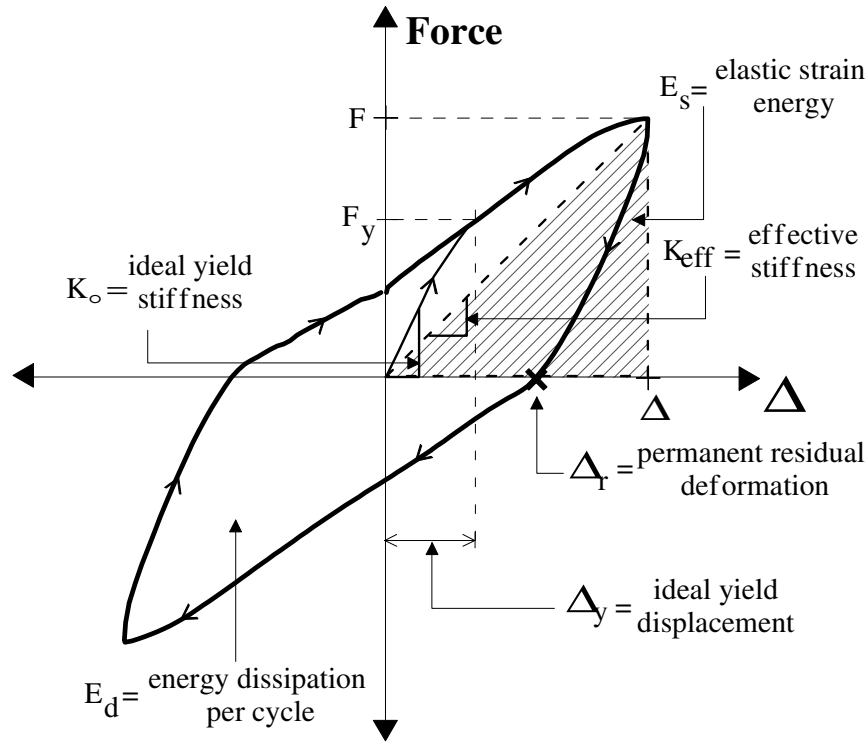


**Fig. 2.2. Residual deformation index (RDI), equivalent viscous damping ratio ( $\xi_{eq}$ ), and effective stiffness ( $K_{eff}$ ) for symmetric hysteresis loops**

$$K_{eff} = \frac{F}{\Delta} \quad (2.7)$$

$$K_o = \frac{F_n}{\Delta_y} \quad (2.8)$$

$$n_k = \frac{K_{eff}}{K_o} \quad (2.9)$$

Some components and systems may experience asymmetric response in the two loading directions under cyclic loading. The average RDI is reported for these cases. This calculation is described in Equation 2.10 and the necessary dimensions are defined in Fig. 2.3. The same concept of taking the average of the push and pull responses is applied to the determination of the equivalent viscous damping ratio and the equivalent stiffness. The equivalent viscous damping ratio for the full asymmetric cycle at a specific force level is derived in Equation 2.11 and further defined in Fig. 2.3. The energy input or damping energy loss for the push half cycle of the idealized force-displacement loop is represented by area  $E_{d1}$  in Fig. 2.3. Similarly, the energy loss for the pull half cycle is depicted as area  $E_{d2}$ . The hatched regions in Fig. 2.3 define  $E_{s1}$  and  $E_{s2}$ , which represent the elastic strain energy stored in an equivalent linear elastic system for the push and pull half cycles respectively. The normalized equivalent stiffness for an asymmetric structure is given in Equation 2.12. The peak force and displacement values to calculate the effective stiffness for the push and pull half cycles at a given loading level are defined by  $F_1, \Delta_1$ , and  $F_2, \Delta_2$ , respectively.  $K_{o1}$  and  $K_{o2}$  are defined in Fig. 2.3.

$$RDI = \frac{1}{2} \left( \frac{\Delta_{r1}}{\Delta_{y1}} + \frac{\Delta_{r2}}{\Delta_{y2}} \right) \quad (2.10)$$

$$\xi_{eq} = \frac{\xi_{eq1} + \xi_{eq2}}{2} = \frac{1}{2} \left( \frac{2E_{d1}}{4\pi E_{s1}} + \frac{2E_{d2}}{4\pi E_{s2}} \right) = \frac{1}{4\pi} \left( \frac{E_{d1}}{E_{s1}} + \frac{E_{d2}}{E_{s2}} \right) \quad (2.11)$$

$$n_k = \frac{1}{2} \left( \frac{K_{eff1}}{K_{o1}} + \frac{K_{eff2}}{K_{o2}} \right) \quad (2.12)$$

A recent study was performed to quantify the effects of material and system parameters on the cyclic response of reinforced concrete circular columns (Kunnath et al. 1997). Of concern was the effect of load path and ductility on energy dissipation capacity. The Kunnath et al. study, which was limited to seismically detailed flexural circular columns, found that the energy capacity of a member at failure is strongly path dependent. Therefore, standard cyclic testing is

not a good measure of the energy capacity of members. Through the use of the capacity assessment approach presented in this paper, the evaluation of all types of structural components, sub-assemblages and systems can be achieved and included in the database. The database should include results from tests that deviate from the standard cyclic testing protocol by using random loading sequences. By reporting performance/design parameters in the database, we can gain a better understanding about the effects of load path on these parameters. Therefore, the capacity assessment database attempts to include as many parameters as possible to investigate and better understand the capacity of bridge structures. Only after we move towards this standardized assessment approach, which includes studying variable loading histories and a variety of material and geometrical properties, can we develop accurate damage models to be used in performance-based design. This consistent evaluation can lead to a more comprehensive assessment and design approach that is based on quantifiable parameters rather than the simplified physical models and empirical coefficients that are used in current bridge design practice. Although current work focuses on reinforced concrete bridges, it is hoped that a similar procedure will be developed for other types of bridge structures in the future.

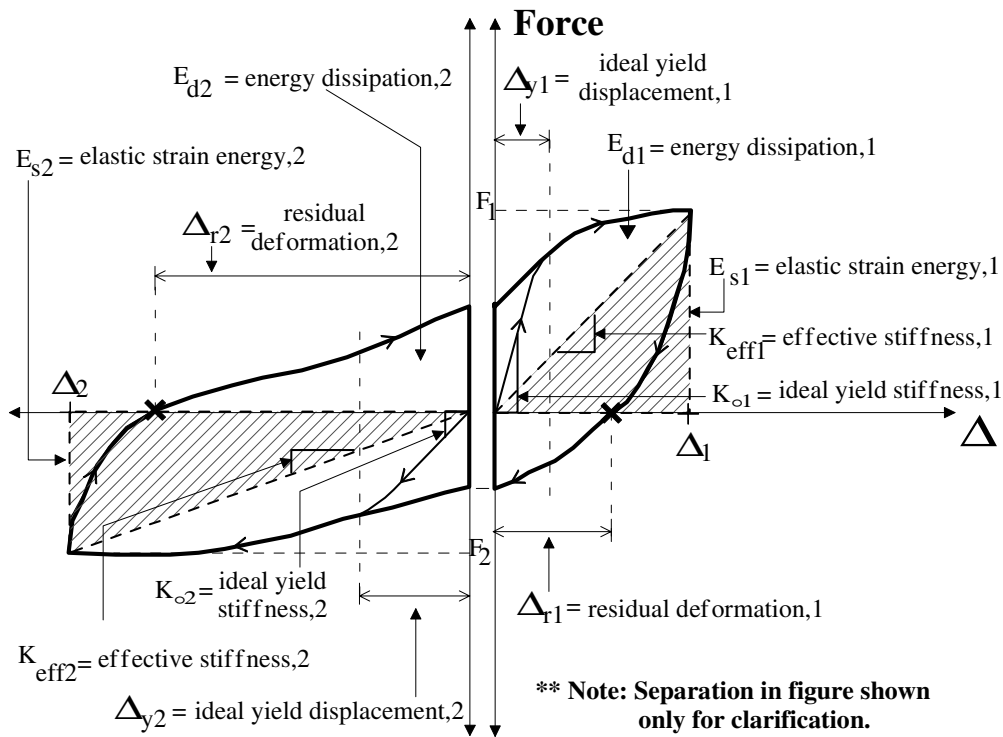


**Fig. 2.3. Residual deformation index (RDI), equivalent viscous damping ratio ( $\xi_{eq}$ ), and effective stiffness ( $K_{eff}$ ) for asymmetric hysteresis loops**

### **3 Case Studies and Performance Evaluation Summaries**

To further develop the capacity evaluation approach, the quantitative parameters associated with the damage and performance levels previously discussed must be defined. This can be achieved only through the formation of a database that consistently evaluates a multitude of case studies. The five levels of bridge damage and performance assessment, as well as the full parameterization of performance indicators, were catalogued to date using results from large scale experiments and associated diagnostic analyses conducted at the Charles Lee Powell Structural Research Laboratories at UCSD. Test units consisting of typical structural and nonstructural bridge components, sub-assemblages, systems, as well as bridge retrofits were analyzed at each of the five levels to determine the numerical values for the engineering parameters outlined in Table 2.3. The results of the evaluations of some of the case studies using the approach outlined in this paper are presented in the Case Study Appendices. The following section describes the proposed standardized template used to evaluate each case study for the uniform database.

#### **3.1 EVALUATION TEMPLATE**

The template shown in Table 3.1 is designed such that a consistent format is used to obtain information from an array of case studies. By making this template available over the Internet, a variety of test units from other institutions outside UCSD and the Pacific Earthquake Engineering Research Center (PEER) can be analyzed and catalogued to develop a consistent performance-oriented design library. Other institutions currently have databases of test results available via the Internet (Univ. of Washington 1999). They provide valuable comprehensive information for test geometry, material properties, and force-displacement histories. However, these databases consist of results from building and bridge column tests under hysteretic loading only, and do not include sub-assemblages and systems. Furthermore, limited data is provided for

columns with varying axial load, columns enclosed in a steel shell or fiber wrap, and non-prismatic columns. Although damage indices are reported for each column to classify performance, they are not applied to actual locations during the response and are not explicitly related to quantifiable performance/design parameters. It is this stage of the capacity evaluation approach that is of primary interest and the objective of the PEER/UCSD database (UCSD 1999). Ultimately, this Bridge Performance Database will evaluate and make available to the public an array of component, sub-assembly, and system case studies from a variety of institutions. The focus of the assessment will be to provide the performance/design parameters that correlate to the multiple performance levels, which are relevant in deriving a reliable performance-based design procedure.

The case studies presented in the appendices of this paper and found in the *Performance/Capacity Catalog* available on the Internet were formulated using the evaluation template outlined in Table 3.1. Instructions on the information required for each section of the template are provided for the user during input, and the completed evaluation templates are submitted over the Internet. The first section of the template provides general information regarding the principal investigators for the case study in question. The assessment area describes the type of test unit under investigation. It consists of *component*, *sub-assembly*, or *system*, while the assessment classification describes whether the case study is *new* or is a *retrofit*. Also included in this *Background Information* section is the reference and sponsoring agency. Following the general information, the test unit designation and a brief discussion about the design of the test unit including relevant experimental test setup information is provided. The reinforcement details are depicted by a cross-sectional figure. For each component, the axial load ratio, which is generally defined in Equation 3.1, is reported. For sub-assemblies and systems, the axial load ratio includes dead load and seismic variations.

$$AxialLoadRatio = \frac{P}{f'_c A_g} \quad (3.1)$$

where,

$P$  = Axial load on the structure

$f'_c$  = Concrete compression strength

$A_g$  = Gross area of critical cross section

**Table 3.1 Evaluation template**

**Background Information:**

P.I.: Name Phone Email		Institution Address	
Co- Name P.I.: Phone Email		Institution Address	
Assessment Area		<b>1. Component</b>	<b>2. Sub-Assemblage</b> <b>3. System</b>
Assessment Classification		<b>N. New</b>	<b>R. Retrofit</b>
Reference			
Sponsoring Agency			

**Test Unit Information:**

Test Unit Designation			
Test Unit Description	Discussion about design of test unit and relevant test setup information		
Reinforcement Details: Cross-section Figure	Material Properties: $f_y, f_u$ , and stress-strain data of reinforcement		
Axial Load Ratio:	$f'_c$ of concrete (day of test value)		

**Bridge Damage Assessment:**

Qualitative description of damage observed in test unit at each of the damage/performance levels that correlate with photographs included in the next section			
Test Setup or Elevation Figure		Level I scanned photograph	
Level II scanned photograph		Level III scanned photograph	
Level IV scanned photograph		Level V scanned photograph	

**Bridge Performance Assessment:**

Discussion of results such as of force, ductility, and drift for significant loading levels and governing failure mechanism as they relate to the force-displacement response of the test unit					
Force-Displacement Hysteresis/Envelope: Force vs. Displacement and %Drift Include ductility levels on figure			Force-Displacement Envelope/Symbols: Symbols indicating location where each damage/performance level was reached (Level I=▲, II=●, III=■, IV=◆, V=✕)		
Bridge Performance/Design Parameters:					
Level	$\epsilon_s$	$\epsilon_c$	$\mu_o$	$\theta_p$	$P_c, P_t$
I					
II					
III					
IV					
V					
Level	% Drift	$\mu_\Delta$	RDI	$\xi_{eq}$	$n_k$
I					
II					
III					
IV					
V					

The *Test Unit Information* section also provides the material properties of each component, which include yield and ultimate stresses for all reinforcement and the day of test unconfined compression strength for concrete. To enable engineers to reproduce results for the case studies analytically, actual stress-strain data for the reinforcement is provided in this section when available.

The *Bridge Damage Assessment* section consists of qualitative descriptions of the damage observed in the test unit, which are correlated to photographs at each of the damage/performance levels. This set of five damage state photographs corresponding to the five performance levels, together with the numerical quantification of performance parameters, forms the main substance of the bridge performance catalog. A figure of the test setup or elevation of the test unit is also provided with the photographs. The goal of this section is to qualitatively demonstrate visual damage that is consistent at the various performance levels. To compliment both the University of Washington and University of California, San Diego efforts in capacity assessment, Table 3.2 was added to the template. It lists milestones in experimental testing with corresponding cycle designation, displacement levels, and comments. This table can be used during future testing as a method to record benchmark observations.

In the *Bridge Performance Assessment* section of the template, qualitative and quantitative performance descriptions of the five performance levels are defined. Initially, a brief discussion indicating relevant results regarding force, ductility, and drift at significant loading levels is provided. Also included is a description of the governing failure mechanism. The force-displacement hysteresis of the test unit with corresponding ductility levels and the response envelope is provided. A figure that shows the force-displacement envelope with symbols indicating the locations in the response of the test unit where each damage/performance level was reached is also given. The values of the performance/design parameters for the test unit under investigation are reported in two tables. The first table consists of the parameters that represent results determined from section properties, while the second table reports values of the parameters used to define overall structural behavior. The evaluation template is useful because the data from different case studies is reported in a consistent and concise format. Also, the page consisting of photographs depicting damage at the five performance levels can be used during post-earthquake field investigations to assess the remaining capacity of bridge structures and help officials determine which structures need to be repaired or replaced.

**Table 3.2 Damage observations during testing**

<b>Damage Type</b>	<b>Criteria to Identify Damage</b>	<b>Cycle</b>	<b>Disp.</b>	<b>Comments</b>
1 <sup>st</sup> “significant” flexural crack	Crack width, $w > 0.5\text{mm}$ (0.02 in)			
1 <sup>st</sup> “significant” shear crack	Diagonal crack extends over 1/4 cross-section depth, $w > 0.5\text{mm}$ (0.02 in)			
1 <sup>st</sup> visible joint-shear crack	Visible crack			
1 <sup>st</sup> residual open crack after unloading	$w > 0.25\text{mm}$ (0.01 in)			
1 <sup>st</sup> yield of longitudinal reinforcement	Strain gauge reading reaches yield strain at any location			
Onset of crushing	Observed flaking. Minor spalling.			
“Significant” spalling	Spall height $> 1/10$ cross-section depth			
Fully spalled	Spall height no longer increases with increasing deformation			
Development of shear mechanism	Diagonal crack extends over 2/3 cross-section depth, $w > 2\text{mm}$ (0.08 in)			
First sign of longitudinal bar buckling	Observation			
Large cracks within concrete core	$w > 2\text{mm}$ (0.08 in) within core			
Spiral/hoop fracture	Observation, sound			
Longitudinal bar fracture	Observation, sound			
Loss of axial load capacity	Instability of member			

## 4 Performance Assessment and Design Methodologies

From the evaluation of an array of case studies using the performance assessment approach defined in this paper, identification curves can be developed to characterize the performance and behavior modes for different classifications of seismic structural response. Preliminary stages of these curves that illustrate the behavior modes of *Brittle*, *Strength Degrading*, and *Ductile* structures as they respond to increasing lateral deformation are given in Fig. 4.1 through Fig. 4.3. These figures are sample curves that will be expanded and finalized as more case studies are evaluated. They are intended to demonstrate where the performance-based design approach is heading. The curves are similar to performance figures for buildings, and represent schematic plots of the lateral force-displacement response (FEMA 274 1997) and (FEMA 306 1999). They are labeled, however, according to the five discrete bridge damage/performance levels discussed in this paper and are also related to specific bridge performance/design parameters such as residual deformation index (RDI), equivalent viscous damping ratio ( $\xi_{eq}$ ), and normalized effective stiffness ( $n_k$ ). It should be noted that for a given bridge component, sub-assembly, or system, the relative horizontal and vertical scales for these figures and the margin of deformation between the damage/performance levels may vary significantly.

It has been recognized that the evaluation of displacements rather than forces is important for defining survival, damage control, and serviceability of a bridge following a major seismic event. Therefore, completely displacement-based design approaches for the seismic response of bridges are under development (Priestley et al. 1996) and (Kowalsky 1997). The two most important parameters required for these displacement-based procedures, effective stiffness  $K_{eff}$  and effective damping  $\xi_{eq}$ , have been observed to vary based on the type of failure mode of the structure. They also change as a function of structural displacement ductility. In many cases, an increasing RDI value indicates fatter hysteresis loops, which relates directly to the amount of equivalent viscous damping and the effective stiffness of the structure. Therefore, understanding

the relationships between these parameters is necessary for new displacement/performance-based design procedures. By evaluating and incorporating the bridge performance/design parameters on Fig. 4.1 through Fig. 4.3, the identification curves become important tools in design. Since these identification curves are in preliminary stages of development, the values for the parameters at each level are based only on average values obtained from a limited number of case studies. As the bridge performance/capacity database expands, more reliable identification curves can be developed.

Two performance ranges, similar to those defined in (FEMA 273 1997), are also labeled on the identification curves in Fig. 4.1 through Fig. 4.3. In order for a sufficient margin of safety to be maintained prior to potential failure, the performance ranges vary depending on what type of governing failure mode occurs in the structural member. For all three failure modes, the *Damage Control* range covers the elastic region, where the force resisting mechanisms of the bridge structures retain most of their pre-earthquake strength and stiffness. In the capacity assessment approach presented in this paper, Levels I and II define this elastic region. The risk of life-threatening injury from structural damage is low and only minor repairs are necessary. For *Brittle* structures shown in Fig. 4.1, the *Damage Control* performance range terminates between Levels II and III of the capacity assessment methodology. For the *Strength Degrading* mode shown in Fig. 4.2, the *Damage Control* performance range includes behavior defined by Level III. Level IV in *Brittle* and *Strength Degrading* structures usually indicates local failure with the onset of buckling, shear failure, or joint shear failure. For *Ductile* structures shown in Fig. 4.3, however, the damage and performance observed at Level IV is more stable, and thus is included in the *Damage Control* performance range. In all three behavior modes, moderate to significant damage is expected in the *Damage Control* range, but partial or total structural collapse is unlikely. Injuries may occur during the earthquake, but the overall risk of life-threatening injury as a result of structural damage is low. It is within this *Damage Control* range that future performance-based design procedures need to be concentrated to minimize repair time, cost, and operation interruption. The second performance range, *Limited Safety*, represents behavior and damage states at large deformations. This range covers Levels III-V in the capacity assessment for *Brittle* structures, Levels IV and V for *Strength Degrading* structures, and Level V for *Ductile* structures. A significant risk of life and economic loss may result if design or assessment procedures that reach performance within this *Limited Safety* range are employed (FEMA 273) 1997). From the preliminary curves it is recognized that the locations

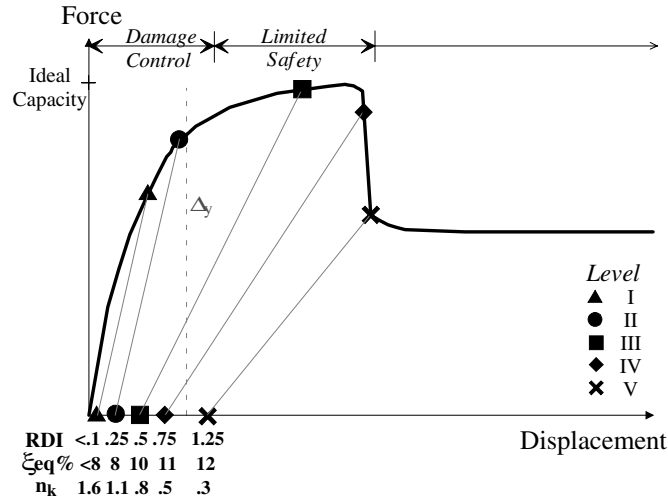


Fig. 4.1. Identification curve for *brittle* behavior mode.

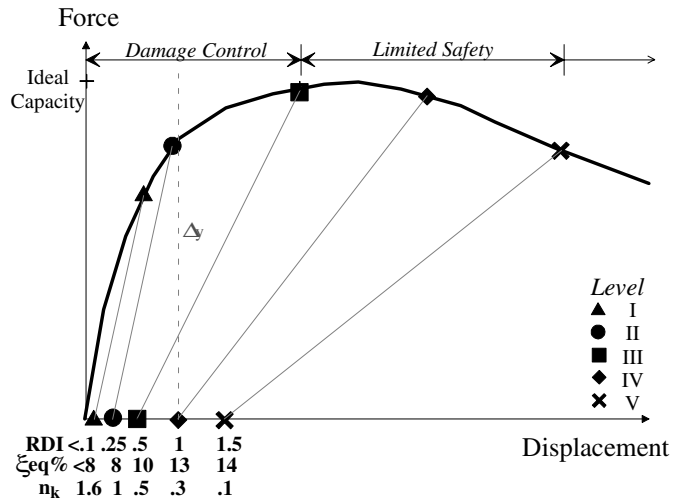


Fig. 4.2. Identification curve for *strength degrading* behavior mode.

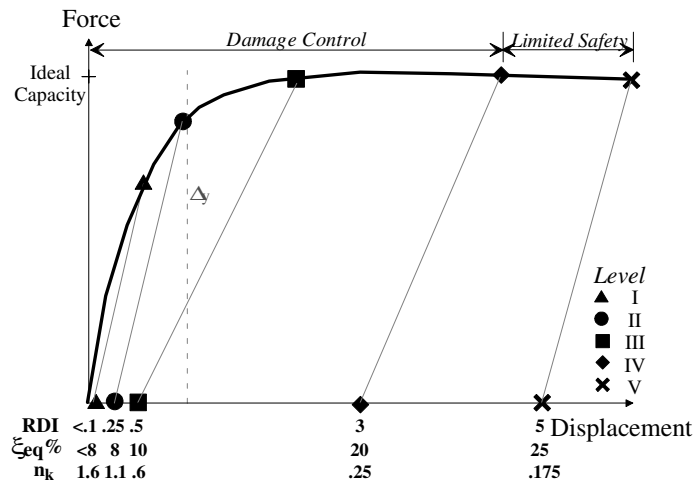


Fig. 4.3. Identification curve for *ductile* behavior mode.

of the performance ranges are not consistent between different behavior modes. The determination of the levels that define these performance ranges can not be finalized until more case studies are investigated. Since performance is defined in terms of damage control and therefore repair effort, future identification curves will attempt to resolve this inconsistency.

## 5 Conclusions

The research described in this paper is part of a comprehensive program instigated by PEER and conducted by UCSD to develop and demonstrate the parametric basis for performance-based bridge engineering in the form of a bridge performance catalog. It focuses on the capacity evaluation of bridge components, sub-assemblages, and systems to accurately characterize and predict structural behavior, such that a multi-step design approach can eventually be implemented. The database presented in this paper consists of a five-level performance evaluation approach that translates performance descriptions into engineering limit states. Qualitative descriptions of structural damage are correlated with photographs at the five designated performance levels. Also evaluated at the five levels is the association between qualitative descriptions and quantification of performance parameters. It is this parameterization of bridge components, sub-assemblages, and systems that is essential in the development of a consistent performance-based design methodology for bridges in seismic zones.

The evaluation template presented in this paper is available over the Internet such that consistent evaluations of numerous case studies for bridges can be performed. This will enhance the development of the identification curves and performance parameters presented in this paper, which characterize performance for different classifications of bridges. The use of a standard evaluation template, specifically correlating the five performance levels to actual photographs, is also convenient as a post-earthquake reconnaissance guide for the evaluation of structural safety. Decisions in the past on what to do about damaged structures were hampered by a lack of technical procedures to evaluate the effects of damage and repair. A better understanding of the capacity of our structures and the establishment of a better method to evaluate damage will allow us to formulate strategies to deal with post-earthquake problems. Furthermore, a major factor that has hindered the development of a performance-based design approach is that no systematic experimental program that is tailored to monitor, model, and calibrate cumulative seismic damage has been formulated. A new testing protocol that addresses performance-based design

issues should be developed (Kunnath et al. 1997).

Currently, the PEER/UCSD web site is accessible to the public. This site can be expanded to remaining PEER institutions and then to the three National Science Foundation (NSF) earthquake engineering research centers. Once extensive test data is collected, a comprehensive performance-based design approach can be investigated and defined. Although the current database applies only to reinforced concrete bridges, the authors anticipate that future phases of the evaluation approach will incorporate steel and composite bridge structures that are more prevalent in the Midwest and East Coast. Furthermore, analytical tools that incorporate the performance levels defined by this approach can be developed such that the capacity of new designs and retrofits of arbitrary structures can be more reliably evaluated.

The theory behind the database is based on observations and results from laboratory tests, as well as damage from past earthquakes. Through the evaluation of more case studies, the specific values of parameters and qualitative and quantitative descriptions may evolve. The identification curves with numerical correlation are a significant contribution to the performance-based design effort, but the characterization of the levels can not be defined until this assessment procedure is exposed to and used by the entire bridge engineering community. This database is essential for the performance-based design process to advance. Since a large portion of performance-based design goals are still undefined in terms of evaluation and application procedures, the capacity assessment database presented in this report provides a means for achieving these goals.

## **CASE STUDY APPENDIXES**

# **APPENDIX A:**

## **Components**

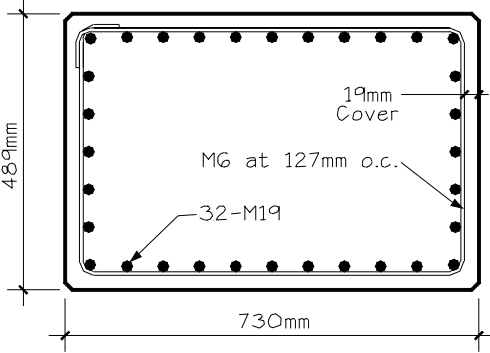
## Performance Parameter Assessment of Bridge Components/Structures

### **Background Information:**

<b>P.I.:</b>	<b>Name</b> Frieder Seible <b>Phone</b> (858) 534-4640 <b>Email</b> seible@ucsd.edu	<b>Institution</b> <b>Address</b>	University of California, San Diego Department of Structural Engineering 9500 Gilman Drive, Mail Code 0085 La Jolla, CA 92093-0085	
<b>Assessment Area</b>	1	<b>1. Component</b>	<b>2. Sub-Assemblage</b>	<b>3. System</b>
<b>Assessment Classification</b>	N	<b>N. New</b>	<b>R. Retrofit</b>	
<b>Reference</b>	Sun, Z., Seible, F., and Priestley, M.J.N., 1993, Diagnostics and Retrofit of Rectangular Bridge Columns for Seismic Loads, <i>Structural Systems Research Program, 93/07</i> , University of California, San Diego, La Jolla, July.			
<b>Sponsoring Agency</b>	California Department of Transportation			

### **Test Unit Information:**

<b>Test Unit Designation</b>	R-1: Rectangular Column with Continuous Longitudinal Reinforcement
<b>Test Unit Description</b>	<p>In 1971, the San Fernando earthquake exposed a number of deficiencies in bridge design guidelines. As a result, Caltrans and UCSD developed a research program to investigate the seismic response of circular and rectangular bridge columns designed prior to 1971. Many of the existing pre-1971 California bridge columns were designed with reinforcement ratios less than 2.5% and lap-splices of the longitudinal reinforcement with the footing starter bars. The lap-splices occurred over a splice length of <math>20d_b</math> in the potential plastic hinge region.</p> <p>The test unit under evaluation, <i>R-1</i>, was based on a prototype rectangular column with a cross section of 1.83m (72 inches) by 1.22m (48 inches), and a height of 9.14m (360 inches). In order to test the prototype column under laboratory conditions, a 40% dimensional scale factor was selected resulting in the 730mm (28.75 inches) by 489mm (19.25 inches) cross section. The continuous longitudinal reinforcement in column <i>R-1</i> consisted of 32 M22 (#6) bars resulting in a longitudinal reinforcement ratio of 2.55%. The transverse reinforcement consisted of 6.4mm (#2) stirrups spaced at 127mm (5 inches), resulting in a transverse reinforcement ratio of 0.184%. The cover concrete was 19mm (0.75 inches) taken from the outside face of the column to the transverse ties. The lap splice length in the plastic hinge region was 381mm (15 inches).</p> <p>The reinforcement details and material properties for column <i>R-1</i> are presented on the following page. The column was tested in the strong direction using the test setup shown in the figure on the following pages. The overall height to centerline of load application for this column was 3.66m (144 inches), and the column was tested in single bending with a 1780 kN (400 kip) applied axial load.</p>

<b>Reinforcement Details:</b> 		<b>Material Properties:</b>  <b>Longitudinal Steel:</b> $f_y = 317 \text{ MPa [46 ksi]}$ $f_u = 476 \text{ MPa [69 ksi]}$  <b>Transverse Steel:</b> $f_y = 276 \text{ MPa [40 ksi]}$ $f_u = 414 \text{ MPa [60 ksi]}$  <b>Concrete:</b> $f'_c = 33 \text{ MPa [4.8 ksi]}$
<b>Axial Load Ratio:</b>	<b>15%</b>	

### **Bridge Damage Assessment:**

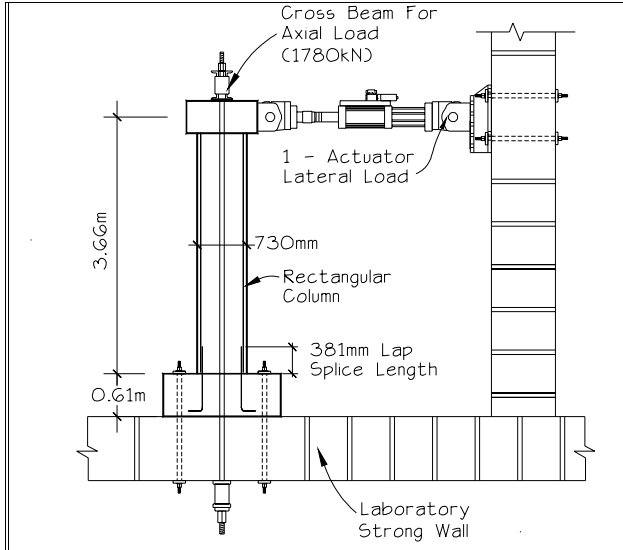
The first photograph on the following page depicts the damage observed in column *R-1* at Performance Level I (CRACKING), as defined in the PBEE Capacity Assessment Methodology. Horizontal cracks, which close upon unloading, are visible up the height of the column. No repair is necessary.

At Level II, significant horizontal flexural cracks were observed up the height of the column. Also, the first vertical cracks were identified near the base of the column, indicating the splitting effect of the column reinforcement lap splices. At the theoretical yield load level of 267 kN (60 kips), the average displacement of the push and pull directions was calculated as 17.5mm (0.69 inches), which resulted in a ductility 1 displacement of 22.6mm (0.89 inches). Little strength degradation was observed at this stage. However, a 15% load drop was recorded in the pull direction of the second cycle at ductility 1 due to debonding of the lap splice.

Level III, shows *R-1* after the third cycle at ductility 1.5. Spalling of the cover concrete was observed indicating the initiation of the local failure mechanism, which consists of debonding of the lap splice on the tension face of the test unit. Considerable degradation in the lateral load capacity of the column was observed during cycling at this ductility. Not only is repair of the damaged cover concrete necessary, but failure of the component is imminent. Therefore, the component has reached the Limited Safety performance range.

Continued spalling of the cover concrete over the entire lap-splice region primarily at the corners of the test unit defines the Level IV damage, which occurred at ductility 2. The damage is illustrated in the fourth photograph on the following page. A 25% degradation in strength was registered relative to the peak lateral load. The test unit does not show signs of extensive damage but the structural integrity of the section is compromised due to initiation of the bond/slip mechanism.

Failure of the test unit, corresponding to Level V, was dominated by bond/slip of the lapped reinforcement in the plastic hinge region. Damage of the column at failure is shown in the final photograph on the following page. During cycling at ductility 3, buckling of the longitudinal reinforcement occurred. At this level, repair of the column is no longer recommended and complete replacement of the component is necessary.



Test Setup



Level I



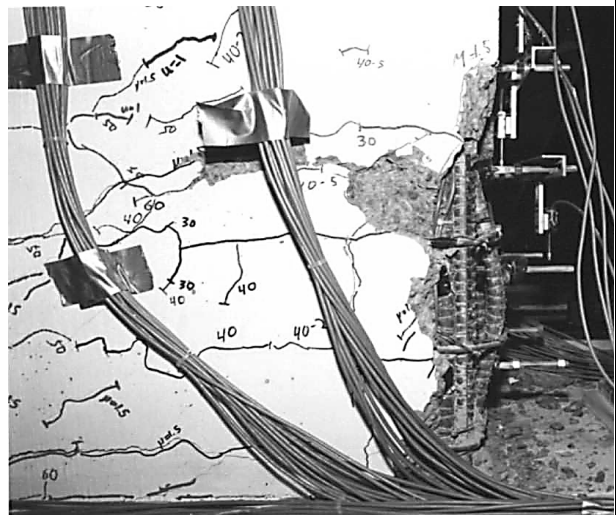
Level II



Level III



Level IV



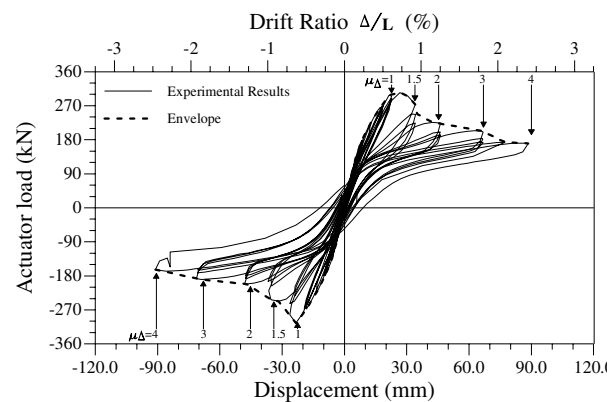
Level V

### Bridge Performance Assessment:

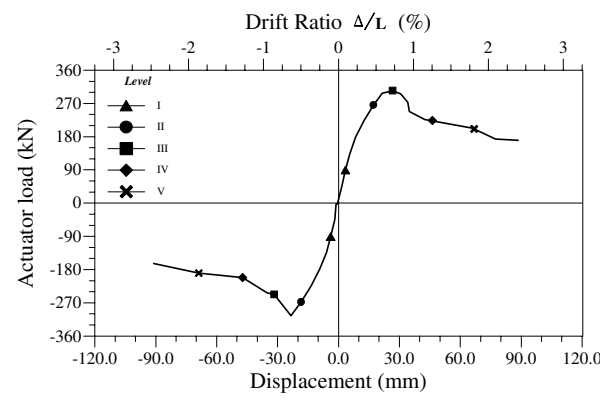
The cyclic force vs. displacement response for  $R-I$  is shown in the first figure below. An envelope profile of the response and displacement ductility levels is also plotted. The ideal yield displacement for the column was approximately 22.6mm (0.89 inches) and the force was 302.5 kN (68 kips). Failure of the column was due to bond/slip of the lapped reinforcement, as a result of the small lap splice length. The behavior of the test unit was fairly symmetric in both loading directions. At Performance Level V, the displacement was 67mm (2.64 inches) corresponding to 1.75% drift, and the lateral force in the push and pull directions was 155.7 kN (35 kips) and 142.3 kN (32 kips), respectively. In the second figure below, the envelope force vs. displacement profile is given with the associated five damage/performance levels. A change in stiffness is observed at Level I. The maximum lateral load was registered at Level III.

The quantitative parametric assessment of  $R-I$  is summarized in the tables below. Values were obtained as a combination of experimental and analytical results. However, drift, displacement ductility, RDI, equivalent viscous damping, and the effective stiffness parameters were based purely on experimental data. Strains were evaluated at the starter bars. The observed decrease in strain at Level V is due to slip of the lap splice connection. The principal stress state parameter does not apply for column components and was therefore not calculated. The low values of the equivalent viscous damping ratio varied between 3.5% and 10%, which are representative of the brittle bond/slip failure mechanism.

Force-Displacement Hysteresis/Envelope:



Force-Displacement Envelope/Symbols:



Bridge Performance/Design Parameters:

Level	$\epsilon_s$	$\epsilon_c$	$\mu_o$	$\theta_p$	$p_c, p_t$
I	$< \epsilon_y$	$< 0.0005^*$	$< 1$	--	--
II	$= \epsilon_y$	$0.001^*$	$< 1$	--	--
III	0.003	$0.002^*$	2	0.0013	--
IV	0.002	$0.003^*$	6	0.005	--
V	0.002	$> 0.005^*$	10	0.01	--
Level	% Drift	$\mu_\Delta$	RDI	$\xi_{eq}$	$n_k$
I	$< 0.50$	$< V_y$	0.02	3.5%	1.67
II	$< 0.50$	$< V_y$	0.08	5.0%	1.0
III	0.75	1	0.15	9.7%	0.67
IV	1.25	2	0.20	9.1%	0.33
V	1.75	3	0.30	8.8%	0.2

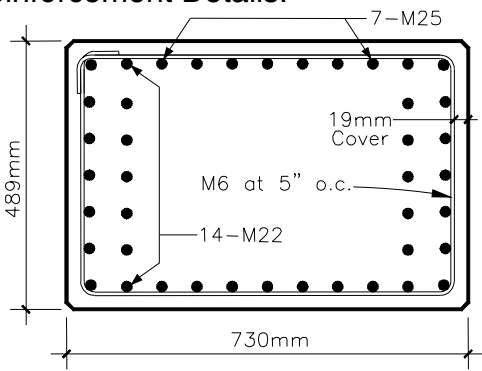
## Performance Parameter Assessment of Bridge Components/Structures

### **Background Information:**

P.I.:	Name Phone Email	Frieder Seible (858) 534-4640 seible@ucsd.edu	Institution Address	University of California, San Diego Department of Structural Engineering 9500 Gilman Drive, Mail Code 0085 La Jolla, CA 92093-0085
Assessment Area	1	1. Component	2. Sub-Assemblage	3. System
Assessment Classification	N	N. New	R. Retrofit	
Reference	Sun, Z., Seible, F. and Priestley, M.J.N., 1993, Diagnostics and Retrofit of Rectangular Bridge Columns for Seismic Loads, <i>Structural Systems Research Program</i> , 93/07, University of California, San Diego, La Jolla, July.			
Sponsoring Agency	California Department of Transportation			

### **Test Unit Information:**

Test Unit Designation	Rectangular Column with Continuous Longitudinal Reinforcement, R-5
Test Unit Description	<p>Many of the existing pre-1971 bridge columns in California with high reinforcement ratios exceeding 5% or more have continuous longitudinal reinforcement that is anchored into the footing. Due to the inadequate transverse reinforcement of these columns, the longitudinal bars start to buckle following spalling of the concrete cover, which limits the displacement capacities of the columns.</p> <p>To test these rectangular bridge columns, the prototype as-built column, which consisted of a 1.83m (72 inches) by 1.22m (48 inches) rectangular column with a height of 9.14m (144 inches), was scaled to 40% resulting in a column that was 730mm (28.75 inches) by 489mm (19.25 inches). The chosen 3.66m (144 inches) model column height provided a column aspect ratio (height to the depth of the column) of more than five to ensure a flexure dominated response.</p> <p>In Column R-5, the longitudinal reinforcement consisted of 14 M25 (#8) and 28 M22 (#7) continuous bars corresponding to a longitudinal reinforcement ratio of 5%. The transverse reinforcement consisted of 9.5mm (#2) hoops spaced at 127mm (5 inches) corresponding to a transverse reinforcement ratio of 0.18%. The cover concrete was 19mm (0.75 inches) taken from the outside face of the column to the transverse ties. Design details and material properties for column R-5 are presented on the following page.</p> <p>The test setup for column R-5, which was tested in the strong direction, is also shown in the following pages. The overall height to centerline of load application was 3.66m (144 inches). The column was tested in single bending with a 1780 kN (400 kip) applied axial load.</p>

<b>Reinforcement Details:</b> 		<b>Material Properties:</b>  <b>Longitudinal Steel:</b> $f_y = 317 \text{ MPa (46 ksi)}$ $f_u = 476 \text{ MPa (69 ksi)}$  <b>Transverse Steel:</b> $f_y = 276 \text{ MPa (40 ksi)}$ $f_u = 414 \text{ MPa (60 ksi)}$  <b>Concrete:</b> $f'_c = 33 \text{ MPa (4.8 ksi)}$
<b>Axial Load Ratio:</b>	<b>15%</b>	

### ***Bridge Damage Assessment:***

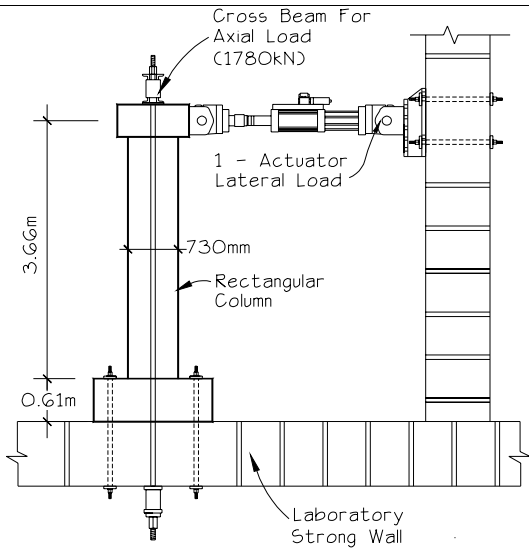
The first photograph on the following page depicts the damage observed in column *R-5* at Performance Level I (CRACKING), as defined in the PBEE Capacity Assessment Methodology. Uniformly distributed horizontal cracks, which close upon unloading, are visible up the height of the column. No repair is necessary.

At Level II, shown in the second photograph, the uniformly distributed horizontal cracking continued with some observed shear inclination of the cracks. At the theoretical yield load level of 478 kN (107.5 kips), the average displacement of the push and pull directions was calculated as 25.5mm (1.0 inch), which resulted in a ductility 1 displacement of 31mm (1.22 inches). Little strength degradation was observed at this stage, and repair, if necessary, is minimal.

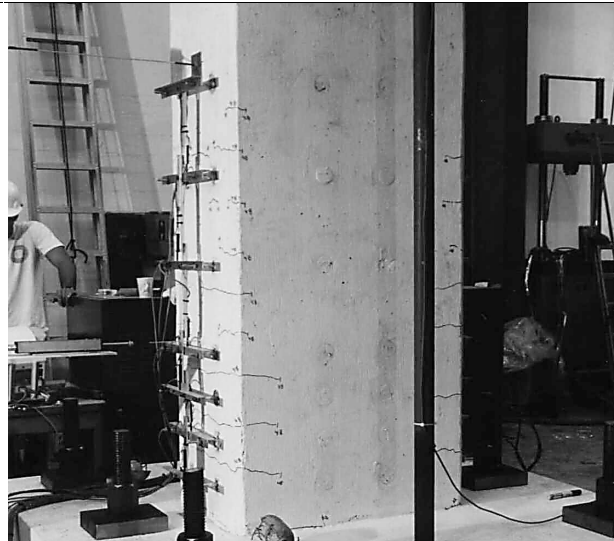
Level III, depicted in the third photograph, shows *R-5* after the first cycle at ductility 2. Significant horizontal and inclined cracks were observed up the height of the column. Also, the flexural shear cracks formed and propagated at an angle of approximately 45 degrees. Although the ideal ultimate lateral load of 580 kN (130.5 kips) was barely reached at ductility 2, the strength degradation in subsequent cycles at this ductility level was small. Spalling of the cover concrete was observed indicating the initiation of the local failure mechanism. At this level, repair to the slightly damaged cover concrete is necessary.

Continued spalling of the cover concrete over the entire plastic hinge region defines Level IV, which occurred at ductility 3. The damage is illustrated in the fourth photograph on the following page. Plastic hinging initiated at the bottom of the column and propagated up from the footing. Since the structural integrity of the section is fairly stable, repair of the damage in the column to maintain serviceability is feasible.

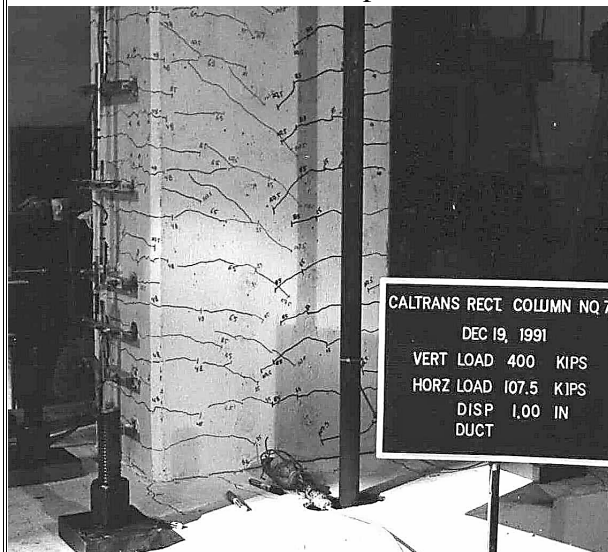
During the first cycle at ductility 4, which correlates to Level V and is shown in the final photograph, buckling of the longitudinal reinforcement occurred over a 635mm (25 inch) region extending from the top of the footing. During continued cycling, the longitudinal bar buckling caused the light transverse reinforcement ties to start opening up at the 90-degree corner laps. The lateral stiffness dramatically decreased and the capacity of the column dropped significantly. At this level, repair of the column is no longer recommended and complete replacement of the component is necessary.



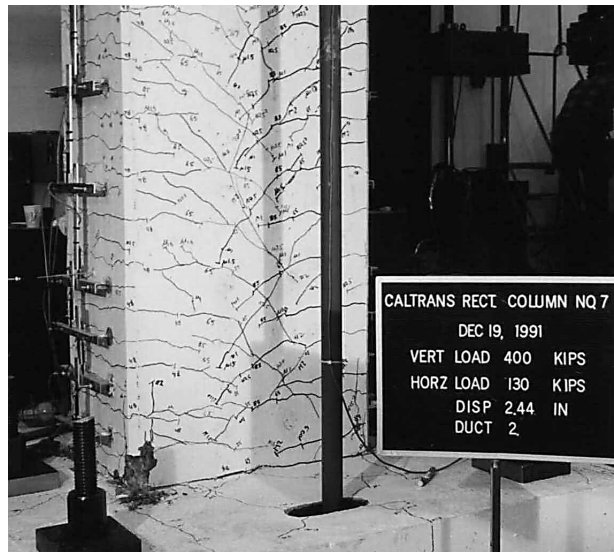
Test Setup



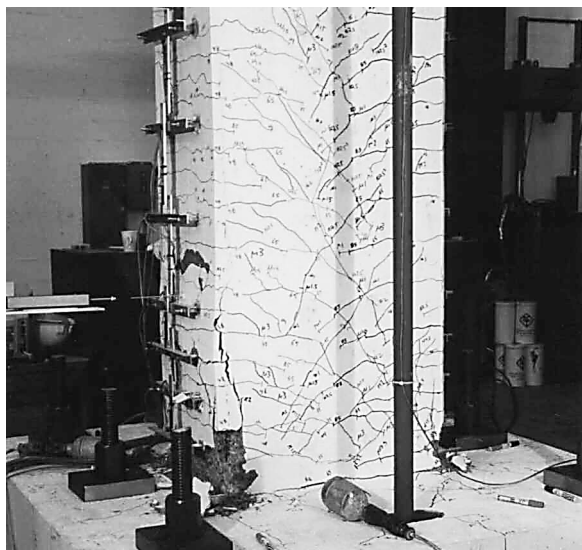
Level I



Level II



Level III



Level IV



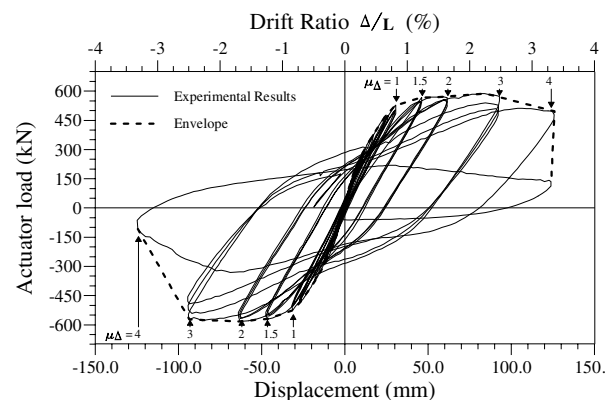
Level V

### Bridge Performance Assessment:

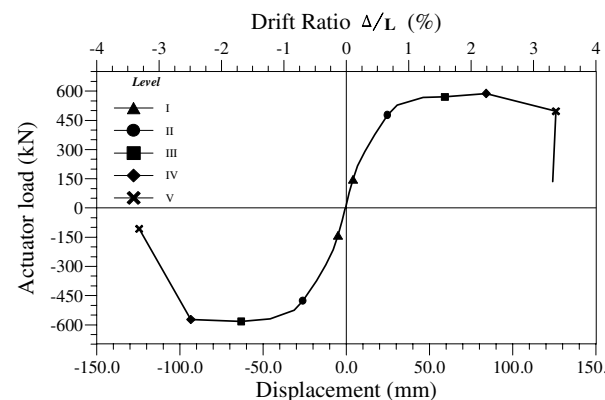
The cyclic force vs. displacement hysteresis for R-5 is shown below. An envelope profile of the response and the displacement ductility levels are also plotted. The ideal yield displacement for the column was approximately 31mm (1.22 inches) and the force was 480 kN (108 kips). Failure of the column consisted of buckling of the longitudinal reinforcement, which was due to the low transverse reinforcement ratio. At Level V of the PBEE capacity assessment methodology, the displacement was 126mm (4.96 inches) corresponding to a 3.4% drift, and the lateral force in the push and pull directions were 496 kN (111.5 kips) and 108 kN (24.3 kips), respectively.

In the second figure below, the force vs. displacement envelope with symbols representing the associated five damage levels is given. A change in stiffness is observed at Level I, while peak response occurred at Level III. The quantitative assessment of R-5 using the previously defined performance/design parameters is summarized in the two tables below. Values were determined from both experimental and analytical results. However, drift, displacement ductility, RDI and the equivalent viscous damping ratio parameters were based purely on experimental data. Since the principal stress state parameter does not apply to columns, it was therefore not calculated. The equivalent viscous damping ratio varied between 3.5% and 25% and the effective stiffness varied between 2.14 and 0.16, which is typical for reinforced concrete sections.

Force-Displacement Hysteresis/Envelope:



Force-Displacement Envelope/Symbols:



Bridge Performance/Design Parameters:

Level	$\epsilon_s$	$\epsilon_c$	$\mu_o$	$\theta_p$	$p_c, p_t$
I	$< \epsilon_y$	$< 0.002^*$	$< 1$	--	--
II	0.002	$< 0.002^*$	$< 1$	--	--
III	0.006*	0.003*	2.5	0.0075	--
IV	0.006*	0.004*	3.5	0.014	--
V	0.012*	0.008*	6	0.026	--
Level	% Drift	$\mu_\Delta$	RDI	$\xi_{eq}$	$n_k$
I	$< 1$	$< V_y$	0.05	3.5%	2.14
II	$< 1$	$< V_y$	0.10	6.5%	1.22
III	1.6	2	0.90	17%	0.61
IV	2.25	3	1.70	22%	0.43
V	3.4	4	2.70	25%	0.16

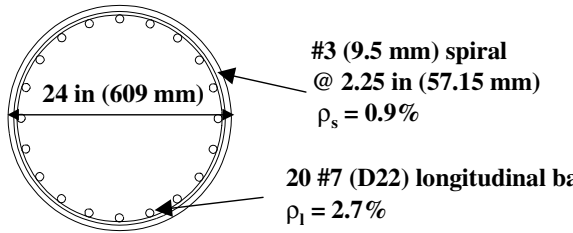
## Performance Parameter Assessment of Bridge Components/Structures

### **Background Information:**

P.I.: Name Phone Email	Frieder Seible (858) 534-4640 seible@ucsd.edu	Institution Address	University of California, San Diego Department of Structural Engineering 9500 Gilman Drive, Mail Code 0085 La Jolla, CA 92093-0085
Co- Name P.I.: Phone Email	Yael D. Hose (858) 534-5529 yhose@ucsd.edu	Institution Address	University of California, San Diego Department of Structural Engineering 9500 Gilman Drive, Mail Code 0085 La Jolla, CA 92093-0085
Assessment Area	1	1. Component	2. Sub-Assemblage 3. System
Assessment Classification	N	N. New	R. Retrofit
Reference	Hose, Y.D., Seible, F., and Priestley, M.J.N., 1997, Strategic Relocation of Plastic Hinges in Bridge Columns, <i>Structural Systems Research Project, 97/05</i> , University of California, San Diego, La Jolla, September.		
Sponsoring Agency	California Department of Transportation		

### **Test Unit Information:**

Test Unit Designation	Strategic Relocation of the Plastic Hinge Reference Column, <i>SRPH-1</i>
Test Unit Description	<p>The column evaluated in this section is part of an experimental program conducted to study the effects of relocating the plastic hinge away from rigid supporting members. Using a conventional design, where the plastic hinge forms at the column/footing interface, the reference column <i>SRPH-1</i> was based on a circular prototype similar to a full-scale bridge column that was previously tested at UCSD. To obtain the model reference column, the prototype was scaled to 40% resulting in a 0.6m (24-inch) column diameter with a longitudinal reinforcement ratio of 2.7% consisting of 20 D22 (#7) bars. The transverse reinforcement ratio of 0.9% was chosen based on the Mander Model energy balance approach, such that the confined column could reach a displacement ductility level of 4. This 0.9% transverse reinforcement ratio corresponds to a 9.5mm (#3) spiral spaced at a 57mm (2.25 inches) pitch. The cover, taken from the outside diameter to just inside the transverse spiral, consisted of 25mm (1-inch).</p> <p>The column cross section for <i>SRPH -1</i> depicting the reinforcement details is presented in the figure on the following page, and the material properties are also reported. Since the Grade 60 transverse reinforcement was prefabricated into a spiral, the material properties obtained from a standard coupon tensile test were unreliable, and only nominal values are reported. A figure of the test setup for <i>SRPH-1</i>, which includes elevation details and instrumentation, is shown in the following pages. The overall height to centerline of load application for this column was 3.66m (144 inches). The column was tested in single bending in the Charles Lee Powell Structures Laboratory at UCSD with a 1780 kN (400 kip) applied axial load.</p>

<b>Reinforcement Details:</b> 		<b>Material Properties:</b> <b>Longitudinal Steel:</b> $f_y = 455 \text{ MPa [66 ksi]}$ $f_u = 745 \text{ MPa [108 ksi]}$ <b>Transverse Steel:</b> $f_y = 414 \text{ MPa [60 ksi]}$ $f_u = 683 \text{ MPa [99 ksi]}$ <b>Concrete:</b> $f'_c = 41.1 \text{ MPa [6.01 ksi]}$
<b>Axial Load Ratio:</b>	14.7%	

### **Bridge Damage Assessment:**

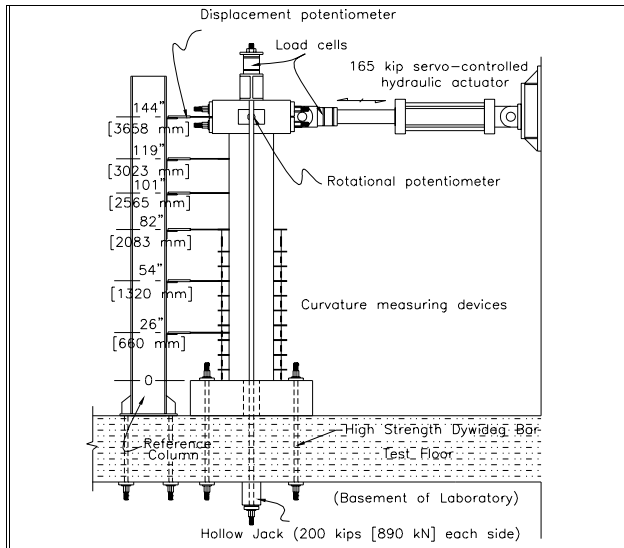
The first photograph on the following page depicts the damage observed in *SRPH-1* at what is considered Performance Level I (CRACKING) in the PBEE methodology. Barely visible horizontal cracks occurring up the height of the column which close upon unloading are depicted in the photograph, which characterizes this limit state. No repair is necessary.

Significant cracking was observed in both the column and footing of this test unit at ductility 1.5 shown in the second photograph on the following page. At this stage of loading, strain profiles of the longitudinal reinforcement in the column indicate that yielding was occurring. The extent of this damage correlates to Performance Level II, YIELDING, of the PBEE methodology. Cracks continue to propagate, and extend further up the column. No other damage is visible, and repair would most likely be unnecessary. During the third cycle at this ductility level, vertical splitting was observed on both sides of the column indicating the initiation of crushing of the cover concrete in the compression toe region.

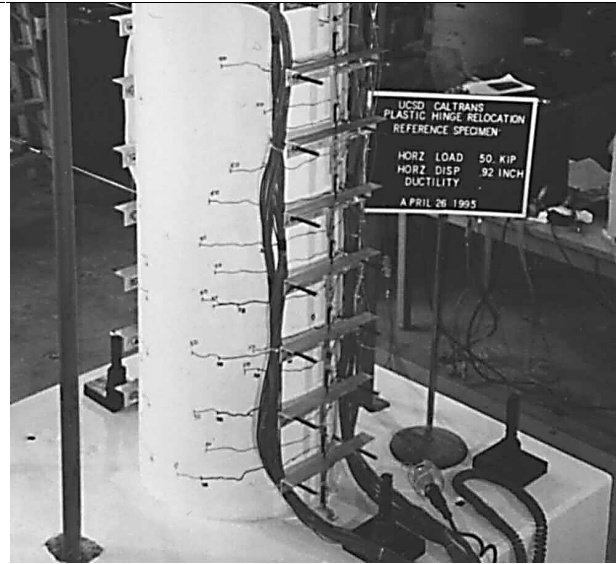
In the first cycle at ductility 2 the column reached the third level of the PBEE methodology, INITIATION OF LOCAL MECHANISM. The onset of spalling of the cover concrete was observed indicating the initiation of the local plastic hinge mechanism. The third photograph shows *SRPH-1* after the third cycle at ductility 2, where spalling of the cover concrete has propagated to a height of 330mm (13 inches) from the base of the column. At this level, the column is structurally sound, but repair to the damaged cover concrete is necessary.

The FULL DEVELOPMENT OF LOCAL MECHANISM of Performance Level IV is shown for *SRPH-1* in the fourth photograph. At this performance level, spalling propagated over the entire plastic hinge mechanism, which is typically over a height of one column diameter. In this column, the spalled region extended up to 762mm (30 inches) above the footing. Inclination of the flexural cracks was also observed. Despite the extensive damage, the column remains structurally sound and can still be repaired.

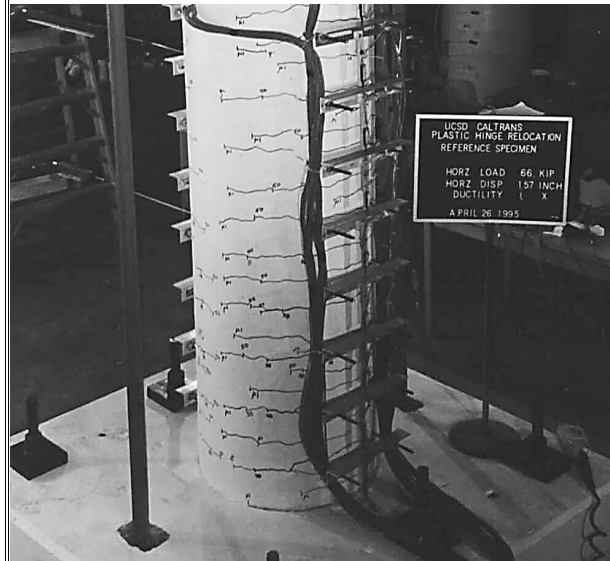
The condition of *SRPH-1* at Performance Level V, STRENGTH DEGRADATION, of the PBEE methodology is shown in the final photograph. During cycling at ductility 8, concrete poured out of the core and buckling of the longitudinal reinforcement occurred in the compression toe region causing spiral fracture. Upon loading in the third cycle, the capacity of the column dropped significantly when several longitudinal bars on the tension side of the column ruptured. At this level, repair of the column is no longer a viable option, and complete replacement of the component is necessary.



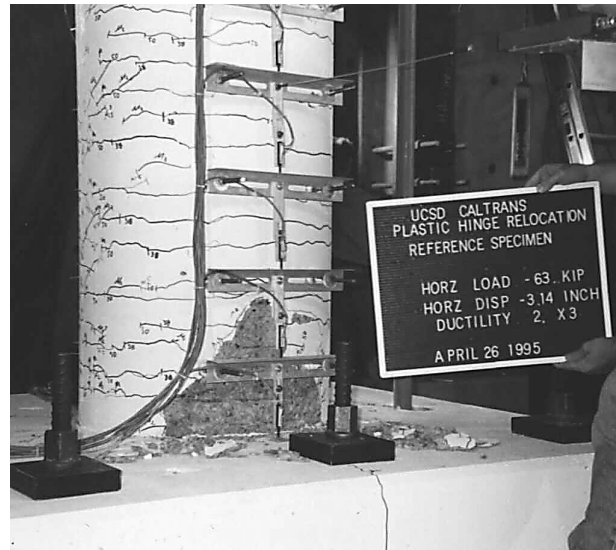
Test Setup



Level I



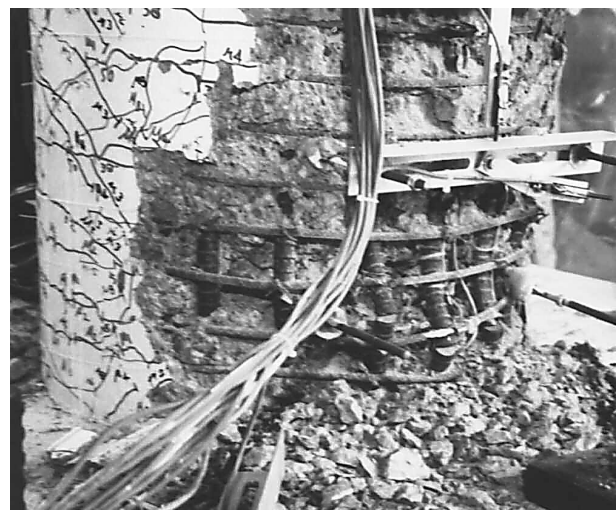
Level II



Level III



Level IV



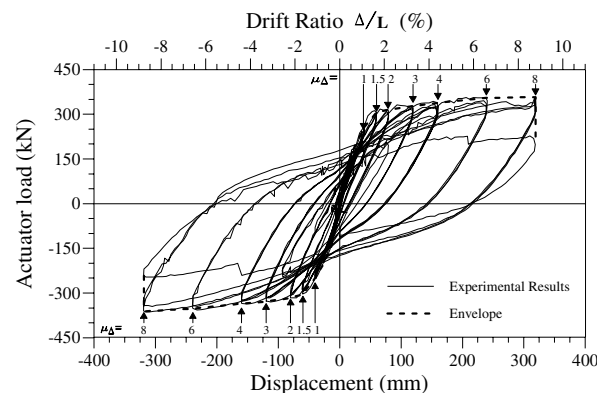
Level V

### Bridge Performance Assessment:

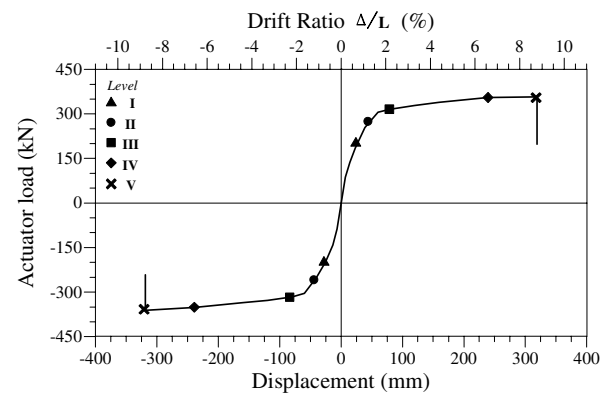
The cyclic force vs. displacement response for *SRPH-1* is shown in the first figure below. An envelope profile of the response and displacement ductility levels is also plotted. The ideal yield displacement for the column was approximately 39.9mm (1.57 inches) corresponding to a 1.1% drift, and the force was 289 kN (65 kips). Failure of the column occurred due to low cycle fatigue of the longitudinal reinforcement in the third cycle of ductility 8. At this Performance Level V, the displacement was at 318mm (12.5 inches) which is an 8.7% drift, and the force was 334 kN (75 kips). In the second figure below, the envelope force vs. displacement profile is given with symbols indicating the locations when the column reached the five damage and performance levels.

The quantification of *SRPH-1* using the PBEE Capacity Assessment parameters is summarized in the tables below. Based on experimental curvatures, the steel and concrete strains were extracted from a simple moment-curvature assessment. These values were in agreement with the values obtained from experimental strain gauges. Since moment-curvature analyses are based on conservative predictions of the ultimate concrete strain, strain values for this *SRPH-1* at final stages of loading were extrapolated. Displacement ductility, drift, and curvature ductility parameters were also taken as a combination of experimental and analytical results, while the RDI, equivalent viscous damping, and effective stiffness parameters were based purely on experimental data. The principal stress state parameter does not apply for these typical components and was therefore not calculated.

Force-Displacement Hysteresis/Envelope:



Force-Displacement Envelope/Symbols:



Bridge Performance/Design Parameters:

Level	$\epsilon_s$	$\epsilon_c$	$\mu_o$	$\theta_p$	$p_c, p_t$
I	< 0.005	< 0.0032*	< 0.771	--	--
II	0.005	0.0032*	0.771	--	--
III	0.019	0.01*	2.77	0.011	--
IV	0.048*	0.027*	7.0	0.054	--
V	0.063*	0.036*	9.26	0.077	--
Level	% Drift	$\mu_\Delta$	RDI	$\xi_{eq}$	$n_k$
I	<1	< $V_y$	< 0.002	< 5%	1.48
II	1	$V_y$	0.002	5%	1.23
III	3	2	0.217	11.9%	0.62
IV	5	6	3.18	23.5%	0.23
V	8.7	8	5.0	12.5%	0.17

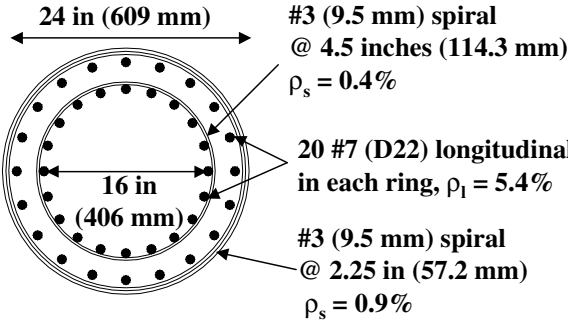
## Performance Parameter Assessment of Bridge Components/Structures

### **Background Information:**

P.I.: Name Phone Email	Frieder Seible (858) 534-4640 seible@ucsd.edu	Institution Address	University of California, San Diego Department of Structural Engineering 9500 Gilman Drive, Mail Code 0085 La Jolla, CA 92093-0085
Co- Name P.I.: Phone Email	Yael D. Hose (858) 534-5529 yhose@ucsd.edu	Institution Address	University of California, San Diego Department of Structural Engineering 9500 Gilman Drive, Mail Code 0085 La Jolla, CA 92093-0085
Assessment Area	1	1. Component	2. Sub-Assemblage 3. System
Assessment Classification	N	N. New	R. Retrofit
Reference	Hose, Y.D., Seible, F., and Priestley, M.J.N., 1997, Strategic Relocation of Plastic Hinges in Bridge Columns, <i>Structural Systems Research Project, 97/05</i> , University of California, San Diego, La Jolla, September.		
Sponsoring Agency	California Department of Transportation		

### **Test Unit Information:**

Test Unit Designation	Strategic Relocation of the Plastic Hinge: Uniform Termination, <i>SRPH-2</i>
Test Unit Description	<p>This column is part of an experimental program conducted to study the effects of relocating the plastic hinge away from rigid supporting members. The method used in this study to relocate the plastic hinge consisted of providing an additional inner concentric reinforcing cage at the column end region. This additional cage was introduced to increase the moment capacity of the column at the column/footing interface, thus forcing the hinge to occur at a weaker section away from the base. The cage originated in the footing and terminated at the desired height of relocation of the hinge. The inner cage bars were terminated in a uniform fashion at 457mm (18 inches) above the footing.</p> <p>The transverse reinforcement ratio of 0.9% was chosen based on the Mander Model energy balance approach, such that the confined column could reach a displacement ductility level of 4. This 0.9% transverse reinforcement ratio corresponds to a 9.5mm (#3) spiral spaced at a 57mm (2.25 inches) pitch. The cover, taken from the outside diameter to just inside the transverse spiral, consisted of 25mm (1-inch).</p> <p>The reinforcement layout is shown for a cross section taken at the base of this column where a double reinforcing cage existed (2 rings of 20 D22 (#7) longitudinal bars). The elevation of <i>SRPH-2</i> is depicted in the test setup figure in the following pages. The height to centerline of the load application for this column was 3.66m (144 inches), and the axial load in the column was 1780 kN (400 kip).</p>

<b>Reinforcement Details:</b> 		<b>Material Properties:</b> <b>Longitudinal Steel:</b> $f_y = 455 \text{ MPa [66 ksi]}$ $f_u = 745 \text{ MPa [108 ksi]}$ <b>Transverse Steel:</b> $f_y = 414 \text{ MPa [60 ksi]}$ $f_u = \text{NA}$ <b>Concrete:</b> $f'_c = 33.7 \text{ MPa [4.89 ksi]}$
<b>Axial Load Ratio:</b>	18%	

### ***Bridge Damage Assessment:***

The damage observed in column *SRPH-2* at each of the five performance levels is depicted in the photographs on the following page.

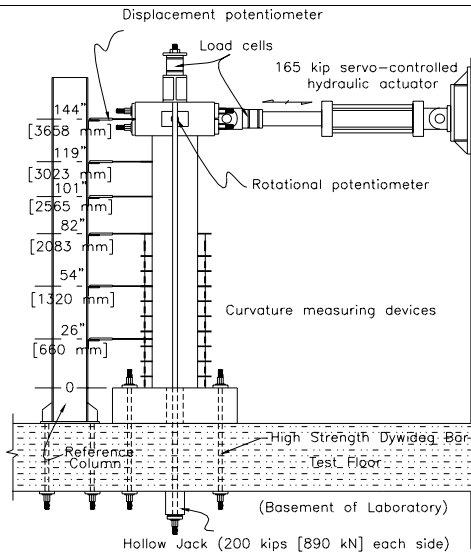
**Performance Level I:** During hookup of the actuator, it pulled with a load of 60 kips and no axial load. This caused cracking up the entire height of the column and softening of the column in the pull direction. During testing, this level was difficult to assess because of the pretest error, however, horizontal flexural cracks that are visible up the height of the column initiated at approximately half the yield force level in the push direction. The damage at this level is shown in the first photograph. The cracks close upon unloading, so no repair is necessary.

**Performance Level II:** Significant cracking was observed in the column at this level, which corresponds to yield. This is shown in the second photograph on the following page. The extent of this damage correlates to Performance Level II, YIELDING, of the PBEE methodology. Cracks continue to propagate, and extend further up the column. No other damage is visible, and repair would most likely be unnecessary.

**Performance Level III:** In the first cycle at ductility 1.5 the column reached the third level of the PBEE methodology, INITIATION OF LOCAL MECHANISM. The onset of spalling of the cover concrete was observed indicating the initiation of the local plastic hinge mechanism, shown in the third photograph. At this level, the column is structurally sound, but repair to the damaged cover concrete is necessary.

**Performance Level IV:** The FULL DEVELOPMENT OF LOCAL MECHANISM of this performance level is shown for *SRPH-2* in the fourth photograph. Spalling propagated over the entire plastic hinge mechanism, which is typically over a height of one column diameter. In this column, the spalled region extended up to 1194mm (47 inches) above the footing. Inclination of the flexural cracks was also observed. Despite the extensive damage, the column remains structurally sound and can still be repaired.

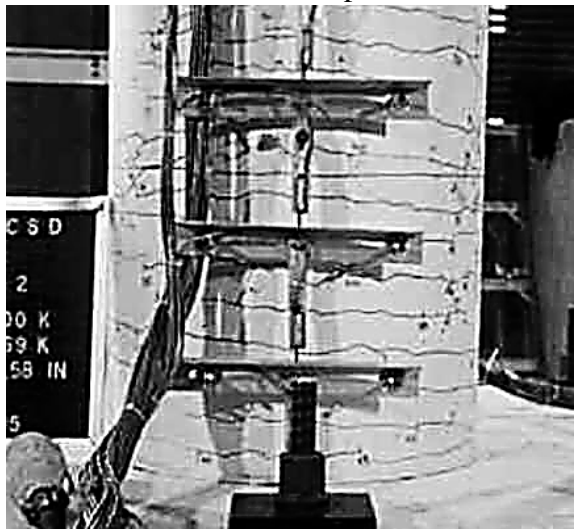
**Performance Level V:** The condition of *SRPH-2* at this performance level is shown in the final photograph. During cycling at ductility 4.5, concrete poured out of the core and buckling of the longitudinal reinforcement occurred in the compression toe region at approximately 432mm (17 inches) above the footing causing spiral fracture. Upon loading in the third cycle, the capacity of the column dropped significantly when several longitudinal bars on the tension side of the column ruptured. At this level, repair of the column is no longer a viable option, and complete replacement of the component is necessary.



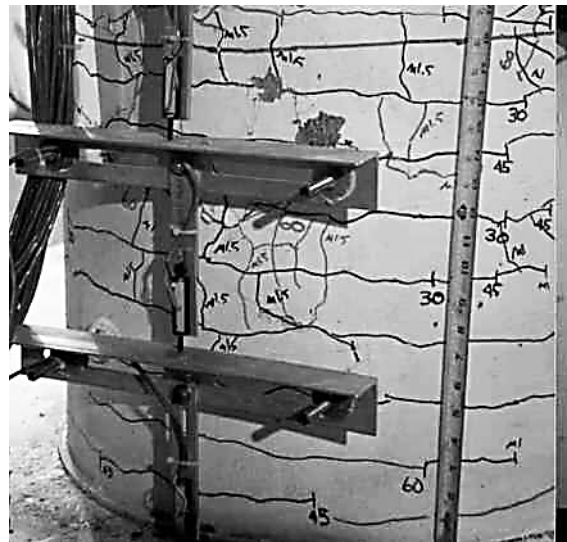
Test Setup



Level I



Level II



Level III



Level IV

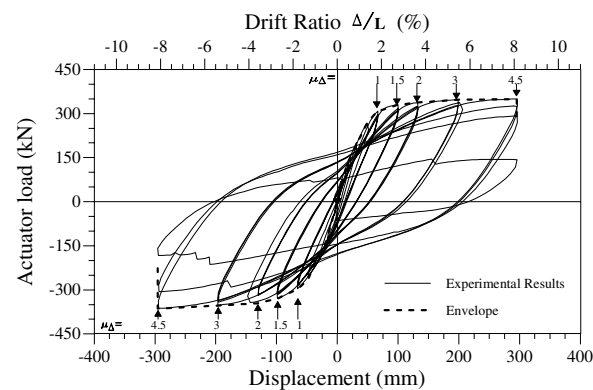


Level V

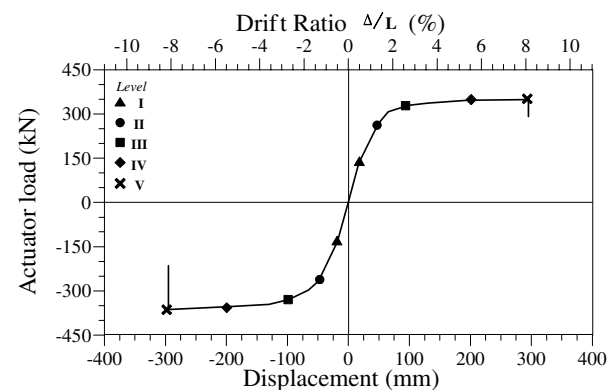
### Bridge Performance Assessment:

The cyclic force vs. displacement response for *SRPH-2* is shown in the first figure below. An envelope profile of the response and displacement ductility levels is also plotted. The ideal yield displacement for the column was approximately 65mm (2.57 inches) corresponding to a 1.8% drift, and the force was 303 kN (68 kips). Failure of the column occurred due to buckling of the longitudinal at ductility 4.5. At this Performance Level V, the displacement was at 295mm (11.6 inches) which is an 8.1% drift, and the force was 356 kN (80 kips). In the second figure below, the envelope force vs. displacement profile is given with symbols indicating the locations when the column reached the five damage/performance levels. The parameters for *SRPH-2* are summarized in the tables below. Based on experimental curvatures, the steel and concrete strains were extracted from a moment-curvature assessment. These values agreed with initial values obtained from experimental strain gauges. Despite the use of the relocation design concept for this *SRPH-2*, the observed behavior resembles that of the reference column, *SRPH-1*. However, *SRPH-2* successfully relocated the plastic hinge region one column diameter away from the footing. Values of other parameters at each level for column *SRPH-2* are consistent with results from other flexural tests.

Force-Displacement Hysteresis/Envelope:



Force-Displacement Envelope/Symbols:



Bridge Performance/Design Parameters:

Level	$\epsilon_s$	$\epsilon_c$	$\mu_\phi$	$\theta_p$	$p_c, p_t$
I	< 0.001	< 0.0001*	< 0.5	--	--
II	0.005	0.0025*	0.72	--	--
III	0.01	0.0055*	1.6	0.010	--
IV	0.029*	0.015*	4.15	0.041	--
V	0.055*	0.028*	7.8	0.072	--
Level	% Drift	$\mu_\Delta$	RDI	$\xi_{eq}$	$n_k$
I	< 0.5	$V_y/2$	< 0.1	< 7%	1.72
II	1.3	$V_y$	0.184	7%	1.2
III	2.7	1.5	0.46	13%	0.72
IV	5.3	3	1.65	19.6%	0.38
V	8.1	4.5	3.1	22.1%	0.26

## Performance Parameter Assessment of Bridge Components/Structures

### **Background Information:**

P.I.: Name Phone Email	Frieder Seible (858) 534-4640 seible@ucsd.edu	Institution Address	University of California, San Diego Department of Structural Engineering 9500 Gilman Drive, Mail Code 0085 La Jolla, CA 92093-0085
Co- Name P.I.: Phone Email	Yael D. Hose (858) 534-5529 yhose@ucsd.edu	Institution Address	University of California, San Diego Department of Structural Engineering 9500 Gilman Drive, Mail Code 0085 La Jolla, CA 92093-0085
Assessment Area	1	1. Component	2. Sub-Assemblage 3. System
Assessment Classification	N	N. New	R. Retrofit
Reference	Hose, Y.D., Seible, F., and Priestley, M.J.N., 1997, Strategic Relocation of Plastic Hinges in Bridge Columns, <i>Structural Systems Research Project, 97/05</i> , University of California, San Diego, La Jolla, September.		
Sponsoring Agency	California Department of Transportation		

### **Test Unit Information:**

Test Unit Designation	Strategic Relocation of the Plastic Hinge: Staggered Termination with $\rho_s=0.9\%$ , <i>SRPH-3</i>
Test Unit Description	<p>This column is part of an experimental program conducted to study the effects of relocating the plastic hinge away from rigid supporting members. The method used in this study to relocate the plastic hinge consisted of providing an additional inner concentric reinforcing cage at the column end region. This additional cage was introduced to increase the moment capacity of the column at the column/footing interface, thus forcing the hinge to occur at a weaker section away from the base. The cage originated in the footing and terminated at the desired height of relocation of the hinge. The inner cage bars were terminated in a uniform fashion at 457mm (18 inches) above the footing.</p> <p>The transverse reinforcement ratio of 0.9% was chosen based on the Mander Model energy balance approach, such that the confined column could reach a displacement ductility level of 4. This 0.9% transverse reinforcement ratio corresponds to a 9.5mm (#3) spiral spaced at a 57mm (2.25 inches) pitch. The cover, taken from the outside diameter to just inside the transverse spiral, consisted of 25mm (1-inch).</p> <p>The reinforcement layout is shown for a cross section taken at the base of this column where a double reinforcing cage existed (2 rings of 20 D22 (#7) longitudinal bars). The elevation of <i>SRPH-2</i> is depicted in the test setup figure in the following pages. The height to centerline of the load application for this column was 3.66m (144 inches), and the axial load in the column was 1780 kN (400 kip).</p>

<p><b>Reinforcement Details:</b></p> <p>24 in (609 mm) → #3 (9.5 mm) spiral @ 4.5 inches (114.3 mm) <math>\rho_s = 0.4\%</math></p> <p>← 16 in (406 mm) ← 20 #7 (D22) longitudinal in each ring, <math>\rho_1 = 5.4\%</math></p> <p>#3 (9.5 mm) spiral @ 2.25 in (57.2 mm) <math>\rho_s = 0.9\%</math></p>	<p><b>Material Properties:</b></p> <p>Longitudinal Steel:  <math>f_y = 455 \text{ MPa [66 ksi]}</math>  <math>f_u = 745 \text{ MPa [108 ksi]}</math></p> <p>Transverse Steel:  <math>f_y = 414 \text{ MPa [60 ksi]}</math>  <math>f_u = \text{NA}</math></p> <p>Concrete:  <math>f'_c = 33.7 \text{ MPa [4.89 ksi]}</math></p>
<p><b>Axial Load Ratio:</b></p>	<p>16.5%</p>

***Bridge Damage Assessment:***

The damage observed in column *SRPH-3* at each of the five performance levels is depicted in the photographs on the following page.

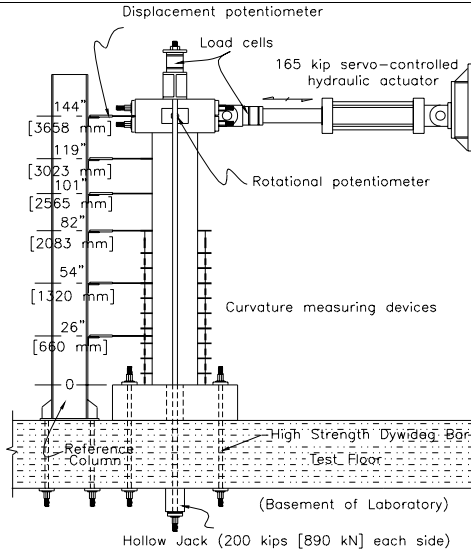
Performance Level I: This performance level occurred at approximately half the yield force level with the observation of horizontal flexural cracks that are visible up the height of the column. The damage at this level is shown in the first photograph. The cracks close upon unloading, so no repair is necessary.

Performance Level II: Significant cracking was observed in the column at this level, which corresponds to yield. This is shown in the second photograph on the following page. The extent of this damage correlates to Performance Level II, YIELDING, of the PBEE methodology. Cracks continue to propagate, and extend further up the column. No other damage is visible, and repair would most likely be unnecessary.

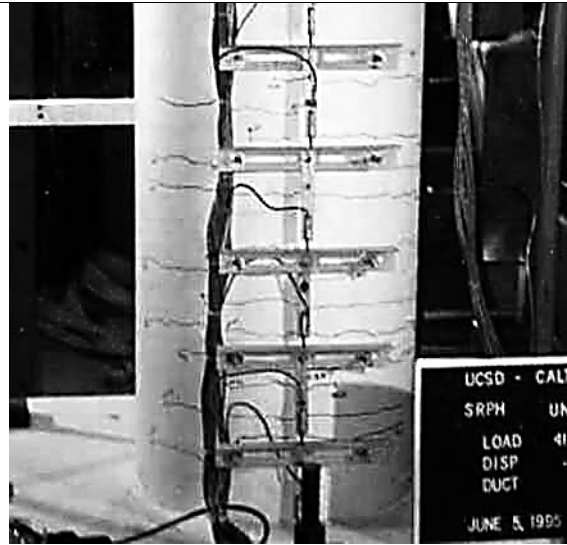
Performance Level III: In the first cycle at ductility 2 in the column, which when calculated based on the ideal yield displacement of the reference column *SRPH-1* was ductility 2.5, the third level of the PBEE methodology was reached. The onset of spalling of the cover concrete was observed indicating the initiation of the local plastic hinge mechanism, shown in the third photograph. Spalling occurred at multiple levels at approximately 178mm (7 inches) and 559mm (22 inches). At this level, the column is structurally sound, but repair to the damaged cover concrete is necessary.

Performance Level IV: The FULL DEVELOPMENT OF LOCAL MECHANISM of this performance level is shown for *SRPH-3* in the fourth photograph. Spalling propagated over the entire plastic hinge mechanism, which is typically over a height of one column diameter. In this column, the spalled region extended from 127mm (5 inches) to 1016mm (40 inches) above the footing. After cycling at this level, the spalled region extended down to the footing. Longitudinal bars were exposed. Despite the extensive damage, the column remains structurally sound and can still be repaired.

Performance Level V: The condition of *SRPH-3* at this performance level is shown in the final photograph. During cycling at ductility 7.3, concrete poured out of the core and buckling of the longitudinal reinforcement occurred in the compression toe region at approximately 483mm (19 inches) above the footing causing spiral fracture. Upon loading in the third cycle, the capacity of the column dropped significantly when several longitudinal bars on the tension side of the column ruptured. At this level, repair of the column is no longer a viable option, and complete replacement of the component is necessary.



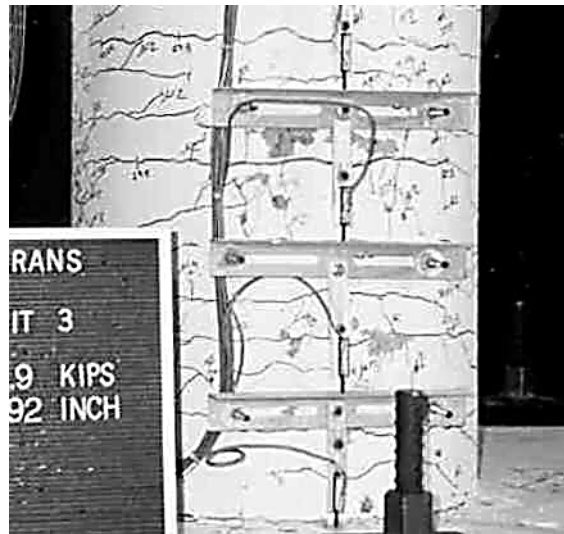
Test Setup



Level I



Level II



Level III



Level IV

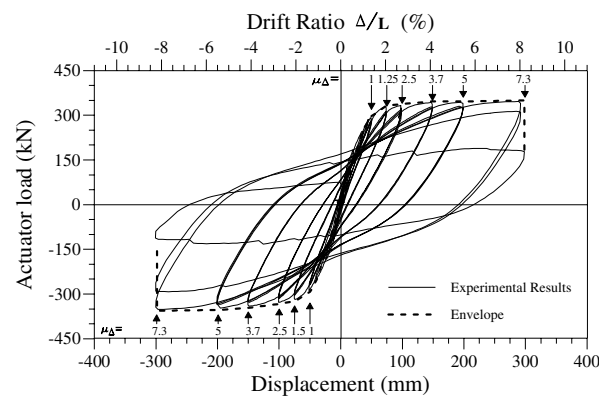


Level V

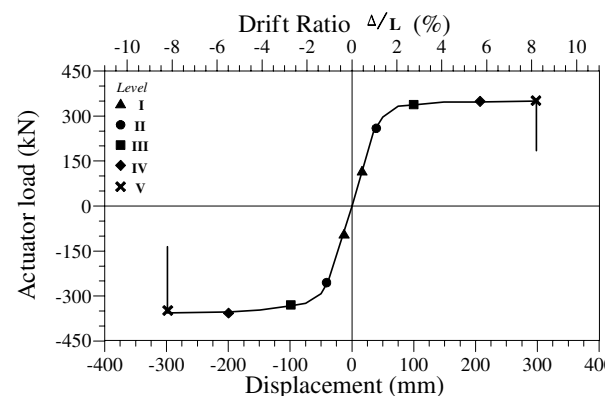
### Bridge Performance Assessment:

The cyclic force vs. displacement response for *SRPH-3* is shown in the first figure below. An envelope profile of the response and displacement ductility levels is also plotted. The ideal yield displacement for the column was approximately 50 mm (1.96 inches) corresponding to a 1.4% drift, and the force was 294 kN (66 kips). Failure of the column occurred due to buckling of the longitudinal at ductility 7.3, which is calculated based on the ideal yield displacement of the reference column *SRPH-1*. At this Performance Level V, the displacement was at 298mm (11.75 inches) which is an 8.2% drift, and the force was 349 kN (78.5 kips). In the second figure below, the envelope force vs. displacement profile is given with symbols indicating the locations when the column reached the five damage/performance levels. The observed behavior resembles that of the reference column, *SRPH-1* despite the use of the relocation design concept for this column. *SRPH-3* successfully relocated the plastic hinge region and had an elongated plastic hinge region due to the staggered termination of the inner reinforcement. The parameters for *SRPH-3* are summarized in the tables below. The values are very similar to those obtained in both the reference column, *SRPH-1* and the column employing a uniform inner cage bar termination, *SRPH-2*.

Force-Displacement Hysteresis/Envelope:



Force-Displacement Envelope/Symbols:



Bridge Performance/Design Parameters:

Level	$\epsilon_s$	$\epsilon_c$	$\mu_o$	$\theta_p$	$p_c, p_t$
I	< 0.001	< 0.0005*	< 0.5	--	--
II	0.0027	0.0014*	0.69	--	--
III	0.012	0.006*	3.1	0.015	--
IV	0.02*	0.010*	5.8	0.046	--
V	0.035*	0.016*	9.23	0.076	--
Level	% Drift	$\mu_\Delta$	RDI	$\xi_{eq}$	$n_k$
I	< 0.5	$V_y/2$	< 0.05	< 5%	1.85
II	1.0	$V_y$	0.064	6.2%	1.12
III	2.7	2.5	0.52	12.6%	0.55
IV	5.4	5	2.14	21%	0.295
V	8	7.3	3.82	26%	0.2

## Performance Parameter Assessment of Bridge Components/Structures

### **Background Information:**

P.I.: Name Phone Email	Frieder Seible (858) 534-4640 seible@ucsd.edu	Institution Address	University of California, San Diego Department of Structural Engineering 9500 Gilman Drive, Mail Code 0085 La Jolla, CA 92093-0085
Co- Name P.I.: Phone Email	Yael D. Hose (858) 534-5529 yhose@ucsd.edu	Institution Address	University of California, San Diego Department of Structural Engineering 9500 Gilman Drive, Mail Code 0085 La Jolla, CA 92093-0085
Assessment Area	1	1. Component	2. Sub-Assemblage 3. System
Assessment Classification	N	N. New	R. Retrofit
Reference	Hose, Y.D., Seible, F., and Priestley, M.J.N., 1997, Strategic Relocation of Plastic Hinges in Bridge Columns, <i>Structural Systems Research Project, 97/05</i> , University of California, San Diego, La Jolla, September.		
Sponsoring Agency	California Department of Transportation		

### **Test Unit Information:**

Test Unit Designation	Strategic Relocation of the Plastic Hinge: Staggered Termination with $\rho_s=2.3\%$ , <i>SRPH-4</i>
Test Unit Description	<p>This column is part of an experimental program conducted to study the effects of relocating the plastic hinge away from rigid supporting members. The method used in this study to relocate the plastic hinge consisted of providing an additional inner concentric reinforcing cage at the column end region. This additional cage was introduced to increase the moment capacity of the column at the column/footing interface, thus forcing the hinge to occur at a weaker section away from the base. The cage originated in the footing and terminated at the desired height of relocation of the hinge. In an attempt to elongate the plastic hinge region, the inner cage bars were terminated in a staggered fashion rather than uniformly. For <i>SRPH-4</i>, the average height of the bar cutoffs was set to 457mm (18 inches) up from the footing. <i>SRPH-4</i> was designed with increased confinement in the plastic hinge region based on a required displacement ductility capacity of 8 resulting in a transverse reinforcement ratio of 2.3%. This 2.3% transverse reinforcement ratio corresponds to a 12.7mm (#4) spiral spaced at a 38.1mm (1.5 inches) pitch. The cover, taken from the outside diameter to just inside the transverse spiral, consisted of 25mm (1-inch). The reinforcement layout is shown for a cross section taken at the base of this column where a double reinforcing cage existed (2 rings of 20 D22 (#7) longitudinal bars). The elevation of <i>SRPH-4</i> is depicted in the test setup figure in the following pages. The height to centerline of the load application for this column was 3.66m (144 inches), and the axial load in the column was 1780 kN (400 kip).</p>

<b>Reinforcement Details:</b> 		<b>Material Properties:</b> <b>Longitudinal Steel:</b> $f_y = 455 \text{ MPa [66 ksi]}$ $f_u = 738 \text{ MPa [107 ksi]}$ <b>Transverse Steel:</b> $f_y = 414 \text{ MPa [60 ksi]}$ $f_u = 621 \text{ MPa [90 ksi]}$ <b>Concrete:</b> $f'_c = 36.3 \text{ MPa [5.26 ksi]}$
<b>Axial Load Ratio:</b>	16.5%	

### ***Bridge Damage Assessment:***

The damage observed in column *SRPH-4* at each of the five performance levels is depicted in the photographs on the following page.

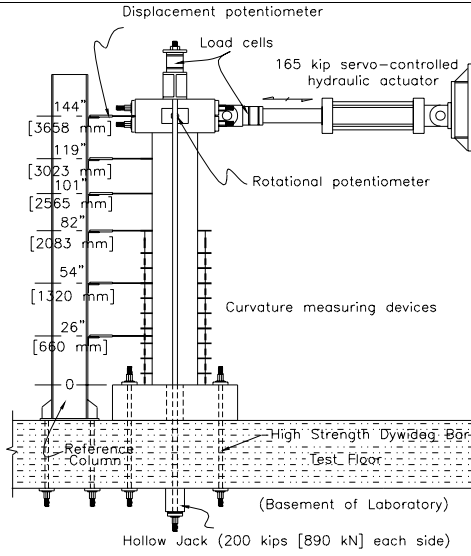
**Performance Level I:** This performance level occurred at approximately half the yield force level with the observation of fine horizontal flexural cracks that are visible up the height of the column. The damage at this level is shown in the first photograph. The cracks close upon unloading, so no repair is necessary.

**Performance Level II:** To verify a cyclic prediction, the test was governed by a predetermined ideal yield displacement, which happened to correspond to the yield level in the column. Therefore, Level II was reached at ideal yield. Significant cracking was observed in the column at this level, which is shown in the second photograph on the following page. Cracks continue to propagate, and extend further up the column. No other damage is visible, and repair would most likely be unnecessary.

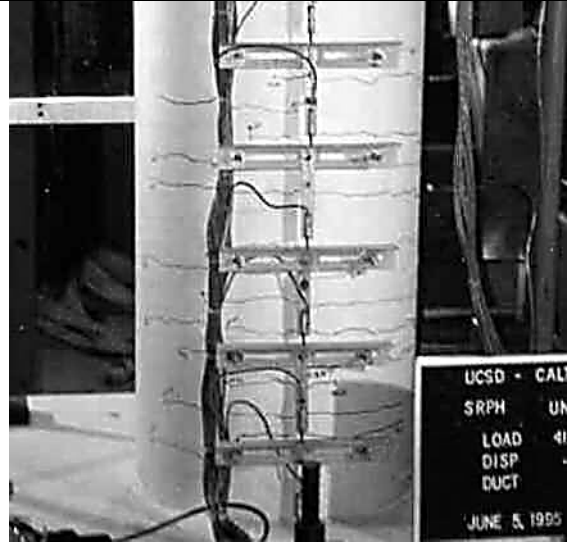
**Performance Level III:** During the final cycle at ductility 2 and the first cycle at ductility 3, the third level of the PBEE methodology was reached. The onset of spalling of the cover concrete was observed indicating the initiation of the local plastic hinge mechanism, shown in the third photograph. The first signs of crushing were seen on the compression face of the column between 381-559mm (15-22 inches). The onset of spalling occurred at approximately 559mm (22 inches). At this level, the column is structurally sound, but repair to the damaged cover concrete is necessary.

**Performance Level IV:** The FULL DEVELOPMENT OF LOCAL MECHANISM of this performance level is shown for *SRPH-4* in the fourth photograph. Spalling propagated over the entire plastic hinge mechanism, extending from the base of the column to approximately 1270mm (50 inches) above the footing. Several longitudinal bars were exposed, but the column core remained completely intact. Despite the extensive damage, the column remains structurally sound and can still be repaired.

**Performance Level V** was never reached because the test was stopped at Level I. The test setup could no longer safely accommodate the extreme column displacement and simultaneous axial load. Overall, the column did not suffer any degradation in strength. The final photograph on the following page depicts the extreme displacement that this column sustained when compared to the steel reference column.



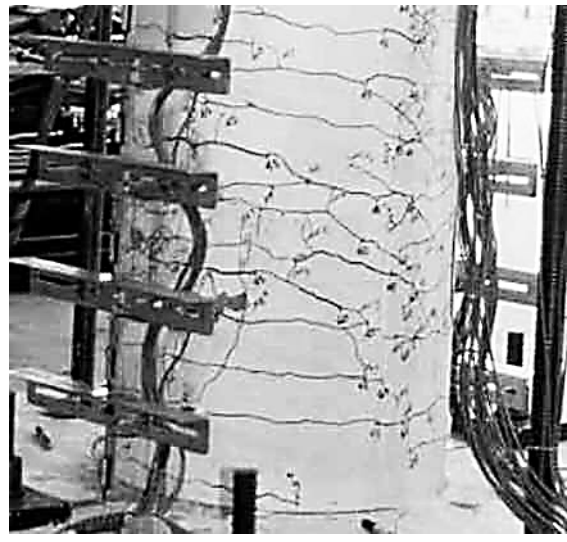
Test Setup



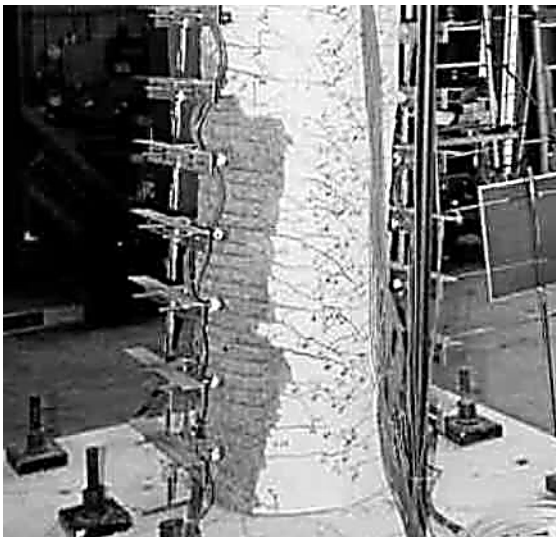
Level I



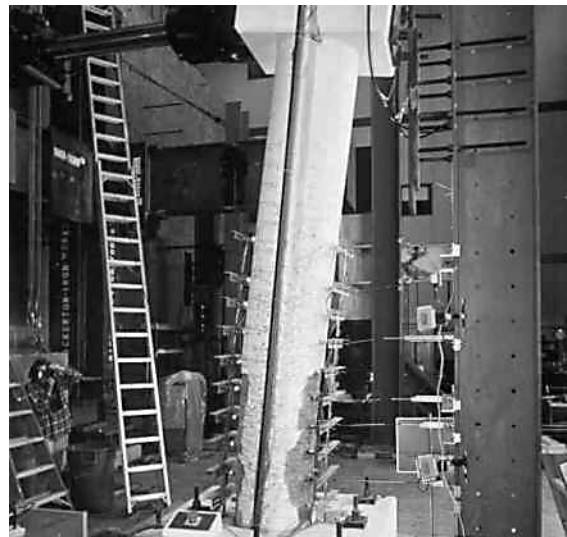
Level II



Level III



Level IV

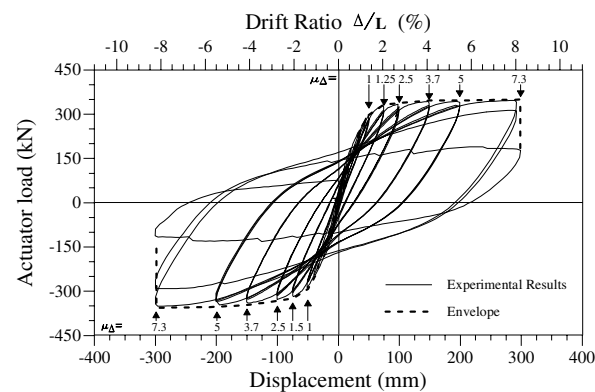


Level IV

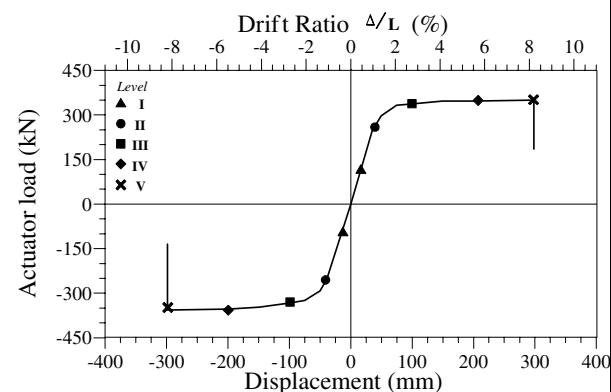
### Bridge Performance Assessment:

The cyclic force vs. displacement response for *SRPH-4* is shown in the first figure below. An envelope profile of the response and displacement ductility levels is also plotted. To verify a cyclic prediction, the test was governed by a predetermined ideal yield displacement of 47.8mm (1.88 inches) corresponding to a 1.3% drift, and the force was 267 kN (60 kips). Testing of the column was stopped at Performance Level IV because the setup could no longer accommodate the extreme column displacement and axial load. The column core was still completely intact. At this level, the displacement was 382 mm (15.05 inches) which is a 10.5% drift, and the force was 400 kN (90 kips). In the second figure below, the envelope force vs. displacement profile is given with symbols of the five damage/performance levels. The observed behavior resembles that of the reference column, *SRPH-1*, despite the use of the relocation design concept for this column. *SRPH-4* successfully relocated the plastic hinge region and had an elongated plastic hinge region due to the staggered termination of the inner reinforcement. The parameters for *SRPH-4* are summarized in the tables below. The values are very similar to those obtained in all previous tests with relocated plastic hinges, as well as the reference column, *SRPH-1*.

Force-Displacement Hysteresis/Envelope:



Force-Displacement Envelope/Symbols:



Bridge Performance/Design Parameters:

Level	$\epsilon_s$	$\epsilon_c$	$\mu_o$	$\theta_p$	$p_c, p_t$
I	< 0.001	< 0.00055*	< 0.5	--	--
II	0.0035	0.002*	1	--	--
III	0.018	0.0095*	5	0.022	--
IV	0.051*	0.028*	14.6	0.104	--
V	--	--	--	--	--
Level	% Drift	$\mu_\Delta$	RDI	$\xi_{eq}$	$n_k$
I	< 0.5	$V_y/2$	< 0.05	< 5%	1.77
II	1.3	$V_y, \mu 1$	0.066	7.1%	1
III	3.25	2.5	0.97	14.4%	0.44
IV	10.5	8	5.4	25.5%	0.18
V	--	--	--	--	--

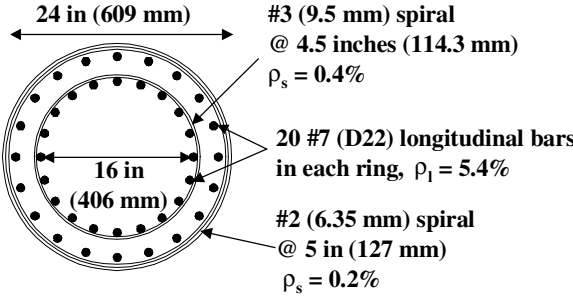
## Performance Parameter Assessment of Bridge Components/Structures

### **Background Information:**

P.I.: Name Phone Email	Frieder Seible (858) 534-4640 seible@ucsd.edu	Institution Address	University of California, San Diego Department of Structural Engineering 9500 Gilman Drive, Mail Code 0085 La Jolla, CA 92093-0085
Co- Name P.I.: Phone Email	Yael D. Hose (858) 534-5529 yhose@ucsd.edu	Institution Address	University of California, San Diego Department of Structural Engineering 9500 Gilman Drive, Mail Code 0085 La Jolla, CA 92093-0085
Assessment Area	1	1. Component	2. Sub-Assemblage 3. System
Assessment Classification	N	N. New	R. Retrofit
Reference	Hose, Y.D., Seible, F. and Priestley, M.J.N., 1997, Strategic Relocation of Plastic Hinges in Bridge Columns, <i>Structural Systems Research Project, 97/05</i> , University of California, San Diego, La Jolla, September.		
Sponsoring Agency	California Department of Transportation		

### **Test Unit Information:**

Test Unit Designation	Strategic Relocation of the Plastic Hinge: Shear Column, <i>SRPH-6</i>
Test Unit Description	<p>This column is part of an experimental program conducted to study the effects of relocating the plastic hinge away from rigid supporting members. To relocate the plastic hinge an additional inner concentric reinforcing cage was provided at the column end region. This additional cage was introduced to increase the moment capacity of the column at the column/footing interface, thus forcing the hinge to occur at a weaker section away from the base. The cage originated in the footing and terminated at the desired height of relocation of the hinge. In an attempt to elongate the plastic hinge region, the inner cage bars were terminated in a staggered fashion rather than uniformly. The average height of the bar cutoffs corresponded to the desired relocation height. For <i>SRPH-6</i>, the average height of the bar cutoffs was set to one column diameter (609mm, 24 inches) up from the footing. The transverse reinforcement was designed based on the UCSD shear model, which predicts the ideal shear strength of a column using a concrete shear-resisting mechanism, transverse reinforcement truss mechanism, and a strength enhancement component resulting from axial compression. <i>SRPH-6</i> was designed for a shear failure at an approximate displacement ductility level of 2. This resulted in a 6.35 mm (#2) spiral spaced at 127mm (5 inches). A 25mm (1-inch) cover was used, as shown in the reinforcement details provided on the following page. The reinforcement layout is shown for a cross section taken at the base of this column where a double reinforcing cage existed. The elevation of <i>SRPH-6</i> is depicted in the test setup figure in the following pages. The height to centerline of the load application for this column was 2.13m (84 inches), and the axial load in the column was 890 kN (200 kips).</p>

<b>Reinforcement Details:</b> 		<b>Material Properties:</b>  <b>Longitudinal Steel:</b> $f_y = 467 \text{ MPa (68 ksi)}$ $f_u = 764 \text{ MPa (111 ksi)}$  <b>Transverse Steel:</b> $f_y = 414 \text{ MPa (60 ksi)}$ $f_u = 662 \text{ MPa (96 ksi)}$  <b>Concrete:</b> $f'_c = 36.3 \text{ MPa (5.26 ksi)}$
<b>Axial Load Ratio:</b>	<b>8.4%</b>	

### **Bridge Damage Assessment:**

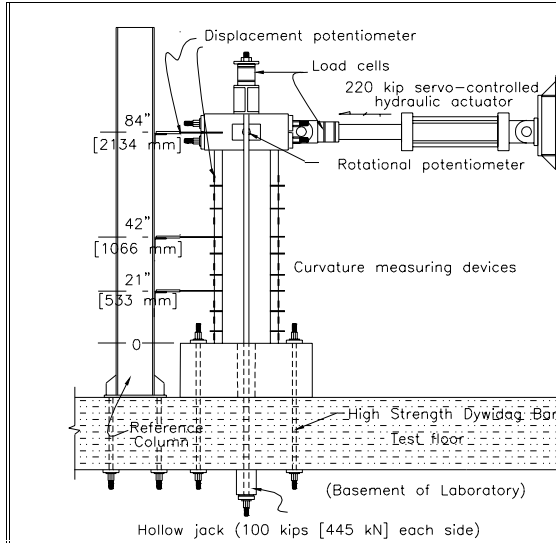
Although the column sustained a brittle shear failure at an early ductility level, the PBEE damage/performance levels are distinctly visible despite being at closer loading intervals. The first photograph on the following page shows the column at Performance Level I. Hairline flexural cracking has initiated at every spiral location, and has already begun to incline due to the light transverse reinforcement. However, upon unloading the cracks close and thus do not require repair.

Performance Level II of the PBEE assessment methodology, YIELDING, is depicted for *SRPH-6* in the second photograph. Flexural cracks that have now propagated up the column show increased inclination, especially in the plastic hinge region, indicating heavy influence of shear behavior. Crack widths, however, remain less than 1mm and repair of the component is possible but not likely.

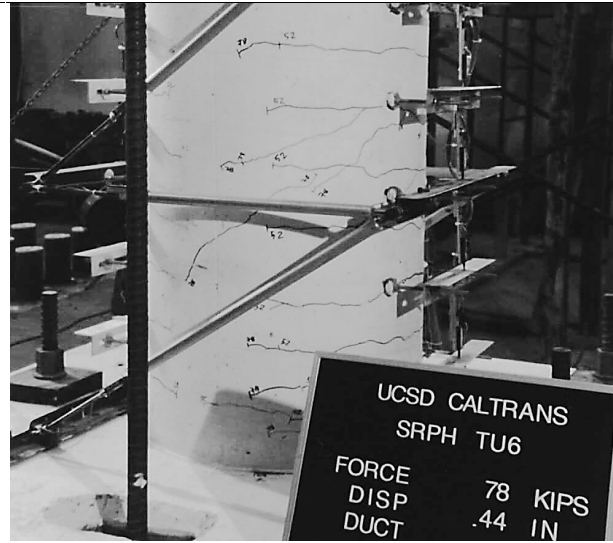
Performance Level III, INITIATION OF LOCAL MECHANISM, is demonstrated in the third photograph, where the shear-sliding failure mechanism has begun to form. This is evident from the extensive diagonal cracking, some as steep as 50 degrees, from top to bottom of the column. The widest cracks on the lateral faces were 2 mm, requiring minimum repair. Bulging of the center of the column was noticeable especially in the relocated plastic hinge region.

The FULL DEVELOPMENT OF LOCAL MECHANISM that categorizes Performance Level IV is apparent in the fourth photograph. Extensive crushing or blowing off of the compression face zone occurred. The extremely wide cracks measuring 8mm propagated along the shear-sliding plane from the plastic hinge all the way to the top of the column. At this level, the strength of the column is still maintained.

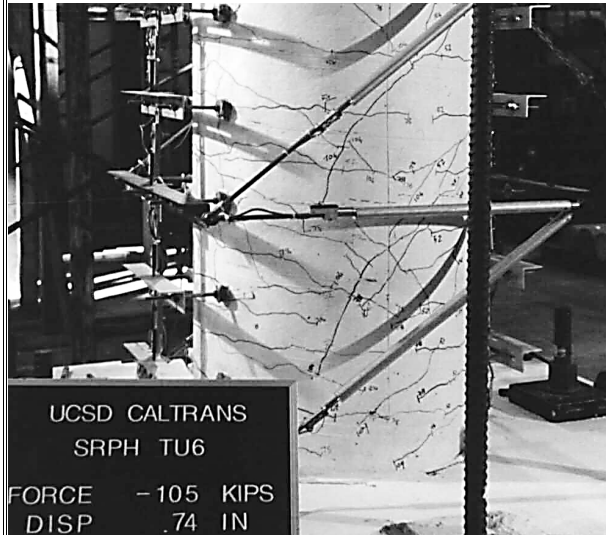
Continued cycling and further loading of the column to ductility 2 causes Performance Level V, STRENGTH DEGRADATION, to be reached as the concrete core is completely obliterated. During the second cycle at this level, the spiral fractured and a complete compression zone failure occurred to complete the test. The final photograph shows the damage of the column at this level, demonstrating that replacement of the component is necessary.



Test Setup



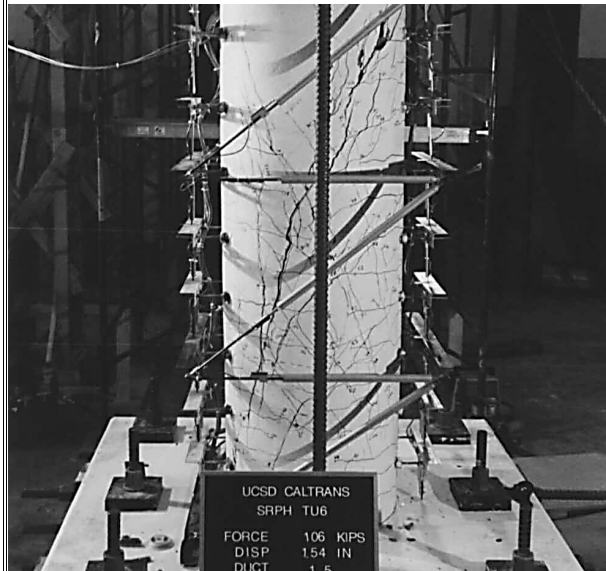
Level I



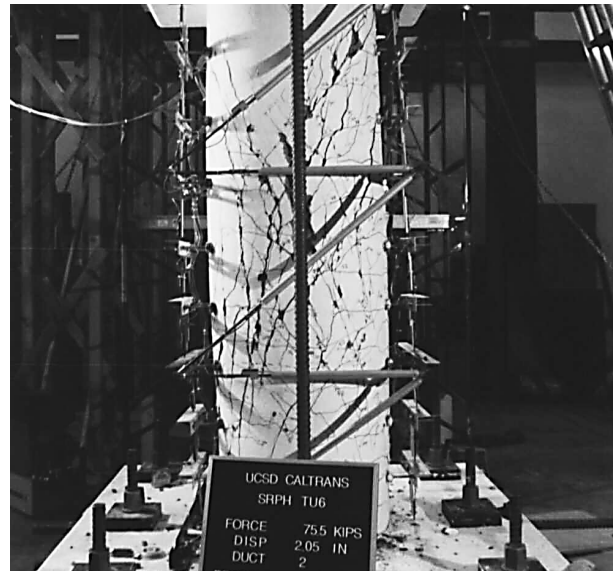
Level II



Level III



Level IV

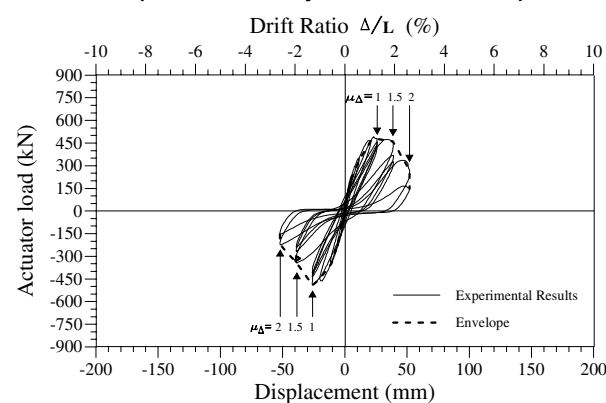


Level V

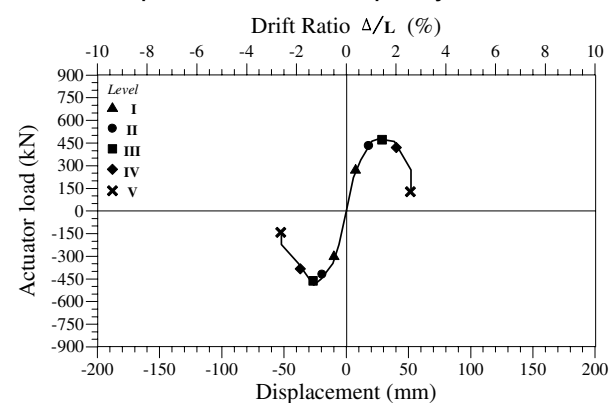
### Bridge Performance Assessment:

The force-displacement response for *SRPH-6*, along with its envelope profile is shown in the first figure below. At ductility 1, the force was 493 kN (110.7 kips) and the displacement was 26mm (1.03 inches). At this load level, a slight dip in the force was observed, indicating imminent shear failure. However, the significant drop in lateral load capacity did not initiate until cycling at ductility 1.5, which corresponds to a force of 472 kN (106.1 kips) and a displacement of 39mm (1.54 inches). Failure of the test unit occurred during the second cycle at ductility 2, where a force of 335 kN (75.3 kips) and a displacement of 52mm (2.05 inches) was registered. The response envelope with symbols depicting the locations where the column reached the five performance levels is given in the second figure below. Despite occurring at closer intervals along the response, all five of the levels were reached. The parameters for *SRPH-6* at each level are also given below. The values for most of the parameters are considerably lower than those observed in flexural columns, because failure of *SRPH-6* occurred at such an early ductility level. RDI values were calculated up to 1.25, which correlate to equivalent viscous damping ratios up to 12.5%. This is nearly half of what is observed in flexural tests, showing limited energy dissipation capacity in shear dominated tests. Evaluation of more case studies demonstrating this brittle behavior will aid in the understanding of the type of behavior that should be avoided in design. Although the shear failure occurred before a plastic hinge could form, strain section profiles demonstrate that failure plane developed from the top of the column down to the flexural compression zone which was now relocated away from the footing. Since the moment-curvature assessment did not take shear degradation into account, strains are not reported for Level V.

Force-Displacement Hysteresis/Envelope:



Force-Displacement Envelope/Symbols:



Bridge Performance/Design Parameters:

Level	$\epsilon_s$	$\epsilon_c$	$\mu_o$	$\theta_p$	$P_c, P_t$
I	< 0.0028	< 0.0015*	< 0.4	--	--
II	0.0056	0.00294*	0.815	--	--
III	0.007	0.0035*	1	0	--
IV	0.011	0.0063*	1.54	0.009	--
V	--	--	2.56	0.017	--
Level	% Drift	$\mu_\Delta$	RDI	$\xi_{eq}$	$n_k$
I	< 0.5	< $V_y/2$	< 0.06	< 8%	1.58
II	1	$V_y$	0.125	8%	1.22
III	1.25	1	0.195	10%	1.0
IV	1.75	1.5	0.49	12.5%	0.65
V	2.5	2	1.25	11.8%	0.285

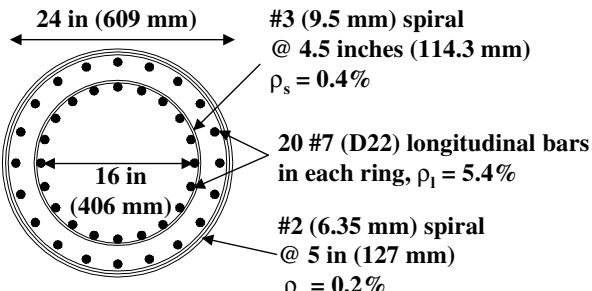
**Performance Parameter Assessment of Bridge Components/Structures**

**Background Information:**

P.I.: Name Phone Email	Frieder Seible (858) 534-4640 seible@ucsd.edu	Institution Address	University of California, San Diego Department of Structural Engineering 9500 Gilman Drive, Mail Code 0085 La Jolla, CA 92093-0085		
	Co- Name P.I.: Phone Email		Yael D. Hose (858) 534-5529 yhose@ucsd.edu	Institution Address	University of California, San Diego Department of Structural Engineering 9500 Gilman Drive, Mail Code 0085 La Jolla, CA 92093-0085
Assessment Area	1	1. Component	2. Sub-Assemblage		3. System
Assessment Classification	N	N. New	R. Retrofit		
Reference	Hose, Y.D., Seible, F., and Priestley, M.J.N., 1997, Strategic Relocation of Plastic Hinges in Bridge Columns, <i>Structural Systems Research Project, 97/05</i> , University of California, San Diego, La Jolla, September.				
Sponsoring Agency	California Department of Transportation				

**Test Unit Information:**

Test Unit Designation	Strategic Relocation of the Plastic Hinge: Flexure-Shear Column, <i>SRPH-7</i>
Test Unit Description	<p>This column is part of an experimental program conducted to study the effects of relocating the plastic hinge away from rigid supporting members. To relocate the plastic hinge an additional inner concentric reinforcing cage was provided at the column end region. This additional cage increased the moment capacity of the column at the column/footing interface, thus forcing the hinge to occur at a weaker section away from the base. The cage originated in the footing and terminated at the desired height of relocation of the hinge. In an attempt to elongate the plastic hinge region, the inner cage bars were terminated in a staggered fashion rather than uniformly. The average height of the bar cutoffs corresponded to the desired relocation height. For <i>SRPH-7</i>, the average height of the bar cutoffs was set to one column diameter (609mm, 24 inches) up from the footing. The transverse reinforcement for <i>SRPH-7</i> was designed based on the UCSD shear model, such that a ductile shear failure would occur at an approximate displacement ductility level of 8. This resulted in a 9.5mm (#3) spiral spaced at 70mm (2.75 inches) corresponding to a transverse reinforcement ratio of 0.7%. A 25mm (1-inch) cover was used, as shown in the reinforcement details provided on the following page. The reinforcement layout is shown for a cross section taken at the base of this column where a double reinforcing cage existed (2 rings of 20 D22 (#7) longitudinal bars). The elevation of <i>SRPH-7</i> is depicted in the test setup figure in the following pages. The height to centerline of the load application for this column was 2.13m (84 inches), and the axial load in the column was 890 kN (200 kips).</p>

<b>Reinforcement Details:</b> 		<b>Material Properties:</b> <b>Longitudinal Steel:</b> $f_y = 462 \text{ MPa (67 ksi)}$ $f_u = 745 \text{ MPa (108 ksi)}$ <b>Transverse Steel:</b> $f_y = 414 \text{ MPa (60 ksi)}$ $f_u = 662 \text{ MPa (96 ksi)}$ <b>Concrete:</b> $f'_c = 35.2 \text{ MPa (5.1 ksi)}$
<b>Axial Load Ratio:</b>	8.7%	

### **Bridge Damage Assessment:**

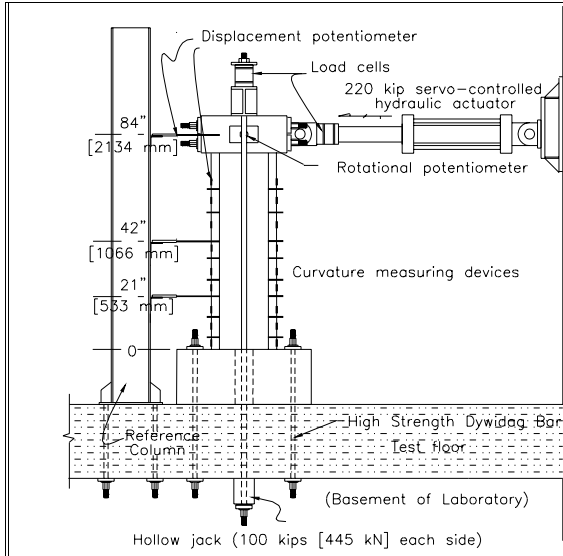
The damage observed in column *SRPH-7* at each of the five performance levels is depicted in the photographs on the following page. Horizontal flexural cracks that are visible up the height of the column initiate at Performance Level I of the PBEE methodology. The damage at this level is shown in the first photograph. However, the cracks close upon unloading, so no repair is necessary.

At Performance Level II of the PBEE methodology, shown in the second photograph, significant horizontal flexural cracks that begin to incline propagate further up the height of the column. The onset of early crack inclination is due to the high aspect ratio of the column. Crack widths, however, remain less than 1mm and repair of the component is possible but not likely.

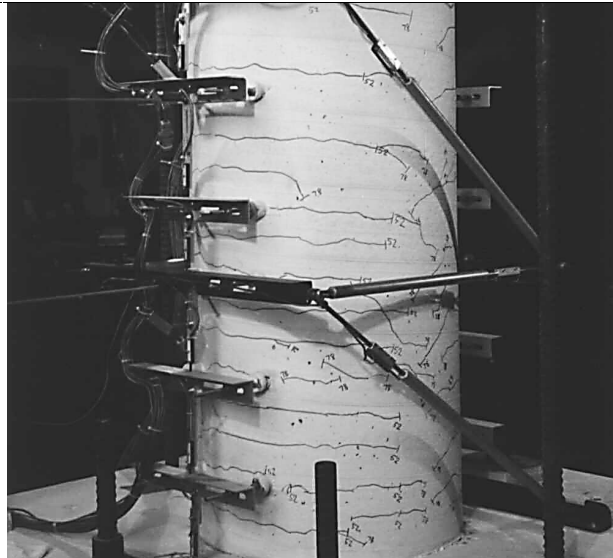
Performance Level III is shown in the third photograph on the following page, where incipient spalling of the cover concrete indicates the initiation of the ductile plastic hinge local mechanism. The critical section of the plastic hinge appeared to be forming slightly lower than expected at approximately 330mm (13 inches) in both loading directions. The propagation of the cracks was even, however, the tension face of the column in the pull direction saw larger amounts of spalling. After three cycles at this ductility 2 level, only minor extension of cracks and marginal amounts of spalling occurred. Repair of the component is possible but not likely.

The full formation of the plastic hinge region, which characterizes Performance Level IV, is evident in the fourth photograph. Cracking was well distributed on all faces of the column. The spalling region spread over approximately one column diameter in height in the relocated hinge region. By the third cycle at this ductility 4 level, the spalled region wrapped entirely around the column. At this level, the strength of the column is still maintained, but repair of the extensive concrete spalling is necessary.

Performance Level V is shown in the final photograph, where imminent failure of the column is evident by the extensive longitudinal bar buckling. During the first push cycle, despite spalling extending completely around the column, the concrete core was still intact. In the reverse loading direction, a spiral ruptured due to buckling of all six extreme longitudinal bars. Upon the next push cycle, the column suffers an extreme degradation in strength as the buckled bars eventually fracture. The damage of the column at this level requires full replacement of the component rather than repair.



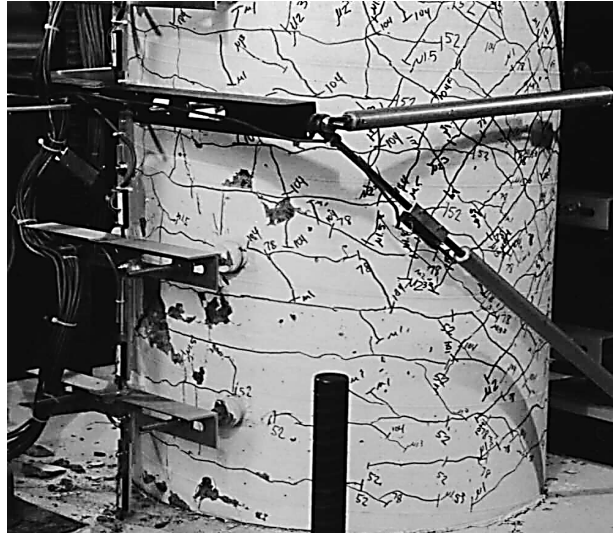
Test Setup



Level I



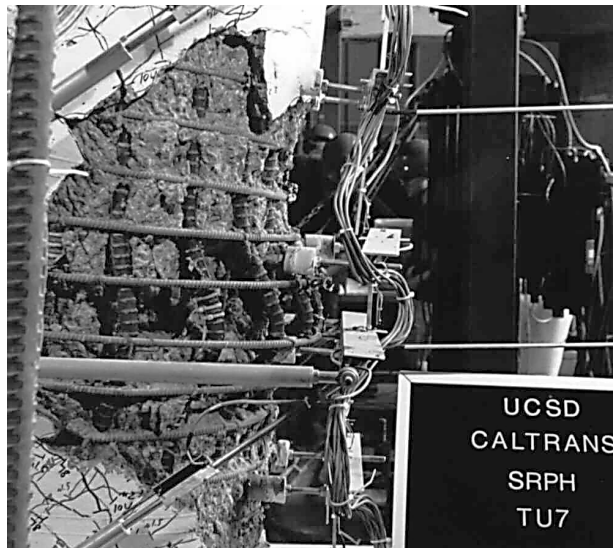
Level II



Level III



Level IV

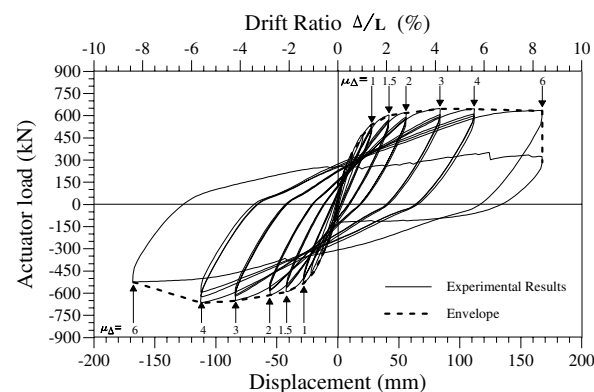


Level V

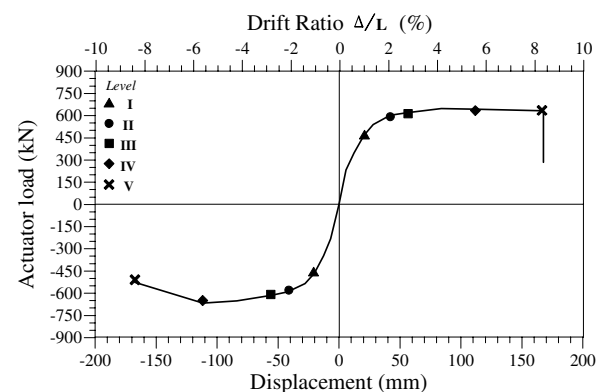
### Bridge Performance Assessment:

The cyclic force vs. displacement response for *SRPH-7*, along with its envelope profile is shown in the first figure below. The ideal yield displacement was 28mm (1.1 inches) corresponding to a 1.3% drift, and the ideal yield force occurred at 543 kN (122 kips). Ultimate displacement was 167mm (6.6 inches) which is a 7.9% drift, and the ultimate force was 632 kN (142 kips). Failure of the column was flexural and occurred at ductility 6 as opposed to the design level of ductility 8. However, a significant influence of shear behavior was observed in the column. The spiral ruptured and the longitudinal bars buckled with one eventually rupturing in the reverse loading direction. The response envelope, with symbols depicting the locations where the column reached each of the damage/performance levels is given in the second figure below. The quantitative parameters for *SRPH-7* at each level are given in the two tables below. Despite the use of the relocation design concept for this *SRPH-7*, the observed behavior resembles that of the reference column, *SRPH-1*. The local failure mechanism in both columns was the formation of a ductile plastic hinge. However, *SRPH-7* successfully relocated the plastic hinge region one column diameter away from the footing, which is demonstrated by regions of high strains concentrated in this relocated plastic hinge area in the longitudinal reinforcement strain profiles. Values of other parameters at each level for column *SRPH-7* are consistent with results from other flexural tests. RDI values ranged from approximately 0-4.2, which correlate to equivalent viscous damping ratios ranging from 8-25%. The consistency between the values of the parameters demonstrates that the formulation of a performance-based methodology for design is viable.

Force-Displacement Hysteresis/Envelope:



Force-Displacement Envelope/Symbols:



Bridge Performance/Design Parameters:

Level	$\epsilon_s$	$\epsilon_c$	$\mu_o$	$\theta_p$	$p_c, p_t$
I	< 0.006	< 0.0031*	< 0.75	--	--
II	0.006	0.0031*	0.75	--	--
III	0.0132	0.00615*	1.6	0.018	--
IV	0.0373*	0.0178*	4.56	0.055	--
V	0.0589*	0.0294*	7.32	0.092	--

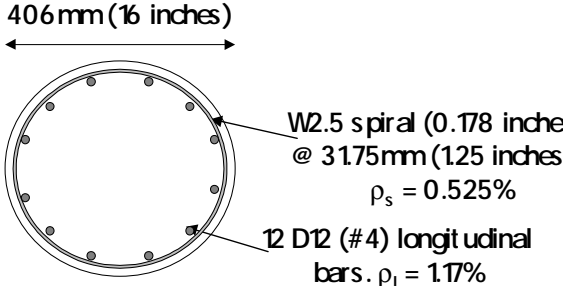
Level	% Drift	$\mu_\Delta$	RDI	$\xi_{eq}$	$n_k$
I	< 1	< $V_y$	< 0.09	< 8%	1.47
II	1	$V_y$	0.09	8%	1.19
III	2.5	2	0.666	13.6%	0.57
IV	5	4	2.31	20.9%	0.30
V	8	6	4.18	24.7%	0.195

## Performance Parameter Assessment of Bridge Components/Structures

### Background Information:

P.I.: Name Phone Email	Frieder Seible (858) 534-4640 seible@ucsd.edu	Institution Address	University of California, San Diego Department of Structural Engineering 9500 Gilman Drive, Mail Code 0085 La Jolla, CA 92093-0085
Co- P.I.: Name Phone Email	Yael D. Hose (858) 534-5529 yhose@ucsd.edu	Institution Address	University of California, San Diego Department of Structural Engineering 9500 Gilman Drive, Mail Code 0085 La Jolla, CA 92093-0085
Assessment Area	1	1. Component	2. Sub-Assemblage 3. System
Assessment Classification	N	N. New	R. Retrofit
Reference	Orozco, G., Cox, K., Hose, Y.D., Ashford, S., and Seible, F., 1999, The Effects of Large Velocity Pulses on Reinforced Concrete Bridge Piers, <i>Structural Systems Research Project, 99/10</i> , University of California, San Diego, La Jolla, August.		
Sponsoring Agency	Pacific Earthquake Engineering Research Center		

### Test Unit Information:

Test Unit Designation	Static Velocity Pulse Test, <i>VP2</i>		
Test Unit Description	<p>This column is part of a joint experimental program conducted by UC San Diego, UC Berkeley, UC Irvine, and University of Southern California, to study the effects of a large velocity pulse “fling type” time history. Many representative time histories were evaluated to establish the large velocity pulse test protocol. <i>VP2</i> was first subjected to the characterized velocity pulse <i>statically</i>, and then loaded using a displacement history based on % drift.</p> <p><i>VP2</i> had a column diameter of 406mm (16 inches), and 12 D12 (#4) longitudinal bars. The transverse reinforcement for <i>VP2</i> consisted of a W2.5 spiral (0.178 inches) spaced at 31.75 mm (1.25 inches) corresponding to a transverse reinforcement ratio of 0.525%. A 12.5mm (0.5 inch) cover was used, as shown in the reinforcement details provided below. The elevation of <i>VP2</i> is depicted in the test setup figure on the following pages. The height to centerline of the load application for this column was 1.83m (72 inches). No axial load was applied to the column.</p>		
Reinforcement Details:	 <p>406mm (16 inches)</p> <p>W2.5 spiral (0.178 inches) @ 31.75mm (1.25 inches) <math>\rho_s = 0.525\%</math></p> <p>12 D12 (#4) longitudinal bars. <math>\rho_l = 1.17\%</math></p>	<b>Material Properties:</b> Longitudinal Steel: $f_y = 455 \text{ MPa (66 ksi)}$ $f_u = 745 \text{ MPa (108 ksi)}$ Transverse Steel: $f_y = 590 \text{ MPa (85.5 ksi)}$ $f_u = 834.5 \text{ MPa (121 ksi)}$ Concrete: $f'_c = 34.5 \text{ MPa (5.0 ksi)}$	
Axial Load Ratio:	0		

### ***Bridge Damage Assessment:***

The damage observed in column *VP2* at each of the five performance levels is depicted in the photographs on the following page. The first three performance levels occurred during the initial velocity pulse in the push direction. Performance Levels IV and V were observed after the cyclic displacement loading history commenced.

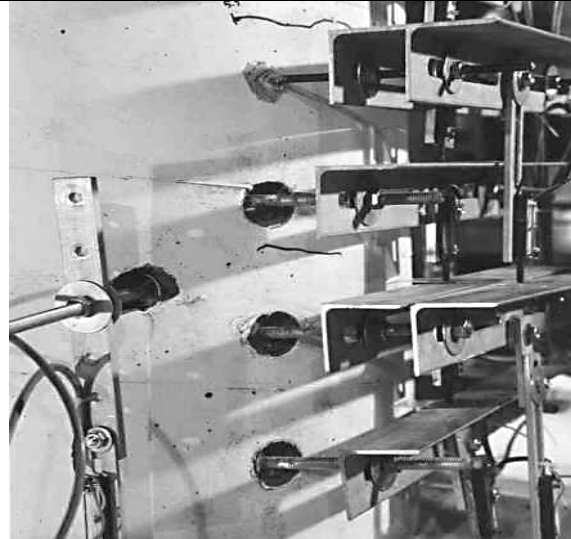
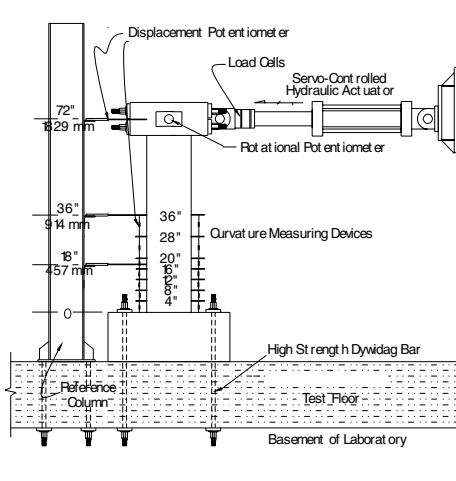
Horizontal flexural cracks located at 254mm (10 inches) and 432mm (17 inches) initiated at Performance Level I of the PBEE methodology. The damage at this level is shown in the first photograph. However, the cracks close upon unloading, so no repair is necessary.

At Performance Level II of the PBEE methodology, shown in the second photograph, yielding of the main longitudinal bar on the tension side of the column was registered. Significant horizontal flexural cracks measuring 0.1mm in width propagated further up the height of the column to approximately 1016mm (40 inches). Cracks wrapped around half of the column. Crack widths, however, remained less than 1mm and repair of the component is possible but not likely.

Performance Level III is shown in the third photograph on the following page, where incipient spalling of the cover concrete indicates the initiation of the ductile plastic hinge local mechanism. The critical section of the plastic hinge appeared to be forming at approximately 38mm (1.5 inches) above the footing. The region of spalling extended 30mm in height (1.2 inches) and 152mm (6 inches) long. The propagation of the cracks wrapped around the column to within 51mm (2 inches) of the curvature rod holes on the compression side. Some slight inclination of cracks was observed on the lateral faces of the column. Average crack spacing outside the plastic hinge region was approximately 152mm (6 inches), as opposed to 102mm (4 inches) inside the plastic hinge region. Crack widths were approximately 1mm. Since only minor extension of cracks and marginal amounts of spalling occurred, repair of the component is possible but not likely.

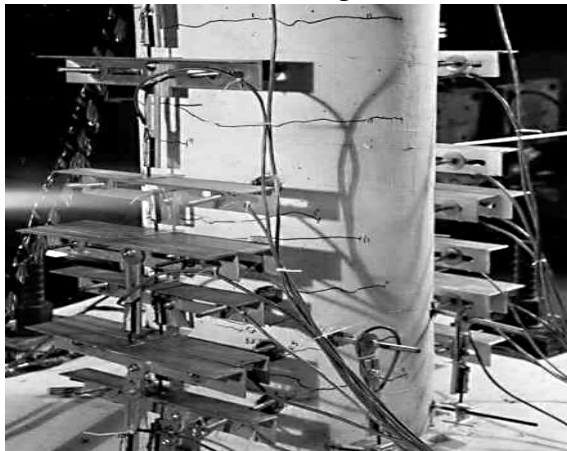
The full formation of the plastic hinge region, which characterizes Performance Level IV, is evident in the fourth photograph. Cracking was well distributed on all faces of the column, and concrete core is being loosened. The spalling regions on push/pull sides of the column are beginning to even out. Unevenness due to larger initial velocity pulse in the push direction. The hinge region on the push side of the column was 292mm (11.5 inches) wide by 191 mm (7.5 inches) high and was centered at 51mm (2 inches) above the footing. The spalling region on the pull side was 318mm (12.5 inches) wide by 121mm (4.75 inches), but penetrated 12.7mm (0.5 inches) into the footing. The center was located at 12.7mm (0.5 inches). Buckling of the longitudinal reinforcement was extremely evident. By the third cycle at this 5% Drift level, the strength of the column is still maintained, but repair of the extensive concrete spalling is necessary.

Performance Level V is shown in the final photograph, where imminent failure of the column is evident by the extensive longitudinal bar buckling. During the first cycle, spiral becomes ineffective since it is no longer touching longitudinal bars. During the second cycle at this 6% Drift level, the spiral ruptured at two locations due to buckling of all extreme longitudinal bars. A strength degradation of approximately 75% is experienced as the bars continue to buckle and the concrete core completely degrades. Eventually during cycling at 7% Drift the buckled longitudinal bars rupture. The damage of the column at this level requires full replacement of the component rather than repair.



Test Setup

Level I



Level II

Level III



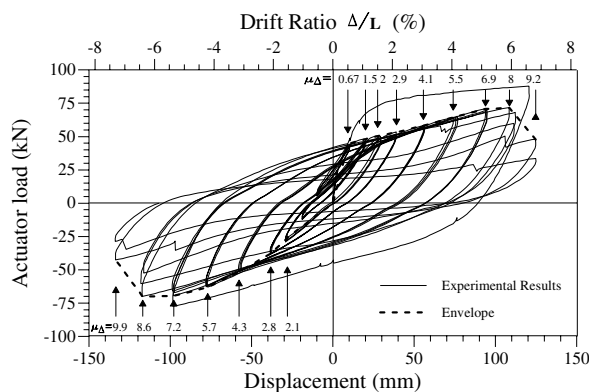
Level IV

Level V

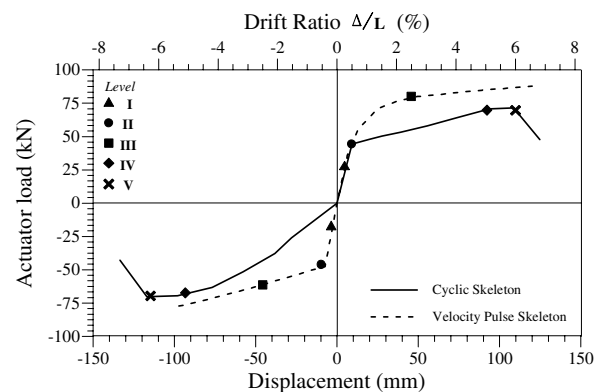
### Bridge Performance Assessment:

The cyclic force vs. displacement response for VP2, along with its envelope profile is shown in the first figure below. To consider damage and performance issues, the testing protocol consisted of stopping when each of the five levels were attained. The first three performance levels were reached during the initial velocity pulse in the push direction. Level I occurred at a force of 24.3 kN (5.47 kips) and a displacement of 3.05mm (0.12 inches), which corresponds to a 0.167% drift. Level II occurred at a force of 48.8 kN (10.96 kips) and a displacement of 10.8mm (0.426 inches), corresponding to a 0.592% drift. Level III occurred at a force of 79.2 kN (17.8 kips) and a displacement of 46.2mm (1.82 inches), corresponding to a 2.5% drift. Levels IV and V were reached during cyclic loading. The full formation of the plastic hinge occurred during cycling at 5% drift at a force of 70.3 kN (15.8 kips) and a displacement of 96mm (3.78 inches). The final performance level was reached during cycling at 6% drift at a force of 70.8 kN (15.9 kips) and a displacement of 113mm (4.45 inches). Actual failure of the column was flexural and occurred during cycling at 7% drift when the longitudinal bars ruptured. The response envelope, with symbols depicting the locations where the column reached each of the damage/performance levels, is given in the second figure below. The quantitative parameters for VP2 at each level are given in the two tables below. Values of strains were determined experimentally. They are not reported for Levels IV and V when the strain gauges were lost. The RDI and  $\xi_{eq}$  values for Level I could not be reported since the column was never cycled at this drift level. For Level III, these parameters were taken as the average of the 2% and 3% values.

Force-Displacement Hysteresis/Envelope:



Force-Displacement Envelope/Symbols:



Bridge Performance/Design Parameters:

Level	$\epsilon_s$	$\epsilon_c$	$\mu_o$	$\theta_p$	$p_c, p_t$
I	0.000897	0.000434	0.32	--	--
II	0.002068	0.000684	1.0	--	--
III	0.01468	0.00211	5.1	0.018	--
IV	--	--	10.8	0.043	--
V	--	--	13.85	0.052	--
Level	% Drift	$\mu_\Delta$	RDI	$\xi_{eq}$	$n_k$
I	0.167	$V_y/2$	--	--	2.22
II	0.59	$V_y$	0.0187	8.74%	1.25
III	2.53	3.4	1.65	16.35%	0.477
IV	5.0	7	4.23	25.6%	0.205
V	6.0	8.25	5.19	28.2%	0.175

## Performance Parameter Assessment of Bridge Components/Structures

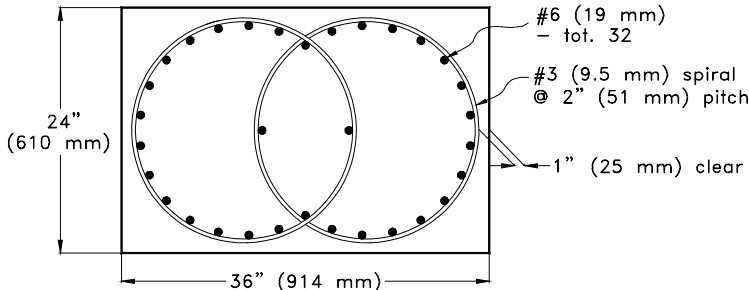
### Background Information:

<b>P.I.:</b>	<b>Name</b> Frieder Seible <b>Phone</b> (858) 534-4640 <b>Email</b> seible@ucsd.edu	<b>Institution Address</b>	University of California, San Diego Department of Structural Engineering 9500 Gilman Drive, Mail Code 0085 La Jolla, CA 92093-0085	
<b>Assessment Area</b>	1	<b>1. Component</b>	<b>2. Sub-Assemblage</b>	<b>3. System</b>
<b>Assessment Classification</b>	N	<b>N. New</b>	<b>R. Retrofit</b>	
<b>Reference</b>	Sánchez, A.V., Seible, F., and Priestley, M.J.N., 1997, Seismic Performance of Flared Bridge Columns, <i>Structural Systems Research Project, 97/06</i> , University of California, San Diego, La Jolla, August.			
<b>Sponsoring Agency</b>	California Department of Transportation			

### Test Unit Information:

<b>Test Unit Designation</b>	<i>RDS-1</i> : Prismatic Reference Column
<b>Test Unit Description</b>	<p><i>RDS-1</i> was part of a research program conducted at UCSD to investigate the seismic performance of columns with nonstructural flares. The column was built at 40-percent scale and tested upside down as a cantilever. The column had 6 feet (1.829 m) long parabolic flares with a clear height of 13 feet (3.962 m). The rectangular cross section design utilized double spirals for confinement. Thus, the test unit is denoted as RDS for Rectangular Double Spiral. <i>RDS-1</i> was the prismatic reference for the Caltrans flared column test phase. It was detailed like the “as-designed” and “improved design” flared columns that were part of the test protocol, but omitted the flare. Reinforcement details and material parameters are shown below.</p>

### Reinforcement Details:



### Material Properties:

**Longitudinal Steel:**  
 $f_y = 68.5 \text{ ksi (473 MPa)}$   
 $f_u = 108.2 \text{ ksi (746 MPa)}$

**Transverse Steel:**  
 $f_y = 68.5 \text{ ksi (473 MPa)}$   
 $f_u = 107.8 \text{ ksi (743 MPa)}$

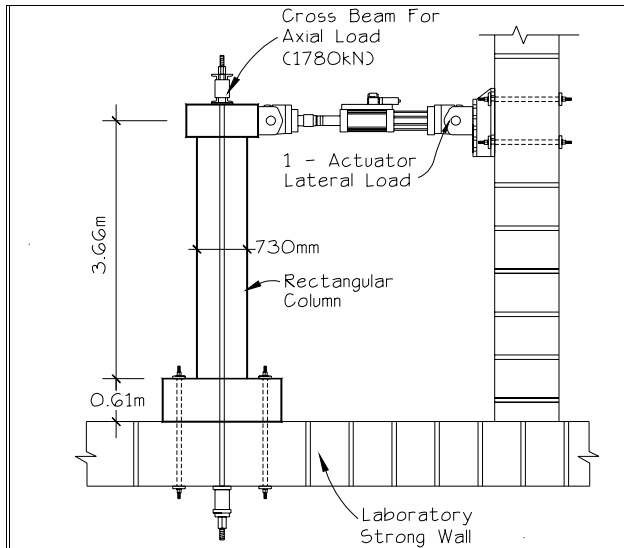
**Concrete:**  
 $f'_c = 4.81 \text{ ksi (33.2 MPa)}$

**Axial Load Ratio:**

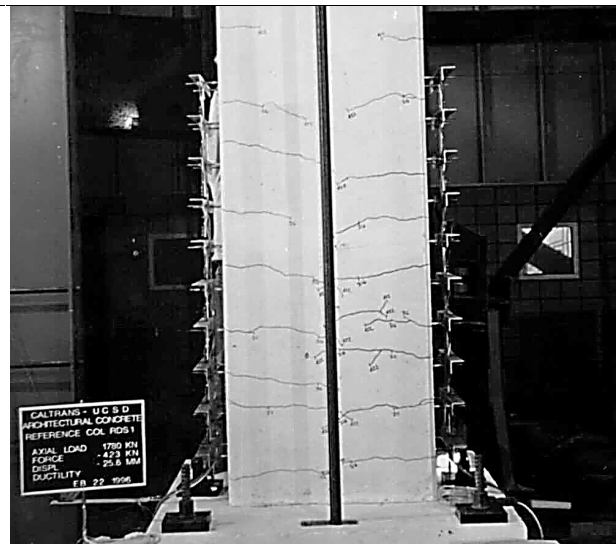
9.6%

### Bridge Damage Assessment:

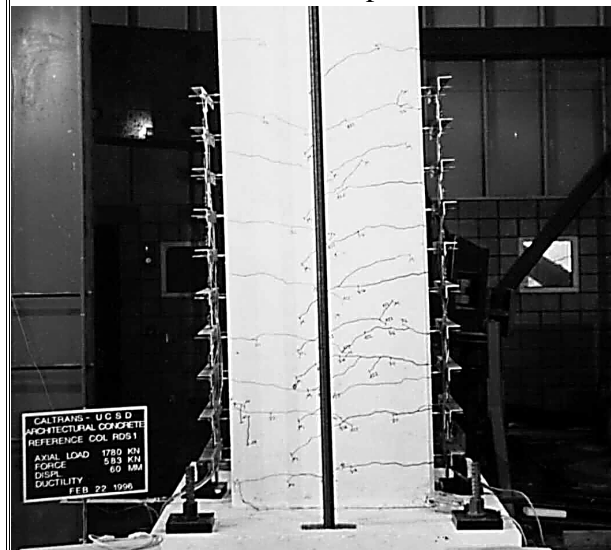
The condition of *RDS-1* at the upper bounds of the performance levels is shown in the following photographs. The first photograph shows *RDS-1* at Level I, where hairline cracks are visible but close upon unloading. No repair is necessary. Level II is shown in the second photograph. The cracks have grown in length and width and extend further up the column. No other damage is visible and only minor repair if any is necessary. Level III is shown in the third photograph, where spalling of the cover concrete at the soffit reveals the formation of the plastic hinge. Cracks have become wider. The column remains structurally sound, but requires repair of the damaged cover concrete. Level IV is shown in the fourth photograph, where spalling has extended over the full length of the plastic hinge. Curvature and strains in this region have increased considerably, and buckling of the longitudinal reinforcement is imminent. Despite considerable damage, the column remains structurally sound and can still be repaired. The condition of *RDS-1* at Level V is shown in the final photograph. At this level, transverse reinforcement has ruptured, longitudinal reinforcement has buckled, and crushing of the core concrete has initiated. The lateral strength of the column has degraded, and the ability of the column to maintain vertical loads has been compromised. Repair is no longer viable.



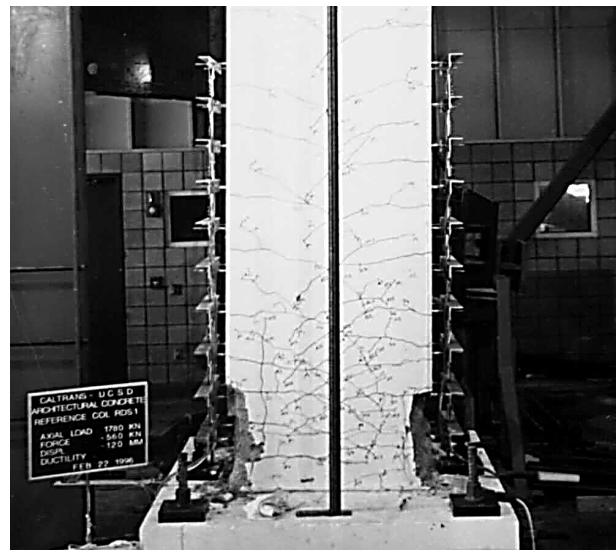
Test Setup



Level I



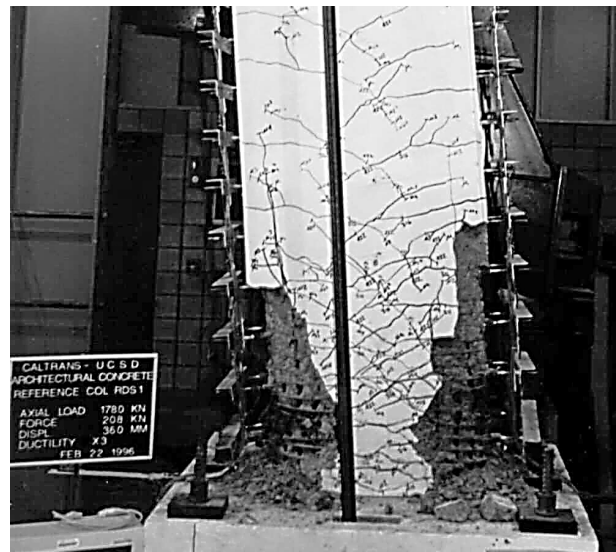
Level II



Level III



Level IV

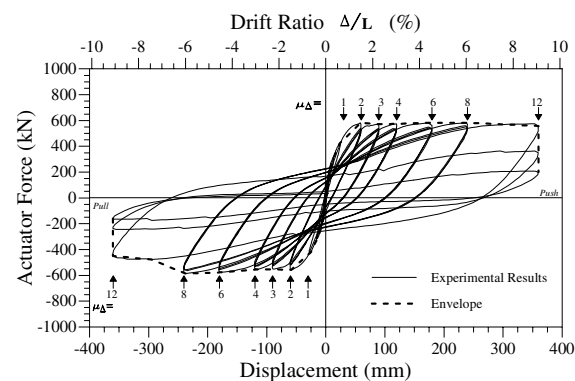


Level V

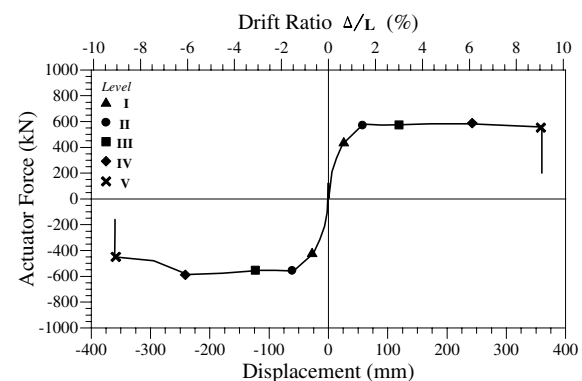
### Bridge Performance Assessment:

The force vs. displacement response of the prismatic reference column can be seen in the first figure below. This figure shows the experimental hysteresis loops and the envelope for the experimental data. Displacement ductility levels are indicated on the plot as well. The experimental envelope is repeated in the second figure, this time with symbols indicating the upper limits of the five performance levels. The triangle symbol is used to mark the end of Performance Level I, CRACKING. The first performance level ends when the column begins to show a significant decrease in stiffness. This corresponds to a displacement ductility,  $\mu_{\Delta} = 1$ , and a drift ratio of 0.76 %. Performance Level II, YIELDING, ends when the force vs. displacement response becomes essentially plastic, with no significant increase in strength due to the initiation of the plastic hinge. This corresponds to  $\mu_{\Delta} = 2$ , a drift ratio of 1.51 %, and cover concrete strains of 0.006. Performance Level IV begins when the plastic hinge is well developed, corresponding to  $\mu_{\Delta} = 4$ , a drift ratio of 3.02 %. As the curvatures in the plastic hinge region increase, and the steel and concrete strain approach their limits, the lateral strength of the column begins to degrade. This corresponds to Performance Level V with an ultimate  $\mu_{\Delta} = 12$ , and a drift ratio of 9.08 %. Performance and design parameters for the prismatic reference column are listed in the tables below. The upper bounds of the five performance levels were chosen based on observed damage corresponding to the experimental displacement ductility levels. Drift, curvature, residual displacement, and equivalent viscous damping were determined from the experimental data. Concrete and steel strains were calculated based on the experimental curvatures and analytically determined neutral axis depths.

Force-Displacement Hysteresis/Envelope:



Force-Displacement Envelope/Symbols:



Bridge Performance/Design Parameters:

Level	$\epsilon_s$	$\epsilon_c$	$\mu_{\theta}$	$\theta_p$	$P_c, P_t$
I	0.009	0.003*	1.0	0	--
II	0.016	0.006*	2.3	0.0077	--
III	0.030	0.012*	4.5	0.023	--
IV	0.075*	0.030*	10.9	0.054	--
V	0.120*	0.047*	17.3	0.085	--

Level	% Drift	$\mu_{\Delta}$	RDI	$\xi_{eq}$	$n_k$
I	0.76	1	0.07	4.7%	1.04
II	1.51	2	0.37	12.4%	1.0
III	3.02	4	0.90	16.6%	0.51
IV	6.05	8	5.00	23.9%	0.13
V	9.08	12	8.83	25.7%	0.09

## Performance Parameter Assessment of Bridge Components/Structures

### Background Information:

<b>P.I.:</b>	<b>Name</b> Frieder Seible <b>Phone</b> (858) 534-4640 <b>Email</b> seible@ucsd.edu	<b>Institution</b> <b>Address</b>	University of California, San Diego Department of Structural Engineering 9500 Gilman Drive, Mail Code 0085 La Jolla, CA 92093-0085
<b>Assessment Area</b>	1	<b>1. Component</b>	<b>2. Sub-Assemblage</b> <b>3. System</b>
<b>Assessment Classification</b>	N	<b>N. New</b>	<b>R. Retrofit</b>
<b>Reference</b>	Sánchez, A.V., Seible, F., and Priestley, M.J.N., 1997, Seismic Performance of Flared Bridge Columns, <i>Structural Systems Research Project, 97/06</i> , University of California, San Diego, La Jolla, August.		
<b>Sponsoring Agency</b>	California Department of Transportation		

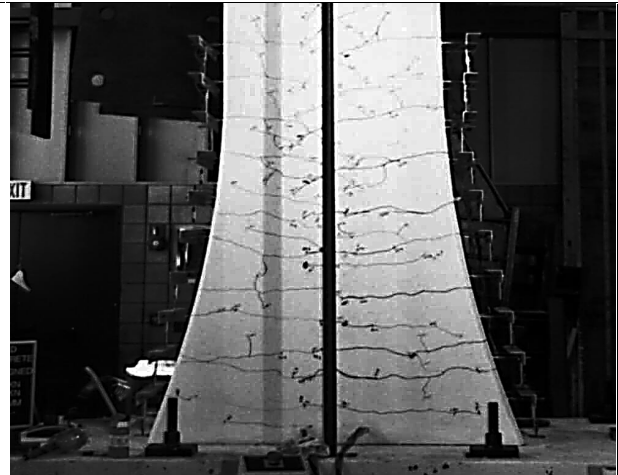
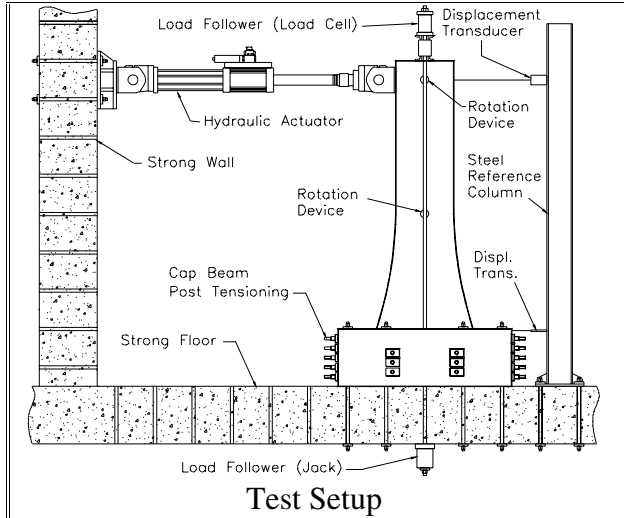
### Test Unit Information:

<b>Test Unit Designation</b>	<i>RDS-2</i> : As-Designed Flared Column
<b>Test Unit Description</b>	<p>The test unit evaluated in this template was part of a research program conducted at UCSD to investigate the seismic performance of columns with nonstructural flares. The column was built at 40-percent scale and tested upside down as a cantilever. The column had 6 feet (1.829m) long parabolic flares with a clear height of 13 feet (3.962 m). The rectangular cross section design utilized double spirals for confinement. Thus, the test unit is denoted with the initials RDS for Rectangular Double Spiral. <i>RDS-2</i> was the as-designed flared column. This column was designed based on current Caltrans flared column details. The 6 feet (1.829m) long parabolic flare transformed the cross section of <i>RDS-1</i>, the reference column, to the soffit cross section shown below.</p>

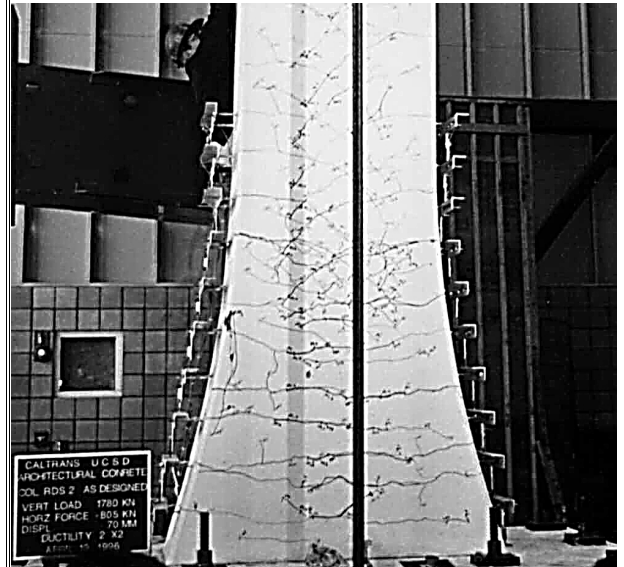
<b>Reinforcement Details:</b> 	<b>Material Properties:</b> <b>Longitudinal Steel:</b> $f_y = 68.5 \text{ ksi (473 MPa)}$ $f_u = 108.2 \text{ ksi (746 MPa)}$ <b>Transverse Steel:</b> $f_y = 68.5 \text{ ksi (473 MPa)}$ $f_u = 107.8 \text{ ksi (743 MPa)}$ <b>Concrete:</b> $f'_c = 5.46 \text{ ksi (37.6 MPa)}$
<b>Axial Load Ratio:</b>	8.5%

### Bridge Damage Assessment:

The condition of *RDS-2* at the upper bounds of the performance levels is shown in the following photographs. The first photograph shows *RDS-2* at Level I, where hairline cracks are visible, but close upon unloading. No repair is necessary. At Level II, shown in the second photograph, cracks have grown in length and width, and extend further up the column. No significant damage is visible, and probably no repair is necessary. Level III is shown in the third photograph. Crushing of the concrete at the critical flexural section 18 inches (460mm) from the start of the flare reveals the formation of the plastic hinge. The column remains structurally sound, but requires repair to the damaged cover concrete. At Level IV, shown in the fourth photograph, the lightly reinforced flared concrete has crushed and spalled over an extensive area as the plastic hinge region lengthens and moves toward the soffit. Non-structural damage is considerable, and repair of the component is necessary. The condition of *RDS-2* at Level V is shown in the last photograph. Structural damage and an excessive amount of damage to the flare exists. Transverse reinforcement has ruptured and longitudinal reinforcement has buckled. The lateral strength of the column has degraded, and repair is no longer viable.



Level I



Level II



Level III



Level IV

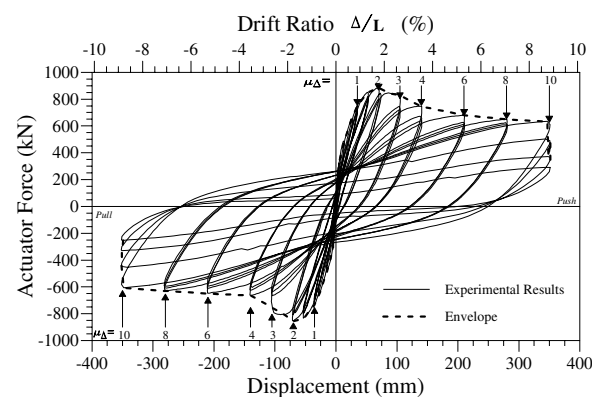


Level V

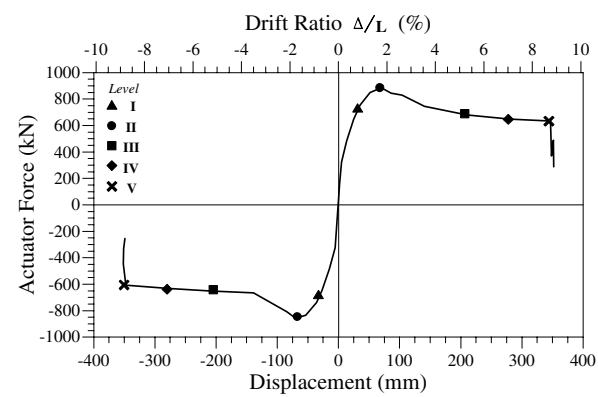
### Bridge Performance Assessment:

The response of *RDS-2* can be seen in the first figure below. This figure shows the experimental force vs. displacement loops, the envelope for the experimental data and markers indicating ductility levels. The experimental envelope is repeated in the second figure, with symbols indicating the upper limits of the five performance levels. The triangle symbol is used to mark the end of Performance Level I. This occurs when the column begins to show a significant decrease in stiffness. This corresponds to a displacement ductility,  $\mu_{\Delta} = 1$ , and a drift ratio of 0.88 %. Performance Level II ends when the force reaches its peak as the formation of the plastic hinge initiates. This corresponds to  $\mu_{\Delta} = 2$  and a drift ratio of 1.77 %. As was observed in the prismatic reference column, cover concrete strains are at 0.006. At the end of Performance Level III, the plastic hinge has lengthened and moved toward the soffit as the lightly reinforced concrete at the start of the flare has spalled away. This corresponds to  $\mu_{\Delta} = 6$ , a drift ratio of 5.30 %, and an equivalent damping ratio of 21.6 %. The long plastic hinge length is responsible for the high level of energy dissipation. Performance Level IV begins when the plastic hinge is well developed and ends upon strength degradation. The performance and design parameters for the *RDS-2* are listed in the two tables below. Values of strain at each of the levels are slightly higher than values reported for other strength degrading structures, possibly due to the higher displacement ductility capacity of this column. Some of the values of the parameters with asterisks were extrapolated beyond the data available from the simple moment-curvature analysis, which was terminated at a conservative estimate of ultimate concrete strain.

Force-Displacement Hysteresis/Envelope:



Force-Displacement Envelope/Symbols:



Bridge Performance/Design Parameters:

Level	$\epsilon_s$	$\epsilon_c$	$\mu_o$	$\theta_p$	$p_c, p_t$
I	0.003	0.002*	1.0	0	--
II	0.015	0.006*	4.2	0.0088	--
III	0.082*	0.035*	23.3	0.044	--
IV	0.112*	0.048*	31.7*	0.062	--
V	0.147*	0.063*	41.7*	0.079	--
Level	% Drift	$\mu_{\Delta}$	RDI	$\xi_{eq}$	$n_k$
I	0.88	1	0.08	4.7%	1.22
II	1.77	2	0.40	12.4%	1.0
III	5.30	6	3.46	16.6%	0.6
IV	7.07	8	5.14	23.9%	0.11
V	8.83	10	7.06	25.7%	0.09

## Performance Parameter Assessment of Bridge Components/Structures

### Background Information:

<b>P.I.:</b>	<b>Name</b> Frieder Seible <b>Phone</b> (858) 534-4640 <b>Email</b> seible@ucsd.edu	<b>Institution</b> <b>Address</b>	University of California, San Diego Department of Structural Engineering 9500 Gilman Drive, Mail Code 0085 La Jolla, CA 92093-0085
<b>Assessment Area</b>	1	<b>1. Component</b>	<b>2. Sub-Assemblage</b> <b>3. System</b>
<b>Assessment Classification</b>	N	<b>N. New</b>	<b>R. Retrofit</b>
<b>Reference</b>	Sánchez, A.V., Seible, F., and Priestley, M.J.N., 1997, Seismic Performance of Flared Bridge Columns, <i>Structural Systems Research Project, 97/06</i> , University of California, San Diego, La Jolla, August.		
<b>Sponsoring Agency</b>	California Department of Transportation		

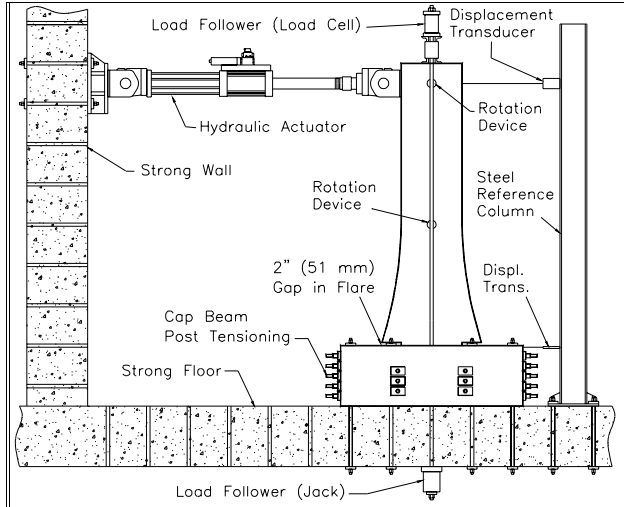
### Test Unit Information:

<b>Test Unit Designation</b>	<b>RDS-6: Uncoupled Flared Column</b>
<b>Test Unit Description</b>	<p>RDS-6 was part of a research program to investigate the seismic performance of columns with nonstructural flares. The column was built at 40% scale and had 6 feet (1.829m) long parabolic flares with a clear height of 13 feet (3.962m). The rectangular cross section used double spirals for confinement and is thus denoted with RDS for Rectangular Double Spiral. RDS-6 was designed with uncoupled flares with increased transverse reinforcement. The flares were discontinuous from the cap beam so that the column would yield at a force similar to the prismatic reference column. The transverse flare reinforcement was increased to reduce nonstructural damage. Reinforcement details and material properties are shown. Transverse reinforcement already yielded when formed into the spiral. Therefore no distinct yield plateau was observed during coupon testing.</p>

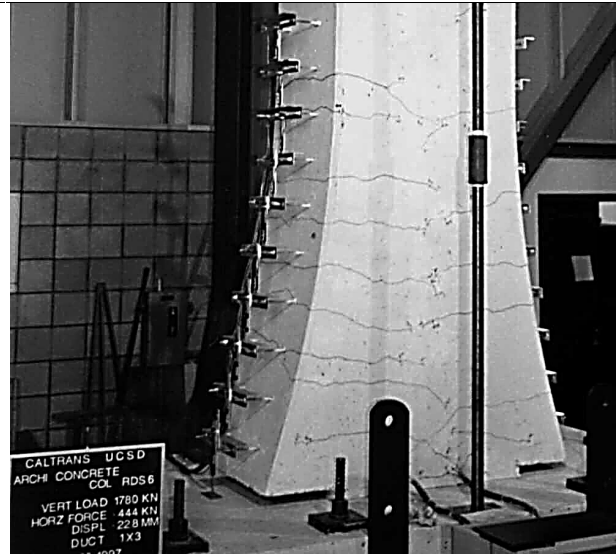
<p><b>Reinforcement Details:</b></p>	<p><b>Material Properties:</b></p> <p><b>Longitudinal Steel:</b>  <math>f_y = 70.8 \text{ ksi (488 MPa)}</math>  <math>f_u = 113.7 \text{ ksi (784 MPa)}</math></p> <p><b>Transverse Steel:</b>  <math>f_y = \text{Unknown}</math>  <math>f_u = 95.5 \text{ ksi (658 MPa)}</math></p> <p><b>Concrete:</b>  <math>f'_c = 4.79 \text{ ksi (33.0 MPa)}</math></p>
<b>Axial Load Ratio:</b>	9.7%

### Bridge Damage Assessment:

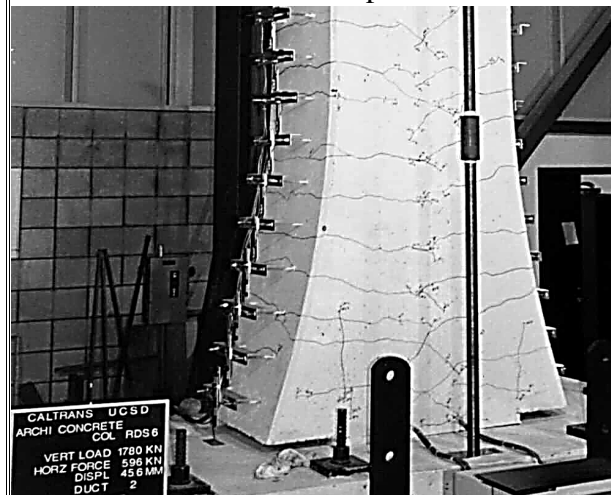
The increased transverse reinforcement in the flared region was successful in reducing non-structural damage. Therefore, little visible damage is apparent in the following photographs. The first photograph shows RDS-6 at Level I, where hairline cracks are visible but close upon unloading. No repair is necessary. At Level II, shown in the second photograph, the cracks have grown in length and width and extend further up the column. No significant damage is visible, and no repair is necessary. Crushing of the cover concrete at the uncoupled soffit correlates with Level III shown in the third photograph as the plastic hinge begins to form. The column remains structurally sound, but requires repair to the damaged cover concrete. Level IV is shown in the fourth photograph, where continued crushing and spalling of the cover concrete at the soffit section occurs. Non-structural damage is light, but repair of the component is necessary. Level V is shown in the final photograph, where the transverse reinforcement has ruptured and longitudinal reinforcement has buckled. The lateral strength of the column has degraded, and repair is no longer viable.



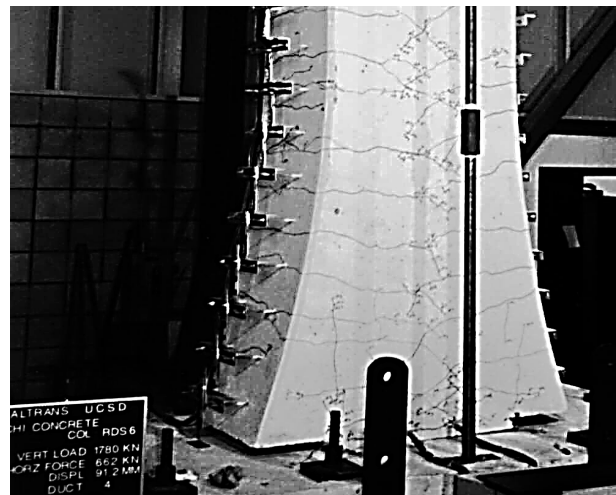
Test Setup



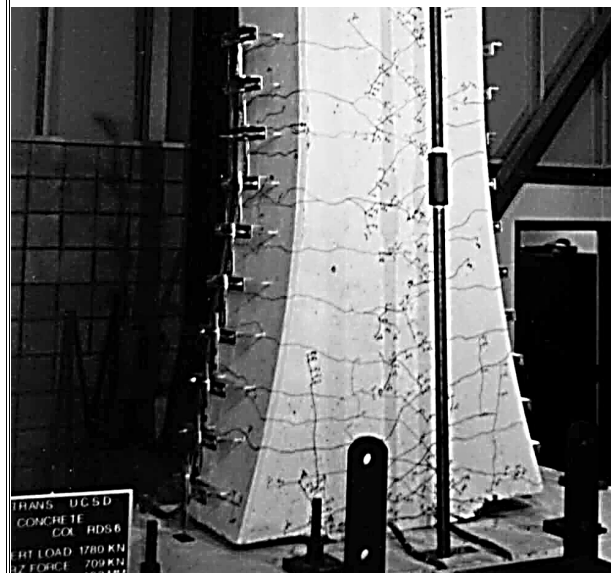
Level I



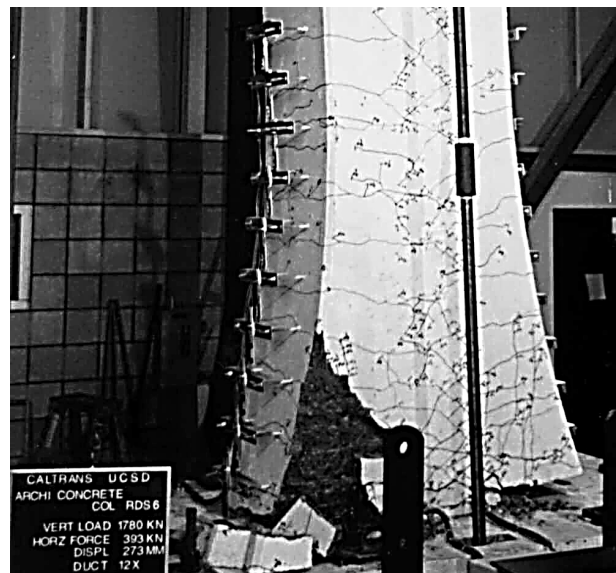
Level II



Level III



Level IV



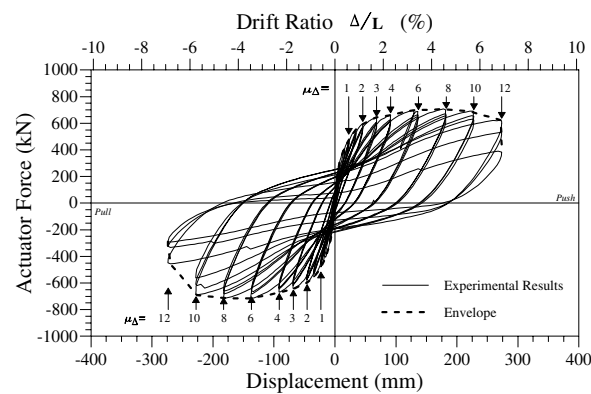
Level V

### Bridge Performance Assessment:

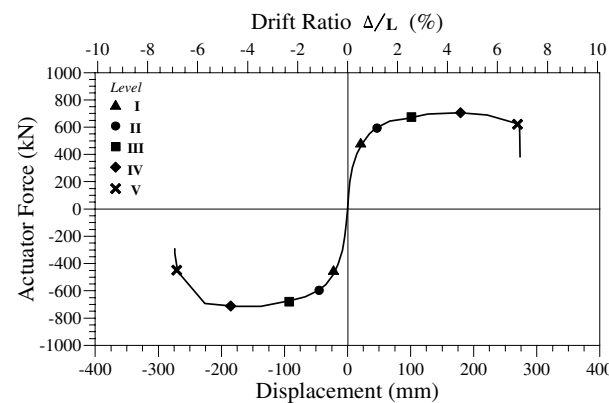
The response of *RDS-6* can be seen in the first figure below. This figure shows the experimental force vs. displacement loops and the envelope for the experimental data. Displacement ductility levels are indicated on the plot as well. The experimental envelope is repeated in the second figure, with symbols indicating the upper limits of the five performance levels. The first performance level ends when the column begins to show a significant decrease in stiffness. This corresponds to a displacement ductility,  $\mu_{\Delta} = 1$ , and a drift ratio of 0.57 %. Performance Level II, YIELDING, ends when the force vs. displacement response begins to flatten, with no significant increase in strength due to the initiation of the plastic hinge. This corresponds to  $\mu_{\Delta} = 2$ , a drift ratio of 1.15 %. As was the case with Test Units *RDS-1* and 2, cover concrete strains are observed at 0.006. Performance Level IV begins when the plastic hinge is well developed, corresponding to  $\mu_{\Delta} = 4$ , a drift ratio of 2.30 %. As the curvatures in the plastic hinge region increase, and the steel and concrete strain approach their limits, the lateral strength of the column begins to degrade. This corresponds to Performance Level V with an ultimate  $\mu_{\Delta} = 12$ , and a drift ratio of 6.90 %.

The performance and design parameters for *RDS-6* are listed in the two tables below. Values of the parameters at each of the levels are comparable to values reported for other ductile structures. Some of the values of the parameters with asterisks were extrapolated beyond the data available from the simple moment-curvature analysis, which was terminated at a conservative estimate of ultimate concrete strain.

Force-Displacement Hysteresis/Envelope:



Force-Displacement Envelope/Symbols:



Bridge Performance/Design Parameters:

Level	$\epsilon_s$	$\epsilon_c$	$\mu_{\phi}$	$\theta_p$	$P_c, P_t$
I	0.010	0.004*	1.0	0	--
II	0.015	0.006*	1.5	0.0057	--
III	0.053	0.021*	5.3	0.017	--
IV	0.113*	0.044*	11.4	0.04	--
V	0.173*	0.068*	17.4*	0.063	--
Level	% Drift	$\mu_{\Delta}$	RDI	$\xi_{eq}$	$n_k$
I	0.57	1	0.07	6.2%	1.33
II	1.15	2	0.25	8.0%	1.0
III	2.30	4	1.40	13.6%	0.65
IV	4.60	8	4.39	19.2%	0.2
V	6.90	12	8.11	20.2%	0.11

## **APPENDIX B:**

### **Sub-Assemblages**

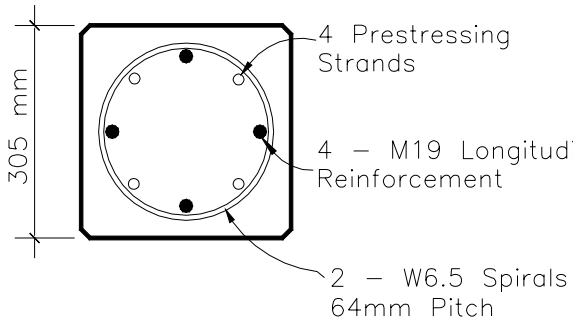
## Performance Parameter Assessment of Bridge Components/Structures

### **Background Information:**

P.I.: Name Phone Email	Frieder Seible (858) 534-4640 seible@ucsd.edu	Institution Address	University of California, San Diego Department of Structural Engineering 9500 Gilman Drive, Mail Code 0085 La Jolla, CA 92093-0085
Co- Name P.I.: Phone Email	Pedro Silva (858) 534-2347 pedrofsilva@hotmail.com	Institution Address	University of California, San Diego Department of Structural Engineering 9500 Gilman Drive, Mail Code 0085 La Jolla, CA 92093-0085
Assessment Area	2	1. Component	2. Sub-Assemblage
Assessment Classification	N	N. New	R. Retrofit
Reference	Silva, P.F., Seible, F., and Priestley, M.J.N., 1997, Response of Standard Caltrans Pile-to-Pile Cap Connections Under Simulated Seismic Loads, <i>Structural Systems Research Project, 97/09</i> , University of California, San Diego, La Jolla, November.		
Sponsoring Agency	California Department of Transportation		

### **Test Unit Information:**

Test Unit Designation	Standard Caltrans Class 625 Alternative X Pile, STD1
Test Unit Description	<p>This section evaluates a pile test unit that was part of a research program conducted at the UCSD Charles Lee Powell Structures Laboratories to model the response of single piles from a pile group. This test unit, defined as <i>STD1</i>, was a full-scale design model of the standard Caltrans Class 625 Alternative X pile. <i>STD1</i> was a 305mm square precast-prestressed concrete pile that was symmetrically reinforced with four M19 (#6) longitudinal bars corresponding to a longitudinal reinforcement ratio of 1.22%. The minimum concrete cover was 51mm. Confinement reinforcement consisted of doubly reinforced W6.5 spirals at 64mm pitch resulting in a volumetric reinforcement ratio of 0.91%. Furthermore, prestressing of the pile consisted of four 7-wire strands with an area per strand of 105mm<sup>2</sup> placed symmetrically around the pile among the longitudinal reinforcement. The pile reinforcement layout and the material properties are presented on the following page.</p> <p>During a seismic event the forces transmitted from the bridge superstructure into the foundation system produce rotation and translation of the pile cap. Thus, under a seismic event the individual piles of a pile group experience reversed cyclic loading in both axial and lateral load. In this pile test series, variations in the axial load were applied by means of two hydraulic actuators installed on the sides of the pile cap. The lateral load was applied by a hydraulic actuator, which was connected to the strong wall and the load stub. The complete test setup for unit <i>STD1</i> is provided in a figure on the following pages.</p>

<b>Reinforcement Details:</b>		<b>Material Properties:</b>
 <p>305 mm</p> <p>4 Prestressing Strands</p> <p>4 - M19 Longitudinal Reinforcement</p> <p>2 - W6.5 Spirals 64mm Pitch</p>		<p><b>Longitudinal Steel:</b></p> <p><math>f_y = 453 \text{ MPa [65.66 ksi]}</math></p> <p><math>f_u = 724 \text{ MPa [105.00 ksi]}</math></p> <p><b>Transverse Steel:</b></p> <p><math>f_y = 598 \text{ MPa [86.73 ksi]}</math></p> <p><math>f_u = 725 \text{ MPa [105.14 ksi]}</math></p>
<b>Axial Load Ratio:</b>	<b>T</b>	<b>-12%</b>
<b>(piles)</b>	<b>C</b>	<b>24%</b>
		<p><b>Concrete:</b></p> <p><math>f'_c = 55 \text{ MPa [7.98 ksi]}</math></p>

### ***Bridge Damage Assessment:***

The damage sustained by unit *STD1* during testing and classified according to the damage description presented in the PBEE Capacity Assessment methodology is depicted in the photographs on the following page and summarized as follows:

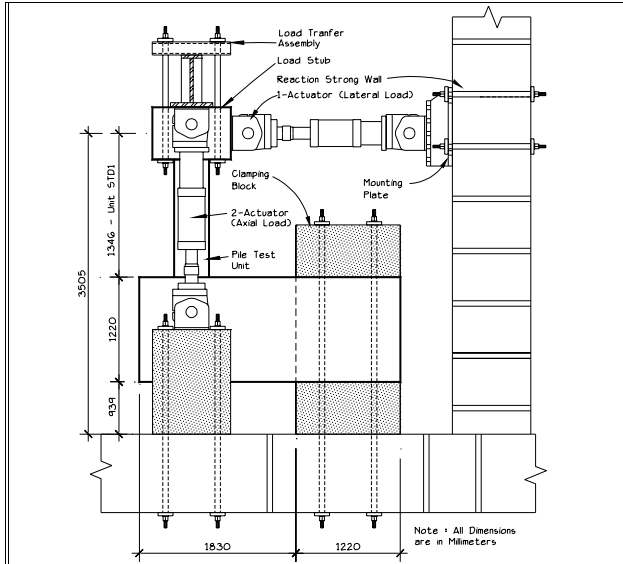
At Performance Level I of the PBEE methodology, shown in the first photograph on the following page, hairline cracks developed at the base of the pile at a spacing of approximately 152mm. These cracks closed under load reversal thus requiring no repair.

At Performance Level II of the PBEE methodology, shown in the second photograph, flexural cracking was recorded over the full length of the pile specimen. Some of the cracks began to incline providing first visual evidence of shear induced cracking. Repair of the component is possible but not likely.

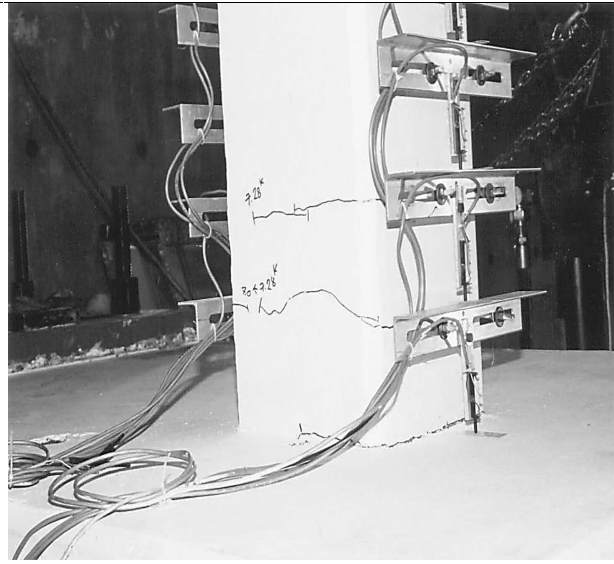
Performance Level III, INITIATION OF LOCAL MECHANISM, is shown in the third photograph on the following page. Onset of spalling of the cover concrete was recorded at the base of the pile indicating the initiation of a flexural plastic hinge behavior mode. Performance at this stage may require repair.

The full formation of the local mechanism, which characterizes Performance Level IV, is evident in the fourth photograph. Extensive spalling of the cover concrete was observed. Furthermore, a decrease in the lateral load-carrying capacity of the section under axial compression loading was registered. At this level, the strength of the sub-assembly is maintained, but repair of the extensive concrete spalling is necessary.

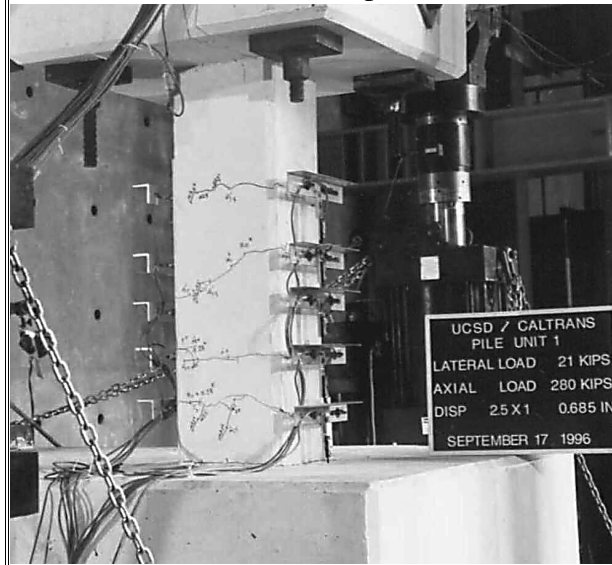
Performance Level V is shown in the final photograph, where imminent failure of the sub-assembly is evident. At this level, the spalling region extended over the full height of the computed plastic hinge. The damage of the sub-assembly at this level requires replacement rather than repair.



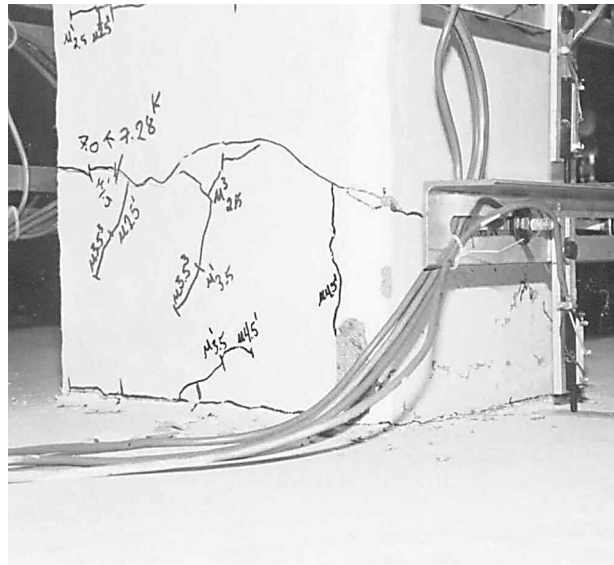
Test Setup



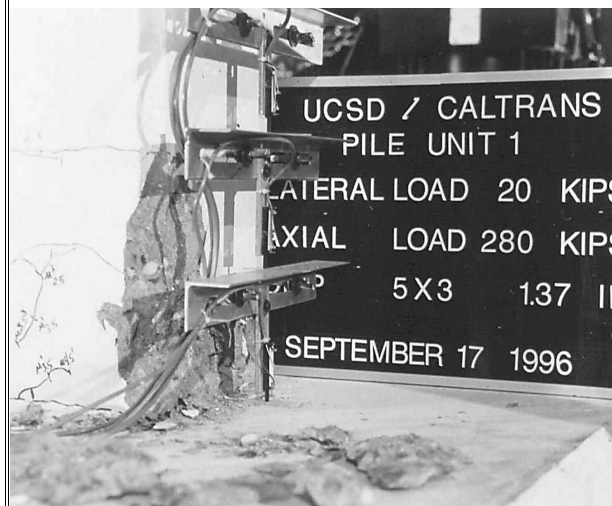
Level I



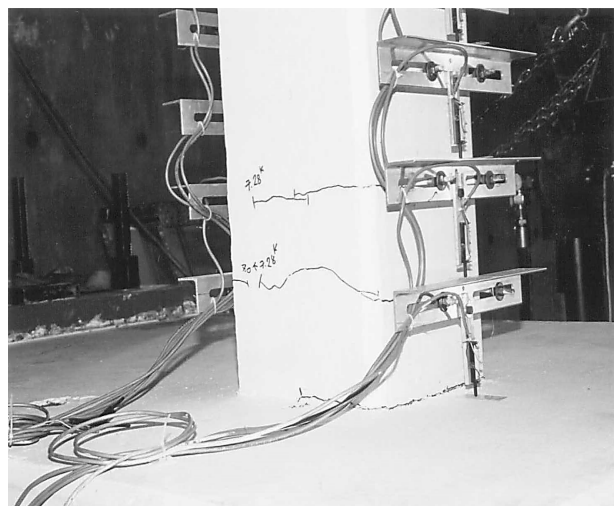
Level II



Level III



Level IV

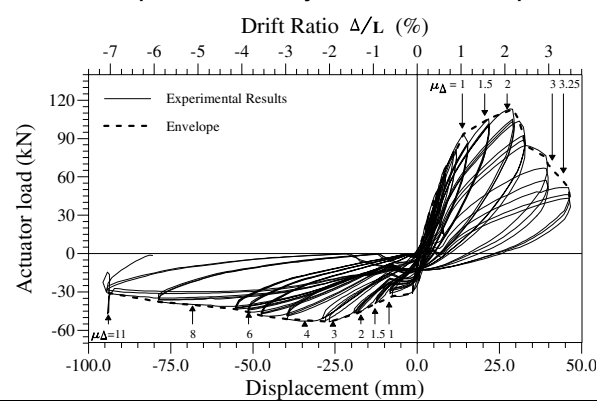


Level V

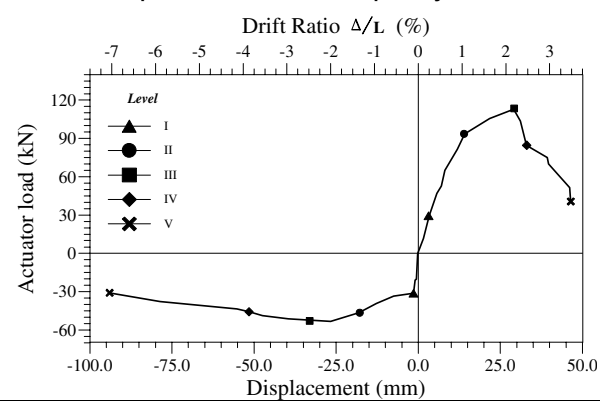
### Bridge Performance Assessment:

The first figure below shows the measured force-displacement response of *STD1*. The asymmetrical response between positive and negative displacements is due to varying axial load. Under positive displacements the section was in axial compression, while under negative displacements a tension load was applied. The axial load varied between +1,246 kN and -445 kN, respectively. Under axial compression, a peak lateral load of +120 kN was observed at ductility +2 (Drift Ratio +2%). This was followed by a rapid decrease in the lateral load-carrying capacity of the section, as a result of spalling of the large cover concrete area. In tension, a maximum lateral load of -45 kN was observed at ductility of -3.5 (Drift Ratio -2%). The second figure below presents the envelope response of unit *STD1* and the associated five damage levels. A drastic change in stiffness is observed at Level I under negative displacements due to cracking of the section and the applied axial tension load. Under positive displacements, only a slight change in stiffness was observed. This demonstrates that under axial compression the section was not significantly influenced by the onset of cracking, as the axial load was adequate in closing these initial cracks. Peak response in both loading directions occurred at Level III. Testing was terminated when excessive concrete spalling was observed over the full height of the computed plastic hinge length, which is associated with Level V. The parameterization of unit *STD1* based on the PBEE performance/design parameters is shown in the two tables below. Because of the unsymmetrical response of the test unit, two values are presented for the different parameters. Positive values were associated with positive deflections (axial compression), while negative values were associated with negative deflections (axial tension). Steel strains evaluated at Level II matched with the first yielding of the longitudinal reinforcement. Concrete strains evaluated at Level III correlate with strains that mark the onset of concrete spalling. RDI values and equivalent viscous damping ratios were obtained for an asymmetric structure. The equivalent viscous damping ratio varied between 10 and 18%, which are values typically found for reinforced concrete sections.

Force-Displacement Hysteresis/Envelope:



Force-Displacement Envelope/Symbols:



Bridge Performance/Design Parameters:

Level	$\epsilon_s$	$\epsilon_c$	$\mu_\phi$	$\theta_p$	$p_c, p_t$
I	+0.0005, -0.0003	+0.0010, -0.0004*	+0.5, -0.25	--	--
II	+0.0022, -0.0023	+0.0025, -0.0014*	+1.75, -2.0	0, 0.0023	--
III	+0.0045, -0.0110*	+0.0057, -0.0027*	+3.5, -4.5	0.011, 0.014	--
IV	+0.0048, -0.0210*	+0.0077, -0.0048*	+4.0, -9.0	0.014, 0.027	--
V	+0.0053, -0.1021*	+0.0121, -0.0451*	+5.75, -15.75	0.024, 0.059	--
Level	% Drift	$\mu_\Delta$	RDI	$\xi_{eq}$	$\eta_k$
I	+0.23, -0.11	+0.25, -0.1	0.14	10.21%	1.37
II	+1.04, -1.32	+1.0, -2.1	0.25	10.43%	0.46
III	+2.17, -2.46	+2.2, -3.9	0.51	10.32%	0.28
IV	+2.45, -3.83	+2.4, -6.0	1.26	11.01%	0.16
V	+3.45, -7.00	+3.4, -11.0	2.05	18.05%	0.05

## Performance Parameter Assessment of Bridge Components/Structures

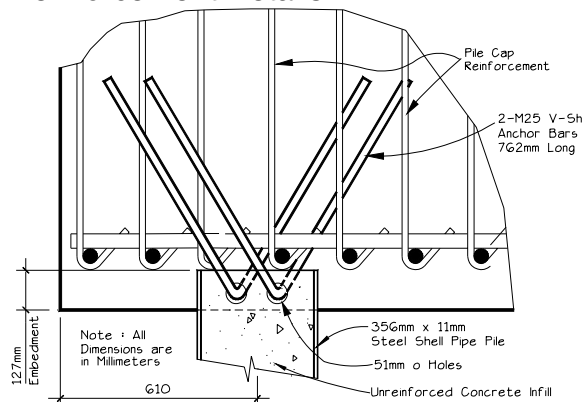
### Background Information:

P.I.:	Name Phone Email	Frieder Seible (858) 534-4640 seible@ucsd.edu	Institution Address	University of California, San Diego Department of Structural Engineering 9500 Gilman Drive, Mail Code 0085 La Jolla, CA 92093-0085
Co-P.I.:	Name Phone Email	Pedro Silva (858) 534-2347 pedrofsilva@hotmail.com	Institution Address	University of California, San Diego Department of Structural Engineering 9500 Gilman Drive, Mail Code 0085 La Jolla, CA 92093-0085
Assessment Area	2	1. Component	2. Sub-Assemblage 3. System	
Assessment Classification	N	N. New	R. Retrofit	
Reference	Silva, P.F., Seible, F., and Priestley, M.J.N., 1997, Response of Standard Caltrans Pile-to-Pile Cap Connections Under Simulated Seismic Loads, <i>Structural Systems Research Project, 97/09</i> , University of California, San Diego, La Jolla, November.			
Sponsoring Agency	California Department of Transportation			

### Test Unit Information:

Test Unit Designation	Standard Caltrans Class 625 Alternative W Pile, STD2
Test Unit Description	This pile test unit that was part of a research program conducted at UCSD to model the response of single piles from a pile group. <i>STD2</i> , was a full-scale design model of the standard class 625 alternative W pile. <i>STD2</i> , designated in the standard B2-5 as alternative W, consisted of a composite steel shell with a 356mm inside diameter unreinforced concrete core. The steel shell was 11mm thick. The connection of the pile to the pile cap consisted of two M25 (#8) V-shaped anchor bars with 64mm long legs that passed through the steel shell in 51mm diameter holes. The cross section of this pile is illustrated below. The complete test setup for unit <i>STD2</i> is provided on the following page. Similar to unit <i>STD1</i> , the axial load was varied during the testing procedure by means of two hydraulic actuators.

#### Reinforcement Details:



#### Material Properties:

##### Longitudinal Steel:

$$f_y = 465 \text{ MPa [67.44 ksi]}$$

$$f_u = 721 \text{ MPa [104.57 ksi]}$$

##### Transverse Steel:

$$f_y = 273 \text{ MPa [40.00 ksi]}$$

$$f_u = \text{unknown}$$

##### Concrete:

$$f'_c = 46 \text{ MPa [6.67 ksi]}$$

Axial Load Ratio:  
(piles)

T	-13%
C	26%

### **Bridge Damage Assessment:**

The damage sustained by unit *STD2* during testing and classified according to the damage description presented in the PBEE Capacity Assessment methodology is depicted in the photographs on the following page and summarized as follows:

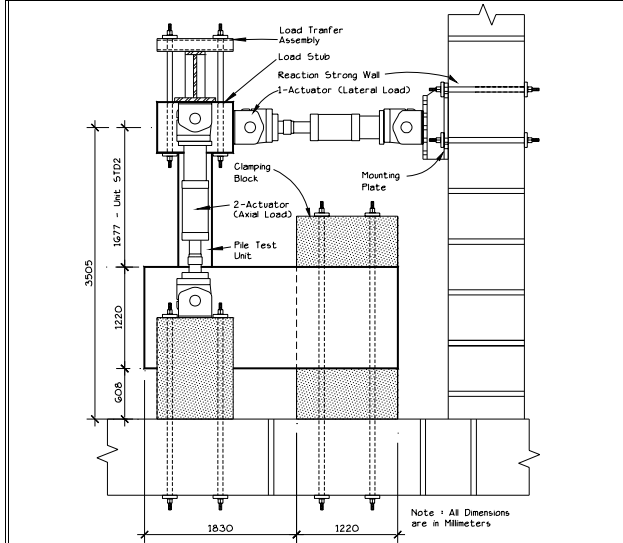
Because of the presence of the steel shell, the damage at Performance Level I of the PBEE methodology was defined in terms of cracking of the pile cap in the pile seating. The cracking pattern is shown in the first photograph on the following page. Although cracking in the adjacent connection occurred, they are minimal and close upon unloading. No repair is necessary.

At Performance Level II of the PBEE methodology, shown in the second photograph, only a few minor cracks were observed. However, a gap between the steel shell and the surrounding concrete was registered, and this damage level may be defined according to the observed gap width. Repair of the component is possible but not likely.

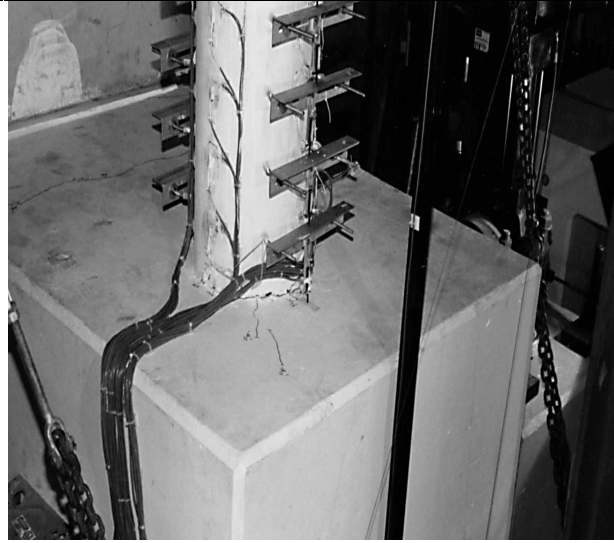
Performance Level III, INITIATION OF LOCAL MECHANISM, is shown in the third photograph on the following page. The lifting of the pile cap cover concrete in the seating area as a result of large rotations of the embedded steel casing is illustrated. Furthermore, the damage in the pile seating is due to tensile strain penetrations of the anchor bars. Performance at this stage shows exposure of the pile cap reinforcement to corrosive attack, which may require repair of the pile seating area.

The full formation of the local mechanism, which characterizes Performance Level IV, is evident in the fourth photograph. Extensive damage to the pile cap cover concrete was observed. A slight decrease in the lateral load-carrying capacity occurred as a result of increasing tension loads and loss of seating around the steel casing. At this level, the strength of the sub-assembly is unstable, and repair of the extensive concrete spalling and unseating of the pile cap is necessary.

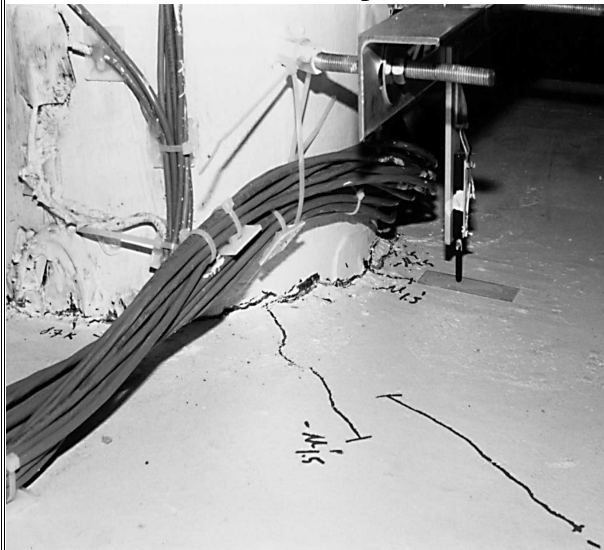
Performance Level V is shown in the final photograph, where imminent failure of the sub-assembly is evident. At this level, fracture of the anchor bars occurred resulting in separation of the pile section from the pile cap. The damage of the sub-assembly at this level requires full replacement of all components rather than repair.



Test Setup



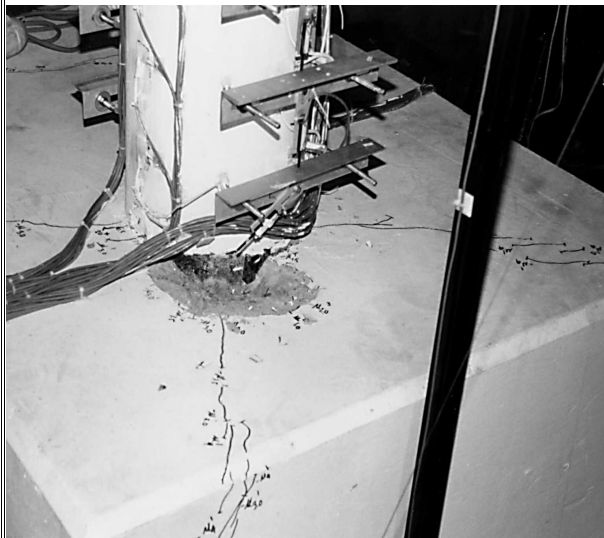
Level I



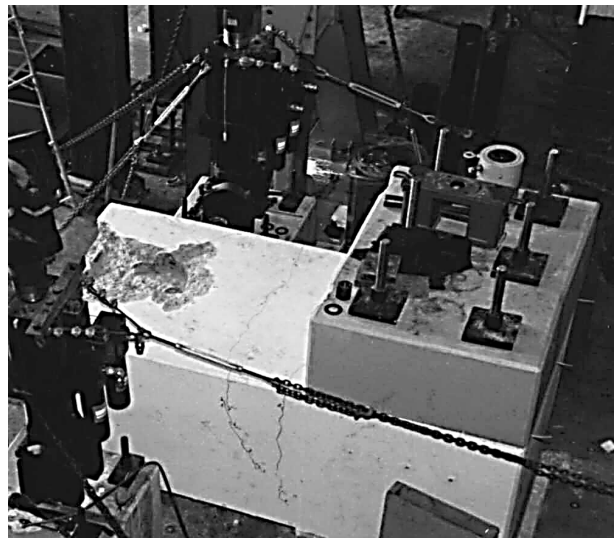
Level II



Level III



Level IV

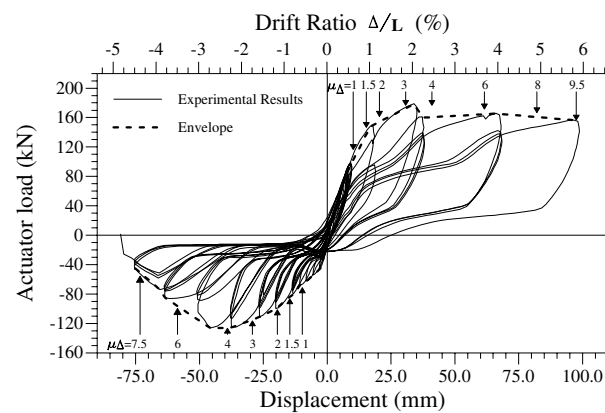


Level V

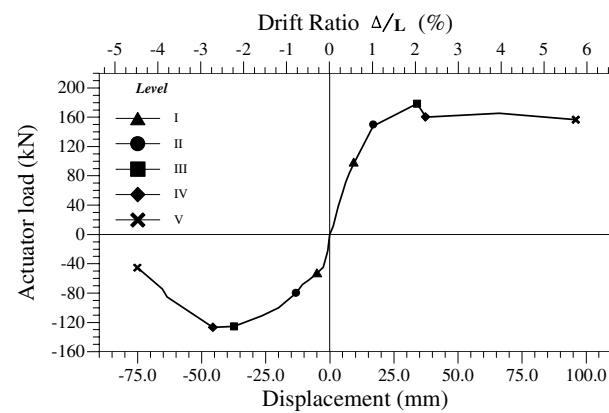
### Bridge Performance Assessment:

The first figure below shows the force-displacement response of *STD2*. Variations in the axial load caused the asymmetric response in the positive and negative displacements. The compression and tension loads varied between +1,246 kN and -445 kN, respectively. Under tension loading a maximum lateral load of -120 kN was observed at ductility -4 (Drift Ratio -2.5%), followed by a rapid decrease in the lateral load-carrying capacity of the section. Degradation in the lateral strength of the pile under axial tension was significant at the maximum displacement due to damage of the seating area, which caused prying of the steel shell on the pile cap seating area concrete. Under axial compression a maximum lateral load of +180 kN was observed at ductility +3.5 (Drift Ratio +2%). After this peak, only a slight decrease in the lateral load-carrying capacity was measured indicating a reduction in prying action of the steel shell under axial compressive loads. The second figure below presents the envelope response of unit *STD2* and the associated five damage levels. Level I occurred at cracking of the seating area. Level II was defined when a wide-open gap developed between the steel shell and the surrounding concrete. Level III occurred at peak response for both loading directions and was marked by the onset of concrete spalling in the seating region. Failure was due to fracture of the anchor bars. The parameterization of unit *STD2* is presented in the two tables below. For some parameters, two values are reported for positive and negative loading. Steel strains evaluated at Level II matched with first yielding of anchor bars, and concrete strains evaluated at Level III correlate with strains that mark the onset of the concrete spalling. The parameters were calculated for an asymmetric structure.

Force-Displacement Hysteresis/Envelope:



Force-Displacement Envelope/Symbols:



Bridge Performance/Design Parameters:

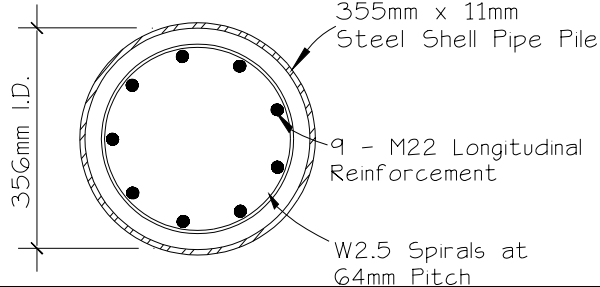
Level	$\epsilon_s$	$\epsilon_c$	$\mu_\phi$	$\theta_p$	$p_c, p_t$
I	+0.0013, -0.0016	+0.0018, -0.0004*	+0.25, -0.5	--	+0.03, -0.13
II	+0.0017, -0.0021	+0.0025, -0.0003*	+1.5, -1.25	0.004, 0.002	+0.07, -0.14
III	+0.0035, -0.0092*	+0.004, -0.0017*	+2.5, -3.75	0.014, 0.016	+0.08, -0.15
IV	+0.0038, -0.011*	+0.0043, -0.0019*	+3.0, -5.75	0.016, 0.021	+0.14, -0.16
V	+0.0058, -0.015*	+0.008, -0.0029*	+8.5, -10.0	0.052, 0.039	+0.13, -0.17
Level	% Drift	$\mu_A$	RDI	$\xi_{eq}$	$n_k$
I	+0.56, -0.30	+0.91, -0.52	0.17	7.6%	1.61
II	+1.01, -0.79	+1.66, -1.35	0.29	9.7%	1.16
III	+2.03, -2.23	+3.31, -3.82	0.52	10.7%	0.65
IV	+2.23, -2.72	+3.64, -4.67	0.63	13.5%	0.53
V	+5.72, -4.48	+9.35, -7.69	1.56	12.0%	0.18

## Performance Parameter Assessment of Bridge Components/Structures

### Background Information:

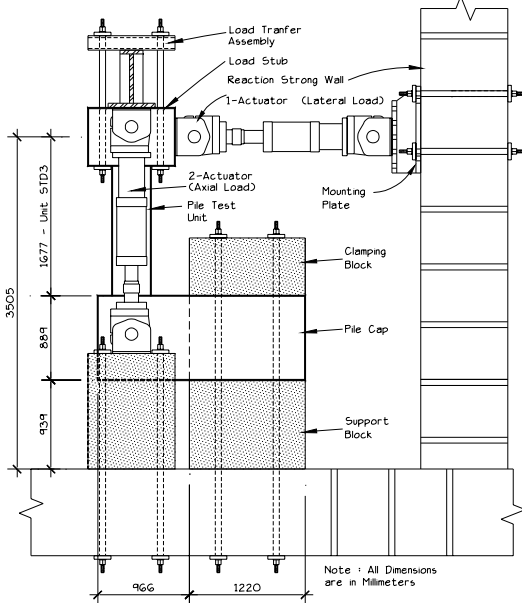
P.I.:	Name Phone Email	Frieder Seible (858) 534-4640 seible@ucsd.edu	Institution Address	University of California, San Diego Department of Structural Engineering 9500 Gilman Drive, Mail Code 0085 La Jolla, CA 92093-0085
Co- P.I.:	Name Phone Email	Pedro Silva (858) 534-2347 pedrofsilva@hotmail.com	Institution Address	University of California, San Diego Department of Structural Engineering 9500 Gilman Drive, Mail Code 0085 La Jolla, CA 92093-0085
Assessment Area	2	<b>1. Component</b>	<b>2. Sub-Assemblage</b>	<b>3. System</b>
Assessment Classification	N	<b>N. New</b>	<b>R. Retrofit</b>	
Reference	Silva, P.F., Seible, F., and Priestley, M.J.N., 1997, Response of Standard Caltrans Pile-to-Pile Cap Connections Under Simulated Seismic Loads, <i>Structural Systems Research Project, 97/09</i> , University of California, San Diego, La Jolla, November.			
Sponsoring Agency	California Department of Transportation			

### Test Unit Information:

Test Unit Designation	Standard Caltrans Class 1780 Pile, STD3		
Test Unit Description	Unit <i>STD3</i> was a 7/12-scale model of the standard Caltrans composite steel shell reinforced concrete core Class 1780 Pile found in route I-880 5th and 6th Street Viaduct bent pile details. Scaling of the prototype pile resulted in a steel shell 11mm in thickness and an inside diameter of 356mm. The core was symmetrically reinforced with 9 M22 longitudinal bars for a reinforcement ratio of 3%, and a minimum concrete cover of 32mm. The transverse reinforcement ratio of 0.30% consisted of a W2.5 spiral at a 64mm pitch.		
Reinforcement Details:			
Material Properties:	<p><b>Longitudinal Steel:</b>  <math>f_y = 465 \text{ MPa [67.44 ksi]}</math>  <math>f_u = 757 \text{ MPa [109.78 ksi]}</math></p> <p><b>Transverse Steel:</b>  <math>f_y = 599 \text{ MPa [86.87 ksi]}</math>  <math>f_u = 717 \text{ MPa [103.94 ksi]}</math></p> <p><b>Concrete:</b>  <math>f'_c = 45 \text{ MPa [6.53 ksi]}</math></p>		
Axial Load Ratio: (Pile)	T	-14%	
	C	28%	

### Bridge Damage Assessment:

The cracking pattern illustrated in the first photograph on the next page shows cracks emanating at 45° from the pile base towards the pile cap side faces. This Level I damage was recorded at first yield of the longitudinal reinforcement. Level II, depicted in the second photograph, shows cracking in the joint region. At Level III, shown in the third photograph, excessive cracking in the pile cap joint region, which may require repair, was observed. Level IV was classified by extensive damage of the pile cap cover concrete in the seating region due to pull out of the steel casing, which is illustrated in the fourth photograph. At Level V, shown in the final photograph, extensive wide-open cracks in the joint region signifying joint degradation, correlated to a 10% decrease in the registered lateral load. Considerable damage to the pile cap cover concrete, due to seating of the steel casing, was observed. At this level, extensive repair of the pile cap may be required.



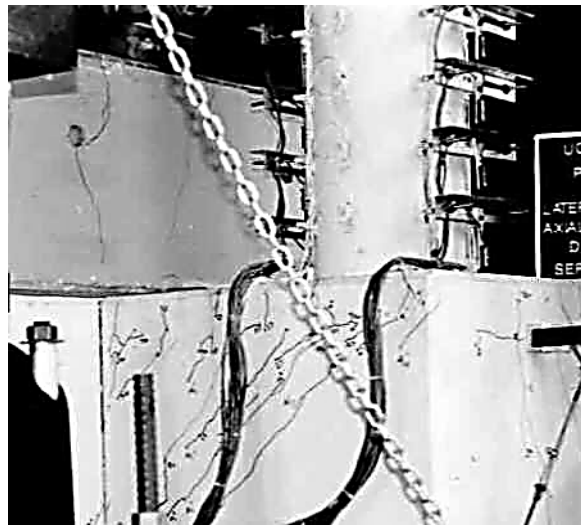
Test Setup



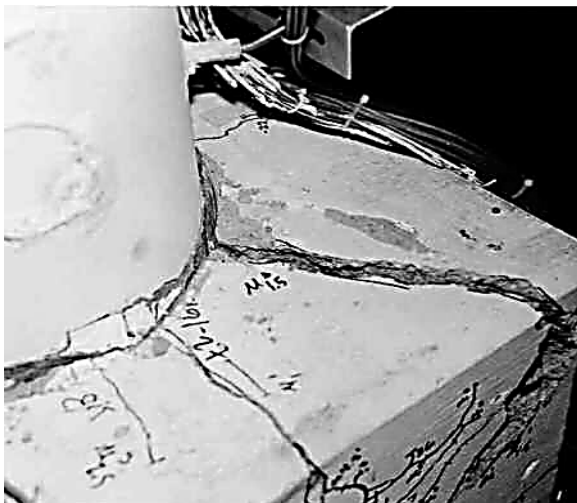
Level I



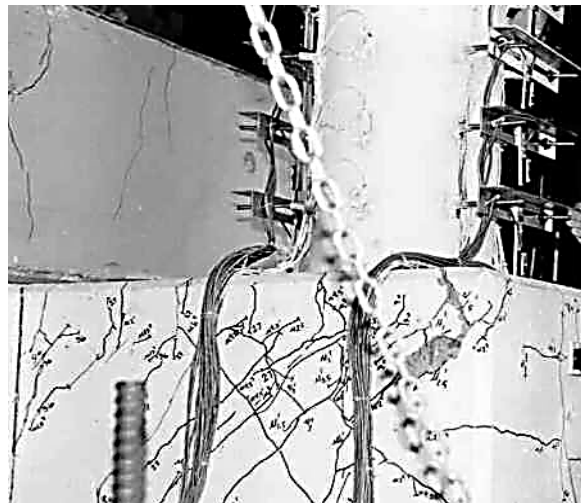
Level II



Level III



Level IV

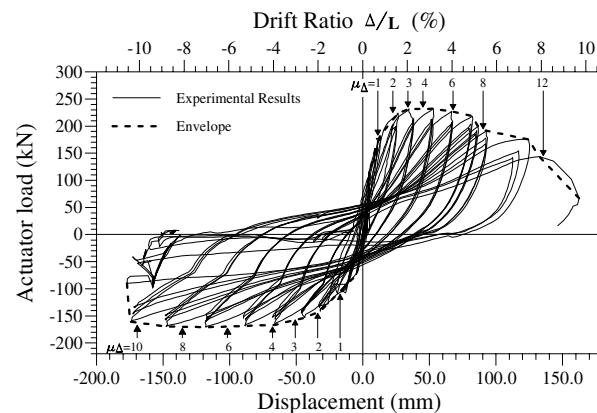


Level V

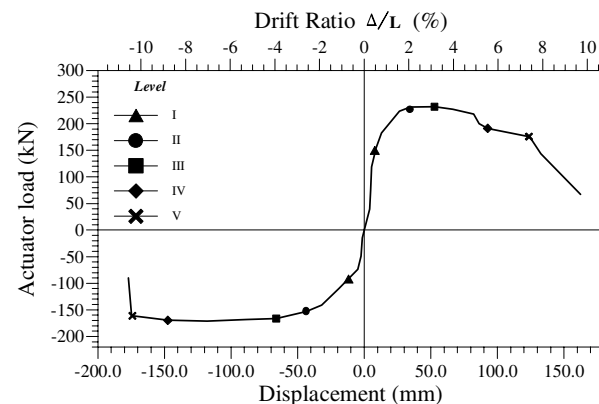
### Bridge Performance Assessment:

The measured lateral force vs. displacement response of unit *STD3* is shown below. The asymmetrical behavior was a result of variations in the axial loading, however, it was not as pronounced as previous tests because the capacity of the section in the range of applied axial loads was approximately the same. The maximum compression and tension loads varied between +1,218 kN and -605 kN, respectively. A maximum lateral force of +232kN was recorded under compressive axial loads at ductility -3 (Drift Ratio -2%). During the final stages of the testing the lateral load was +144kN, which corresponds approximately to 60% of the registered peak load. Under tension loading, a maximum load of -171 kN was observed at ductility -5 (Drift Ratio -5%), followed by a slight decrease in the lateral load-carrying capacity of the section. Due to failure in the joint region, significant strength degradation of the pile section was observed. The envelope response of unit *STD3* and the associated five damage levels is also shown below. Level III was defined at the onset of joint shear failure, which corresponds to the peak response in both loading directions. Level V was marked by extensive damage in the pile cap joint region. Due to the asymmetric response, two values for each level are reported in the performance/design parameter tables below. Steel strains evaluated at Level I matched closely with the first yield of the longitudinal reinforcement in both loading directions, and concrete strains evaluated at Level II correlate with the onset of the concrete spalling. The equivalent viscous damping was obtained for an asymmetric structure type, with values calculated between 9.5 and 26.5%.

Force-Displacement Hysteresis/Envelope:



Force-Displacement Envelope/Symbols:



Bridge Performance/Design Parameters:

Level	$\epsilon_s$	$\epsilon_c$	$\mu_\phi$	$\theta_p$	$p_c, p_t$
I	+0.002,-0.002	+0.001,-0.001	+0.3,-0.5	--	+0.08,-0.15
II	+0.010,-0.013	+0.005,-0.003	+2.0,-2.75	0.0158,0.0189	+0.35,-0.55
III	+0.016,-0.019	+0.007,-0.004	+3.25,-4.0	0.0267,0.0324	+0.42,-0.62
IV	+0.026,-0.039	+0.012,-0.008	+5.0,-7.75	0.0505,0.0809	+0.40,-0.70
V	+0.037,-0.051	+0.017,-0.011	+7.3,-10.5	0.069,0.0968	+0.35,-0.75

Level	% Drift	$\mu_\Delta$	RDI	$\xi_{eq}$	$K_{eff}/K_o$
I	+0.47,-0.70	+0.71,-0.69	0.20	9.3%	1.56
II	+2.06,-2.60	+3.06,-2.57	0.83	14.1%	0.56
III	+3.15,-3.94	+4.68,-3.90	1.65	15.2%	0.44
IV	+5.53,-8.80	+8.21,-8.71	4.90	15.9%	0.33
V	+7.38,-10.38	+10.95,-10.28	7.00	26.5%	0.11

# **APPENDIX C:**

## **Systems**

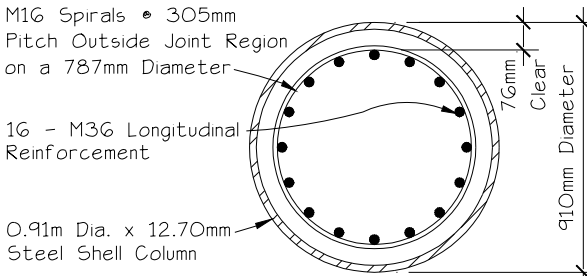
## Performance Parameter Assessment of Bridge Components/Structures

### **Background Information:**

P.I.:	Name Phone Email	Frieder Seible (858) 534-4640 seible@ucsd.edu	Institution Address	University of California, San Diego Department of Structural Engineering 9500 Gilman Drive, Mail Code 0085 La Jolla, CA 92093-0085
Co- P.I.:	Name Phone Email	Pedro Silva (858) 534-2347 pedrofsilva@hotmail.com	Institution Address	University of California, San Diego Department of Structural Engineering 9500 Gilman Drive, Mail Code 0085 La Jolla, CA 92093-0085
Co- P.I.:	Name Phone Email	Sri Sritharan (858) 534-2347 sri@ucsd.edu	Institution Address	University of California, San Diego Department of Structural Engineering 9500 Gilman Drive, Mail Code 0085 La Jolla, CA 92093-0085
Assessment Area	3	1. Component	2. Sub-Assemblage	3. System
Assessment Classification	N	N. New	R. Retrofit	
Reference	Silva, P.F., Sritharan, S., Seible, F., and Priestley, M.J.N., 1998, Full-scale Test of the Alaska Cast-in-Place Steel Shell Three Column Bridge Bent, <i>Structural Systems Research Project, 98/13</i> , University of California, San Diego, La Jolla, November.			
Sponsoring Agency	State of Alaska Department of Transportation and Public Facilities			

### **Test Unit Information:**

Test Unit Designation	Full-scale Test of the Alaska Cast-in-Place Steel Shell Three Column Bridge Bent (Multiple Column Bridge Alaska (MCBA))
Test Unit Description	The test unit consisted of a bridge bent with three cast-in-place steel shell columns that was detailed to ensure ductile performance under simulated seismic loading. The composite columns were composed of steel shells filled with reinforced concrete, with an outside diameter of 910mm (35.8 inches). The longitudinal reinforcement ratio in the columns was selected as $\rho_{cc}=2.5\%$ to avoid problems related to confining large amounts of longitudinal reinforcement, resulting in 16 M36 (#11) longitudinal bars. The cover concrete of the column was 76.2 mm (3 inches). Inside the joints, the transverse reinforcement consisted of an M16 (#5) spiral at a pitch of 127mm (5 inches), while outside the joints, a nominal M16 (#5) spiral at a pitch of 305mm (12 inches) was used. A steel shell gap of 50.8mm (2 inches) was provided at the cap beam interface to avoid damage to the bottom surface cover concrete of the cap beam, which could result from prying action of the embedded portion of the steel shell. The complete test setup for MCBA is shown in the following pages. Gravity loads were simulated at four locations along the cap beam using four loading fixtures. To simulate the seismic lateral forces, two hydraulic actuators were attached to the test specimen on each side of the test unit through load transfer blocks. The columns are designated as EC1, IC, and EC2, while the joints as KJ1, TC, and KJ2.

<b>Reinforcement Details:</b>   <p>M16 Spirals • 305mm Pitch Outside Joint Region on a 787mm Diameter</p> <p>16 - M36 Longitudinal Reinforcement</p> <p>0.91m Dia. x 12.70mm Steel Shell Column</p>		<b>Material Properties:</b> <b>Column:</b> Longitudinal Steel: M36 (#11) $f_y = 453 \text{ MPa [65.7 ksi]}$ $f_u = 724 \text{ MPa [105.0 ksi]}$ Transverse Steel: M16 (#5) $f_y = 598 \text{ MPa [86.7 ksi]}$ $f_u = 725 \text{ MPa [105.1 ksi]}$ <b>Cap Beam:</b> Longitudinal Steel: M29 (#9) $f_y = 455 \text{ MPa [66.0 ksi]}$ $f_u = 772 \text{ MPa [111.9 ksi]}$ Transverse Steel: M13 (#4) $f_y = 425 \text{ MPa [61.6 ksi]}$ $f_u = 716 \text{ MPa [103.8 ksi]}$ <b>Concrete:</b> Column: $f'_c = 55 \text{ MPa [7.98 ksi]}$ Cap Beam: $f'_c = 38 \text{ MPa [5.51 ksi]}$				
		<table border="1"> <tr> <td rowspan="2">Axial Load Ratio: (Columns)</td> <td>EC's</td> <td>3%</td> </tr> <tr> <td>IC</td> <td>5%</td> </tr> </table>		Axial Load Ratio: (Columns)	EC's	3%
Axial Load Ratio: (Columns)	EC's	3%				
	IC	5%				

**Bridge Damage Assessment:**

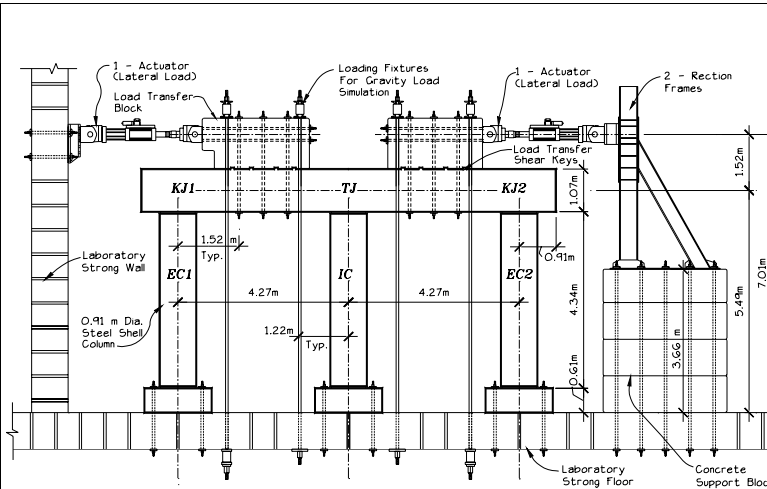
Level I was defined in the PBEE capacity assessment methodology at the onset of flexural cracking. The first photograph on the following page depicts the cracking pattern observed in column *EC1* of test unit *MCBA* at half the theoretical first yield force. Cracking was observed in all three columns in both loading directions.

Level II was characterized by the onset of diagonal shear cracking in the joint region, which was observed in the three joints in both loading directions. The observed damage in the joint region was comparable with the damage criteria used to establish Level I at the component level. The second photograph on the following page depicts the cracking pattern in joint *TJ* at the theoretical first yield force.

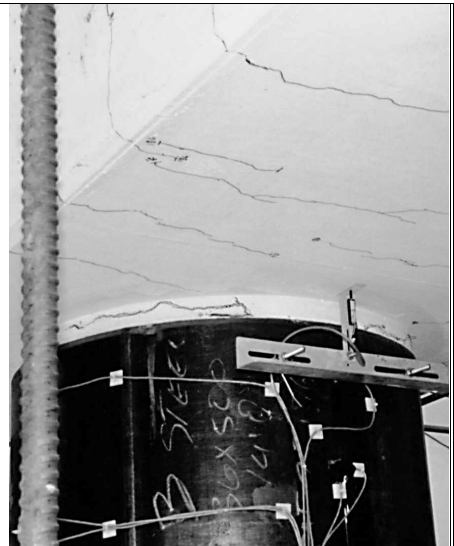
The initiation of the local mechanism, which describes Level III, is shown in the third photograph on the following page. Localized spalling of the cover concrete was recorded in the gap regions at the cap beam. At this pull cycle of displacement ductility 2, wide crack widths were visible in all the three columns at the interface of the cap beam.

The full formation of the plastic hinge mechanism characterizing Level IV is shown in the fourth photograph, where significant damage to the bottom surface of the cap beam indicating full strain penetration of the column longitudinal reinforcement is observed.

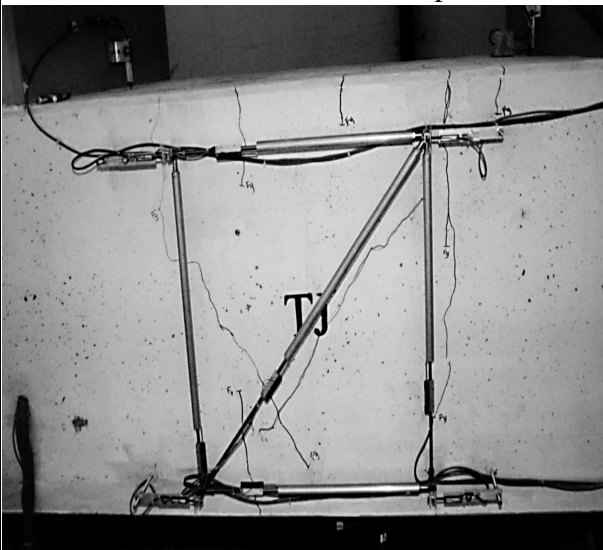
Extensive damage of the test unit, shown in the final photograph, was observed at Level V. The column longitudinal reinforcement fractured in all three columns, indicating that the ultimate flexural strength of the columns was reached. Failure of the test unit, therefore, occurred in the columns rather than the joint regions.



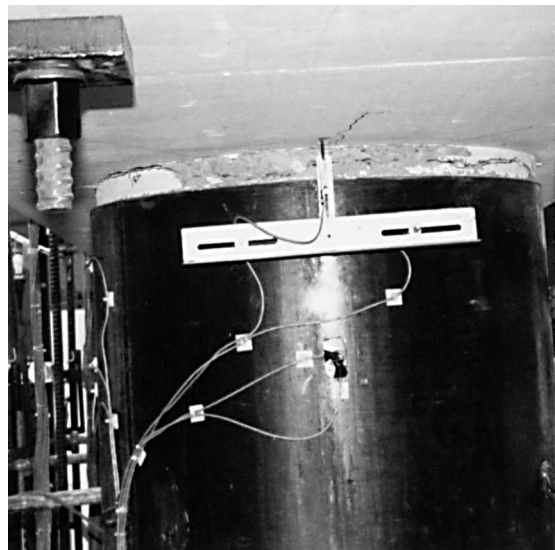
Test Setup



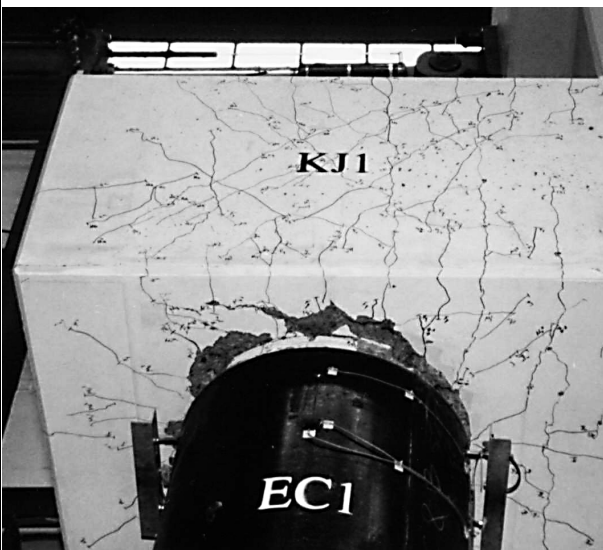
Level I



Level II



Level III



Level IV

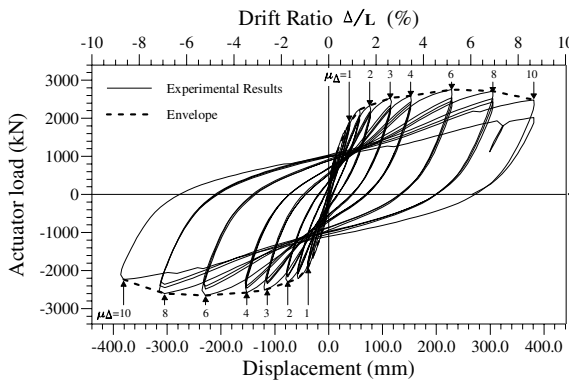


Level V

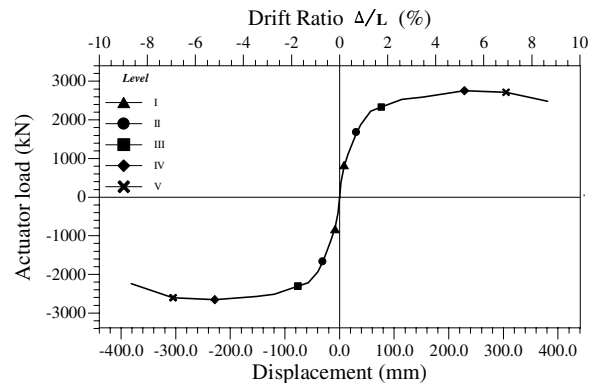
### **Bridge Performance Assessment:**

The measured lateral force vs. displacement response of unit MCBA is shown below. The maximum lateral force applied to the test specimen was recorded during the first cycle at ductility level 6. At this cycle, in the push and pull directions, the lateral force was +2,756 kN and -2,654 kN, respectively. During the first cycle at ductility 8 in the push direction, the lateral load was 2,486 kN, which corresponds to a reduction of approximately 10% from the maximum registered lateral load. During the first cycle to ductility 10, at a deflection corresponding to ductility 8, failure of the longitudinal bars in the columns occurred. The envelope response and the associated five damage levels described in this paper are also shown below. Peak response in both loading directions occurred at Level III, which corresponds to onset of concrete spalling in the column gap region at the column/cap beam interface. Testing was terminated when failure of the column longitudinal reinforcement occurred, which is associated with Level V. The performance and design parameters for test unit MCBA are reported in the tables below. The first table presents the performance/design parameters for unit MCBA at the component level. In this test unit three components were identified. However, the exterior columns (EC's) exhibited similar response, and therefore, the values presented in the table represent the maximum value calculated for columns EC1 and EC2. The Level II steel strains evaluated for all the columns in this test unit correspond to yielding of the longitudinal reinforcement, while the concrete strains evaluated at Level III correlate with strains that mark the onset of concrete spalling. The final table presents the parameters that were evaluated on the system level.

**Force-Displacement Hysteresis/Envelope:**



**Force-Displacement Envelope/Symbols:**



**Bridge Performance/Design Parameters:**

Level	$\epsilon_s$		$\epsilon_c$		$\mu_o$		$\theta_p$	$P_c, P_t$	
	EC	IC	EC	IC	EC	IC	EC & IC	KJ	TJ
I	0.0007	0.0004	0.0007	0.0004	0.3	0.2	--	0.07	0.05
II	0.002	0.0022	0.0022	0.0023	0.9	0.8	0.0	0.24	0.21
III	0.010	0.0042	0.0041	0.0038	4	4	0.0011	0.53	0.47
IV	0.032	0.0339	0.0131	0.0113	11	10	0.0455	0.67	0.62
V	0.040	0.0338	0.0162	0.0143	12	11	0.0631	0.70	0.64

Level	% Drift	$\mu_A$	RDI	$\xi_{eq}$	$K_{eff}/K_o$
I	0.20	0.22	0.05	6.50%	1.87
II	0.70	0.82	0.10	7.25%	1.0
III	1.75	2	0.55	10.5%	0.57
IV	5.20	6	3.90	20.5%	0.22
V	7.00	8	5.75	23%	0.167

## Performance Parameter Assessment of Bridge Components/Structures

### **Background Information:**

P.I.: Name Phone Email	Frieder Seible (858) 534-4640 seible@ucsd.edu	Institution Address	University of California, San Diego Department of Structural Engineering 9500 Gilman Drive, Mail Code 0085 La Jolla, CA 92093-0085		
Co- P.I.'s: Name Phone Email	Donato Innamorato (858) 534-5685 dinnamorato@ucsd.edu	Institution Address	University of California, San Diego Department of Structural Engineering 9500 Gilman Drive, Mail Code 0085 La Jolla, CA 92093-0085		
Assessment Area	3	1. Component	2. Sub-Assemblage	3. System	
Assessment Classification	B	A. New	B. Retrofit		
Reference	Innamorato, D., Seible, F., Hegemier, G.A., Priestley, M.J.N., and Ho, F., 1996, Full Scale Test of a Two Column Bridge Bent with Carbon Fiber Jacket Retrofit, <i>Advanced Composites Technology Transfer Consortium, 96/10</i> , University of California, San Diego, La Jolla, August.				
Sponsoring Agency	Advanced Research Projects Agency (ARPA) and Federal Highway Administration (FHWA)				

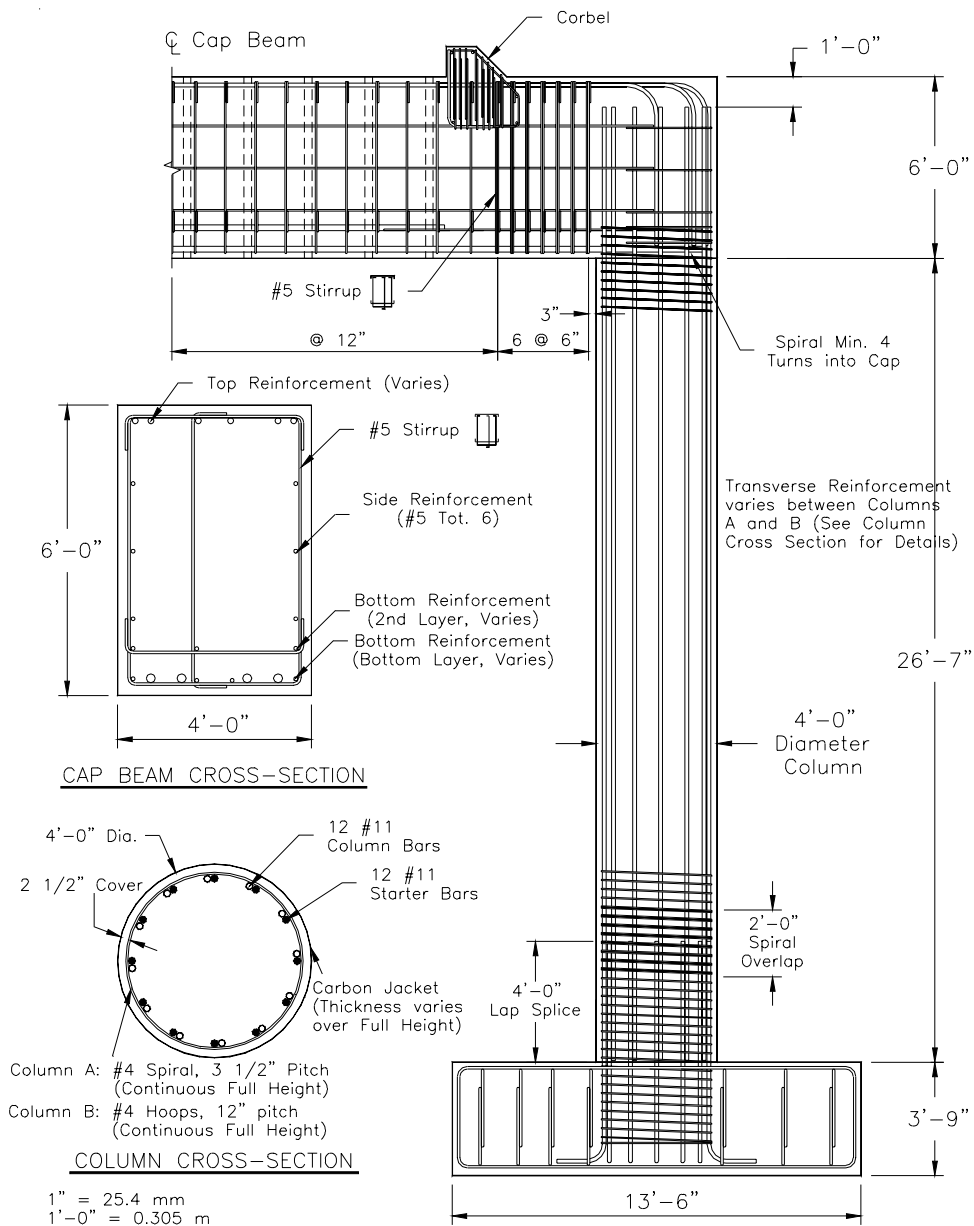
### **Test Unit Information:**

Test Unit Designation	Full Scale Two Column Bridge Bent test of the Santa Monica Viaduct with Carbon Fiber Jacket Retrofit: Phase I, SMV-I
Test Unit Description	<p>The test unit evaluated in this section consists of the phase I retrofit of a full scale two column bridge bent from the Santa Monica Viaduct, defined as <i>SMV-I</i> in this document. Phase I of the testing protocol increased the capacity of the columns by applying a carbon fiber jacket retrofit in order to validate the design criteria for the retrofit scheme used in the field. The purpose of the phase I testing was to determine the onset of failure of the knee joints. Testing was terminated prior to complete knee joint failure, such that the retrofit scheme in phase II could be evaluated. The column cross sections for test unit <i>SMV-I</i> are shown in the figure on the following page. Both columns had an outside diameter of 1219mm (48 inches), 12 M36 (#11) bars lapped over one column diameter to 12 M36 (#11) starter bars, and a 63.5mm (2.5 inch) cover. The transverse reinforcement in Column A was similar to the prototype Santa Monica Viaduct structure consisting of a 13mm (#4) continuous spiral at a 89mm (3.5 inch) pitch which is atypical of columns designed prior to 1971 guidelines. Therefore, the typical pre-1971 detail of 13mm (#4) hoops spaced at 305 mm (12 inches) was used for Column B. Since Column A was fairly well confined, the carbon jacket retrofit was localized top and bottom in the plastic hinge regions. For Column B, a similar jacket thickness was used for the plastic hinge region, but a nominal thickness was employed over the full column height for shear requirements. The cap beam cross section and elevation showing joint details are also shown in the figure. The lateral load was applied by two servo-controlled 2670 kN (600 kip) actuators, and an axial load of 1780 kN (400 kips) representing the bridge superstructure self-weight was applied. The material properties for each component and the complete test setup are presented on the following pages.</p>

**Material Properties:**

Footing/Column Steel			Cap Beam Steel			Concrete	
Bar size	$f_y$	$f_u$	Bar size	$f_y$	$f_u$	Component	$f'_c$
#3	N/A	N/A	#5	459 MPa (66.5 ksi)	733 MPa (106 ksi)	Columns	43 MPa (6.24 ksi)
#4	438 MPa (63.2 ksi)	691 MPa (100 ksi)	#6	486 MPa (70.5 ksi)	777 MPa (113 ksi)		
#8	463 MPa (67.1 ksi)	586 MPa (84.9 ksi)	#11	452 MPa (65.5 ksi)	741 MPa (108 ksi)	Cap Beam	44.9 MPa (6.51 ksi)
#11	454 MPa (65.9 ksi)	745 MPa (108 ksi)	#18	N/A	805 MPa (117 ksi)	Footing	--

**Reinforcement Details:**



<b>Axial Load Ratio: (Columns)</b>	<b>T</b>	<b>3.5% to 0.3%</b>	<b>C</b>	<b>3.5% to 6.1%</b>
--	----------	---------------------	----------	---------------------

### **Bridge Damage Assessment:**

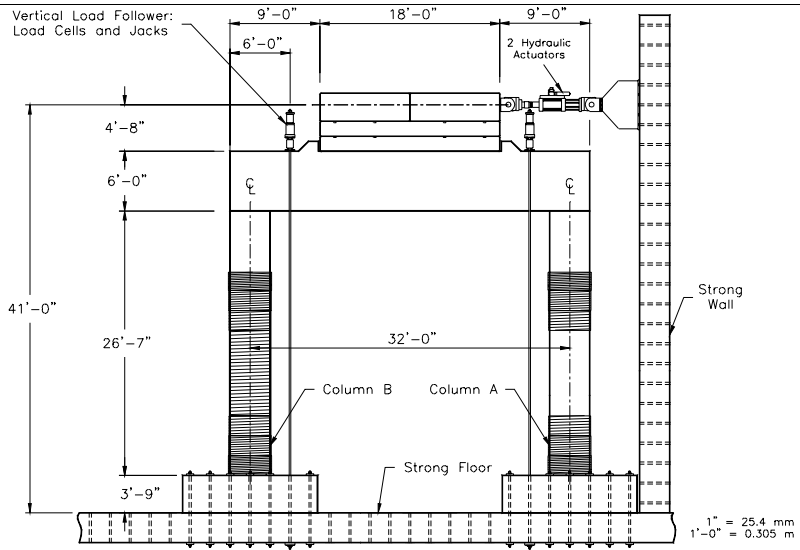
The damage observed in *SMV-I* at what is considered Performance Level I (CRACKING) in the PBEE methodology occurred at approximately 75% of the yield force. Cracking was observed at 305mm (12 inches) in the columns just below the cap beam soffit. Vertical cracks propagated in the cap beam upon application of the vertical load. Horizontal joint cracks and vertical flexural cracks in the cap beam began to develop. No repair is necessary. Unfortunately, no photograph was taken of the test unit at this earlier loading stage.

Flexural cracks developed between the top and bottom jackets of column A. During closing moments vertical joint cracks formed along the end faces of each knee joint. Slight downward inclination of horizontal joint cracks was observed. Minor jacket splits occurred in horizontal directions possibly indicating the onset of flexural cracking in the columns. The extent of this damage correlates to Performance Level II, YIELDING, of the PBEE methodology. The observed damage in the columns was comparable with the damage criteria used to establish Level I at the component level. The first photograph on the following page depicts the knee joint at this yield force level, demonstrating that repair would most likely be unnecessary.

Level III of the PBEE methodology, the initiation of the failure mechanism, which consisted of pullout failures of the cap beam longitudinal reinforcement in the knee joints, was observed at this ductility 2 level. Significant joint shear cracking and widening of existing cracks occurred. Yield penetration of the column longitudinal reinforcement was demonstrated by the formation of shallow splitting or fan cracks at the cap beam soffit and footing top. Pullout failure was represented by a splitting crack pattern around the bottom layer of cap beam reinforcement and the formation of a horizontal crack at 102mm (4inches). The second photograph shows the damage observed at this level.

The FULL DEVELOPMENT OF LOCAL MECHANISM of Performance Level IV for *SMV-I* shows significant damage to the cap beam. This damage is depicted in the third photograph on the following page. The fourth photograph on the following page shows an elevation view of the cap beam/joint connection, demonstrating that testing of the overall system was terminated prior to failure of the knee joint component. Splitting cracks associated with the pullout failure mechanism were more pronounced indicating the onset of failure of the knee joints. Flexural column cracks below the cap beam soffit at both columns opened significantly indicating the onset of flexural plastic hinge formation in the columns. Concrete in the gaps at the footings crushed slightly. Despite significant damage, the columns remained structurally sound and can still be repaired for Phase II of the testing.

Level V in the PBEE assessment methodology was not reached during phase I of the testing because testing was terminated prior to failure of the test unit.



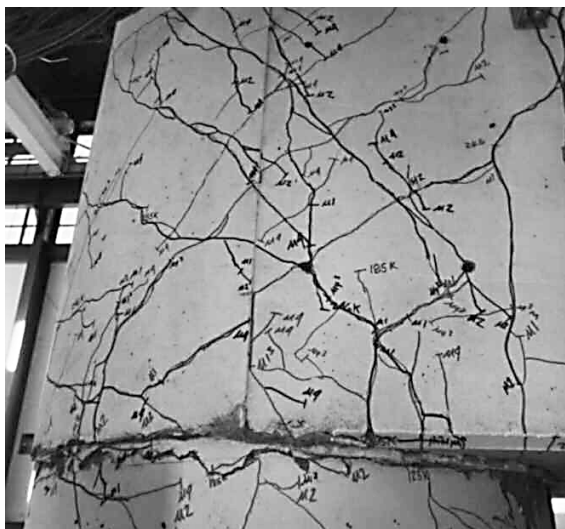
Test Setup



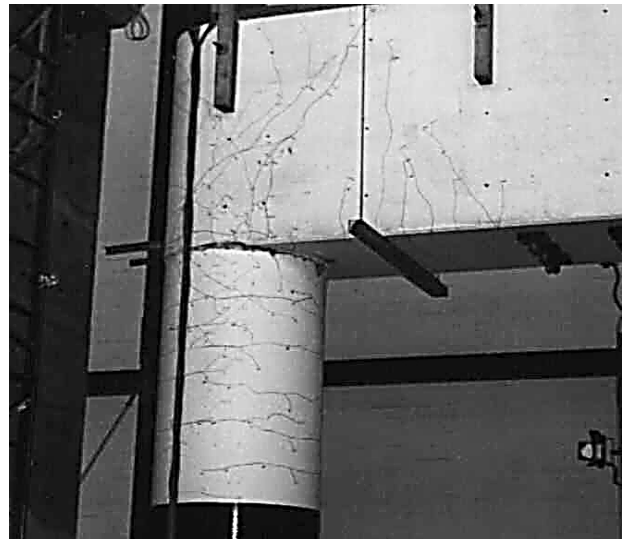
Level II



Level III



Level IV

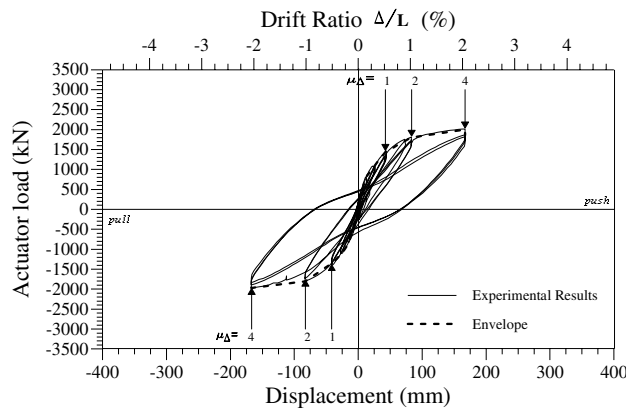


Level IV

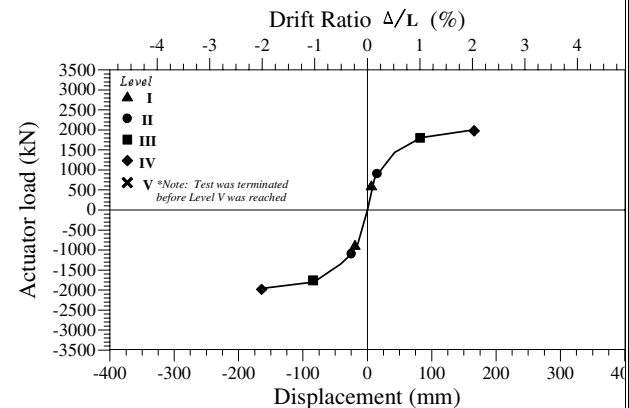
### Bridge Performance Assessment:

The first figure below shows the measured lateral force vs. displacement response of unit *SMV-I*. Testing of the system was terminated at displacement ductility 4, which was the onset of knee joint failure. The columns at this stage, however, were just reaching Level III. Peak lateral load capacity dropped approximately 7% between cycles at displacement ductility 4 and coincided with some loop pinching. The column drift levels were calculated as the overall lateral displacement divided by the clear column height of 8.11m (26 feet, 7 inches). The second figure below presents the envelope response and the associated PBEE damage/performance levels. Peak response in both loading directions occurred at Level IV, which corresponds to the onset of failure of the knee joints with only incipient spalling in the column gap region at the column/cap beam interface. The performance and design parameters for *SMV-I* are reported in the tables below. Since this system was not loaded to failure, Level V of the performance assessment was not reached and therefore values of the parameters are not reported. To determine strain levels at each performance level, a simple moment curvature analysis was performed using an equivalent transverse reinforcement ratio that considered the carbon jacket and internal column confinement. The variation in axial load in the two columns was also taken into account in the moment-curvature assessment of each column. The strains reported in the table below represent values obtained in the extreme cases. The steel and concrete strains were extracted from Column A in Compression, which considered the effects of an increase in axial load contribution. The principal stress state parameter was also computed for the worst case scenario, which consisted of the knee joint of the tension column.

Force-Displacement Hysteresis/Envelope:



Force-Displacement Envelope/Symbols:



Bridge Performance/Design Parameters:

Level	$\epsilon_s$		$\epsilon_c$		$\mu_\theta$	$\theta_p$	$p_c, p_t$
	Columns	Cap Beam	Columns	Cap Beam	Columns	Columns	Knee Joints
I	0.0015	0.0019	0.00067*	0.00029*	0.3	--	0.26
II	0.0031	0.00376	0.00109*	0.00049*	0.6	--	0.36
III	0.0162	0.01884	0.00324*	0.00066*	2.75	0.005	0.46
IV	0.0389*	0.044*	0.00826*	0.0034*	6.65	0.015	0.51
V	--	--	--	--	--	--	--

Level	% Drift	$\mu_\Delta$	RDI	$\xi_{eq}$	$\eta_k$
I	< 0.3	$0.75 V_y$	0.02	< 9%	2.09
II	0.3	$V_y$	0.06	9%	1.29
III	1	2	0.4	10.4%	0.64
IV	2	4	1.64	16.9%	0.34
V	--	--	--	--	--

## Performance Parameter Assessment of Bridge Components/Structures

### **Background Information:**

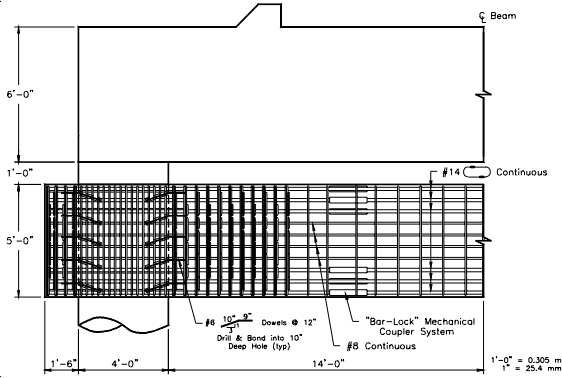
P.I.: Name Phone Email	Frieder Seible (858) 534-4640 seible@ucsd.edu	Institution Address	University of California, San Diego Department of Structural Engineering 9500 Gilman Drive, Mail Code 0085 La Jolla, CA 92093-0085		
Co- Name P.I.'s: Phone Email	Donato Innamorato (858) 534-5685 dinnamorato@ucsd.edu	Institution Address	University of California, San Diego Department of Structural Engineering 9500 Gilman Drive, Mail Code 0085 La Jolla, CA 92093-0085		
Assessment Area	3	1. Component	2. Sub-Assemblage	3. System	
Assessment Classification	B	A. New	B. Retrofit		
Reference	Innamorato, D., Seible, F., Hegemier, G.A., Priestley, M.J.N., and Ho, F., 1996, Full Scale Test of a Two Column Bridge Bent with Carbon Fiber Jacket Retrofit, <i>Advanced Composites Technology Transfer Consortium, 96/10</i> , University of California, San Diego, La Jolla, August.				
Sponsoring Agency	Advanced Research Projects Agency (ARPA) and Federal Highway Administration (FHWA)				

### **Test Unit Information:**

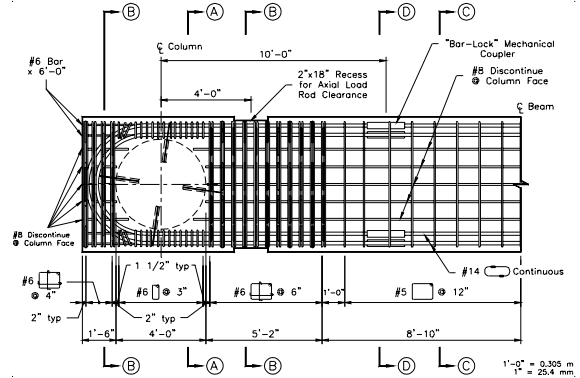
Test Unit Designation	Full Scale Two Column Bridge Bent test of the Santa Monica Viaduct with Carbon Fiber Jacket Retrofit: Phase II, SMV-II
Test Unit Description	<p>The test unit evaluated in this section consists of the phase II retrofit of the full scale two column bridge bent from the Santa Monica Viaduct presented in a previous case study template. In this document, the test unit is defined as <i>SMV-II</i>. Phase II of the testing protocol consisted of installing a link beam just below the cap beam to enhance structural performance by reducing seismic input to the cap beam and knee joints. The link beam was positioned high on the columns to force plastic hinging into the column below the beam away from the joint. With the installation of the link beam, the column stiffness and lateral strength typically increase and the location of the plastic hinges change to the bottom of the link beam. Therefore, the jacketing of the columns in conjunction with the link beam might be necessary to ensure satisfactory behavior of the bent system. It is difficult however, to separate the effects of each retrofit scheme since retrofitting for one deficiency may only shift the seismic problem to another location and failure mode without necessarily improving the overall deformation capacity.</p> <p>The column cross sections for test unit <i>SMV-II</i> and steel properties for the footing, columns, and cap beam are the same as <i>SMV-I</i> reported in a previous template. The details for the link beam and the link beam reinforcement are given in a figure on the following page. The concrete properties for each component of the two-column bent system for phase II are also presented. As in the testing of Phase I, the lateral load was applied by two servo-controlled 2670 kN (600 kip) actuators, and an axial load of 1780 kN (400 kips) representing the bridge superstructure self-weight was applied. The complete test setup is shown in a figure on the following pages.</p>

**Material Properties:**

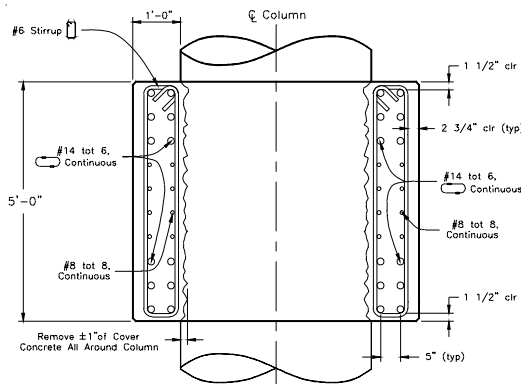
Link Beam Steel			Concrete	
Bar size	$f_y$	$f_u$	Component	$f'_c$
#5	425 MPa (61.6 ksi)	664 MPa (96.3 ksi)	Columns	44.8 MPa (6.49 ksi)
#6	499 MPa (72.4 ksi)	691 MPa (114.5 ksi)		
#8	485 MPa (70.3 ksi)	779 MPa (113.0 ksi)	Cap Beam	47.6 MPa (6.9 ksi)
#14	429 MPa (62.2 ksi)	626 MPa (90.7 ksi)	Footing	35.1 MPa (5.09 ksi)



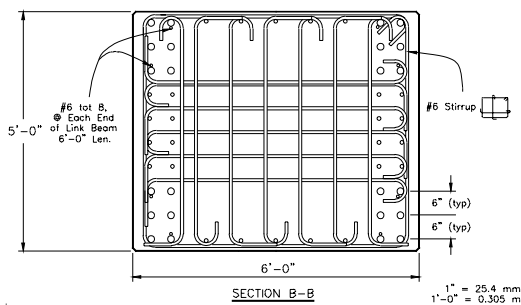
**Link Beam Elevation**



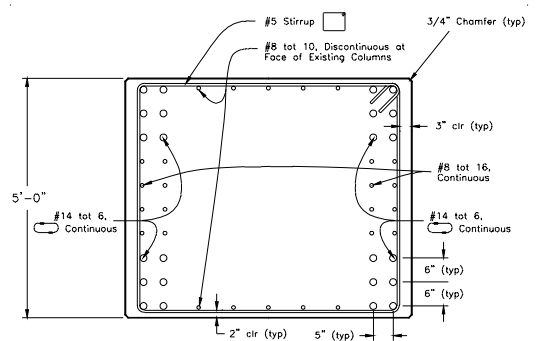
**Link Beam Plan**



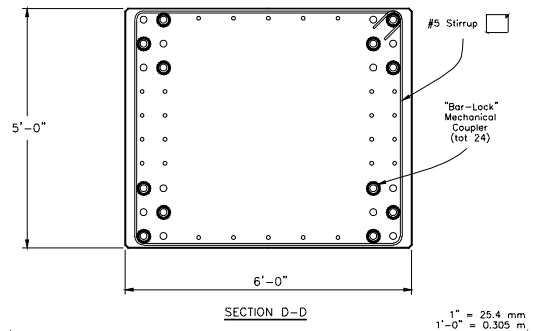
**SECTION A-A**



**SECTION B-B**



**SECTION C-C**



**SECTION D-D**

**Link Beam Cross-section Details**

<b>Axial Load Ratio: (Columns)</b>	<b>T</b>	<b>3.4% to -0.5%</b>	<b>C</b>	<b>3.4% to 6.3%</b>
--	----------	----------------------	----------	---------------------

### ***Bridge Damage Assessment:***

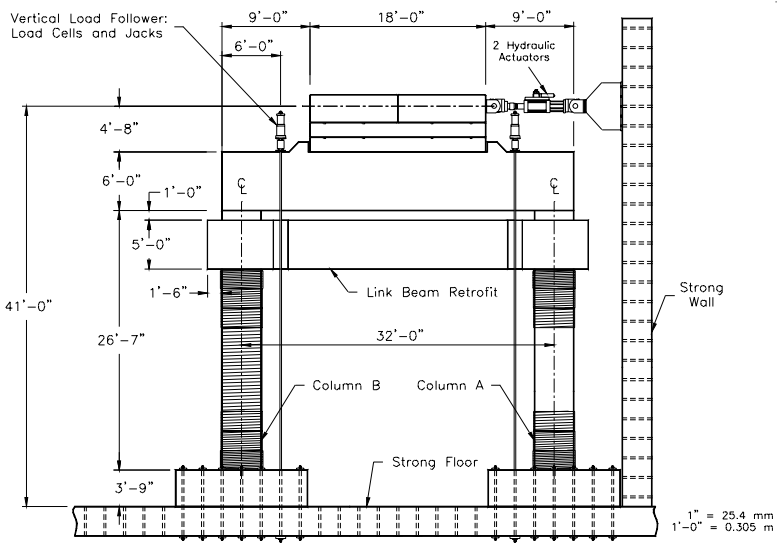
Because the test unit had been previously loaded in phase I, cracking of the specimen, which describes Level I of the PBEE methodology, had already occurred and therefore this level could not be accurately assessed in phase II. No photograph of this level is provided.

At this ductility 2 level, yield strains were measured in the column longitudinal reinforcement at the link beam interface. Since the link beam relocated the plastic hinge to a location in the column that was undamaged in phase I, these yield strain values in the columns are true indicators that the specimen reached this PBEE Performance Level II. Initial cracking of the link beam top and soffit in the form of through beam-width flexural cracks that propagated from the column centerline to 1.83m (6 feet) into the link beam were observed. Existing joint cracks reopened, widened, and extended. The first photograph on the following page shows the minimal damage observed at the link beam/column interface at this level in which repair would most likely be unnecessary.

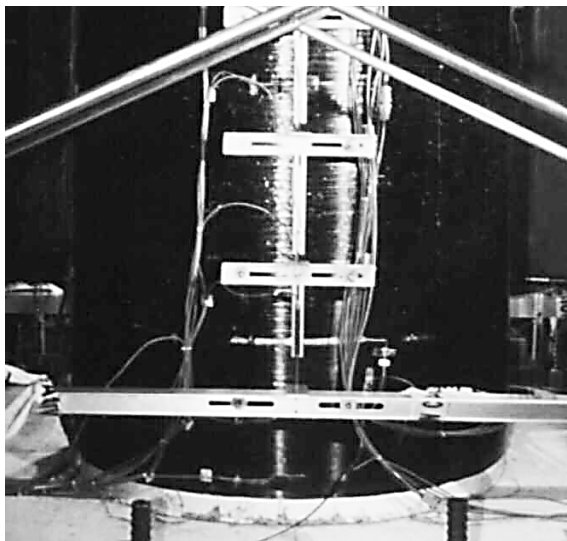
At ductility 3, the first cracks between jacket filaments formed just below the link beam soffit of each column while additional column flexural cracks developed in the gaps in the columns. But, initiation of the failure mechanism that characterizes Level III of the PBEE methodology was not quite apparent until ductility 4. Cracks in the jackets opened over 1.22m (4 feet) below the link beam, which is a result of dilation of the column indicating the initiation of the formation of the plastic hinge region. The second photograph shows the damage observed in the test unit at this level, which would most likely require repair.

Performance Level IV of the PBEE methodology for *SMV-II* occurred at displacement ductility 10, when the plastic hinges in the gaps of the columns reached full development. Significant yield penetration of the column longitudinal reinforcement at both top and bottom created 152mm (6 inches) spalling zones around the column perimeter and link beam soffit exposing link beam reinforcement, and 305mm (12 inch) spalling zones around the column perimeter at the top of the footing exposing starter bars. All other cracking remained stable indicating flexural action being concentrated at the column/footing, column/cap beam interfaces of each column. Despite the extensive damage, the column remains structurally sound and can still be repaired.

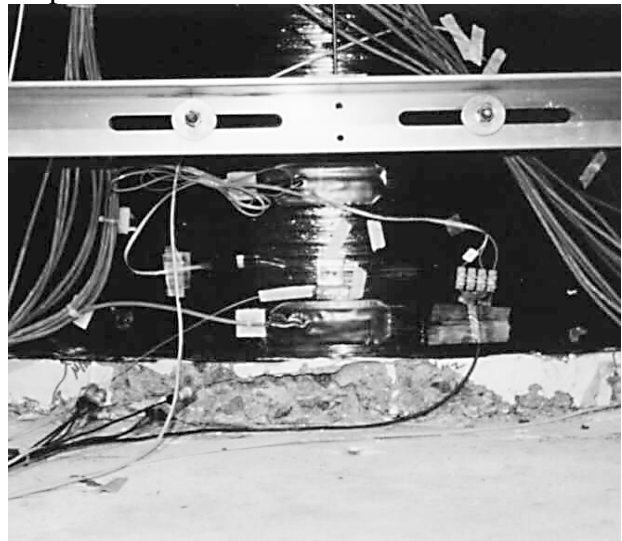
Level V in the PBEE assessment methodology initially occurred at ductility 10 when a starter bar ruptured during cycling. Additional starter bars ruptured as the test unit was displaced to ductility 13. Ten of the 24 starter bars ruptured (7 in column A and 3 in column B). Jacket cracks in column A opened as wide as 9.5mm (3/8 inch) while jacket cracks in B opened as much as 6.4mm (1/4 inch) exposing the column concrete surface. At this level, replacement of the structure is necessary.



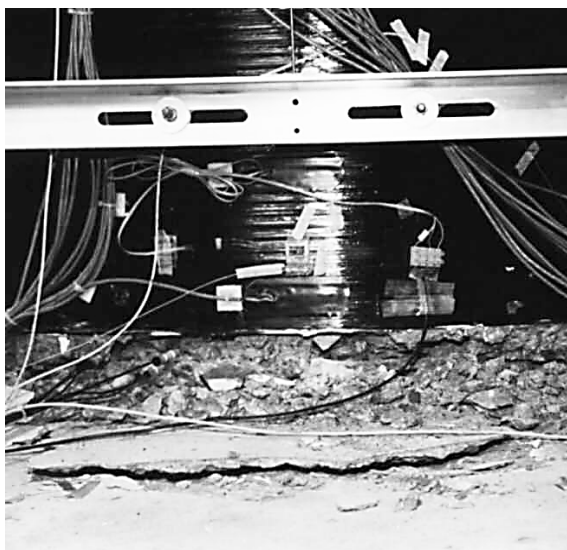
Test Setup



Level II



Level III



Level IV

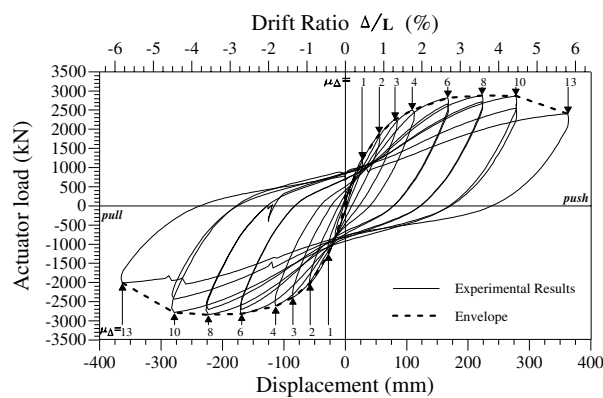


Level V

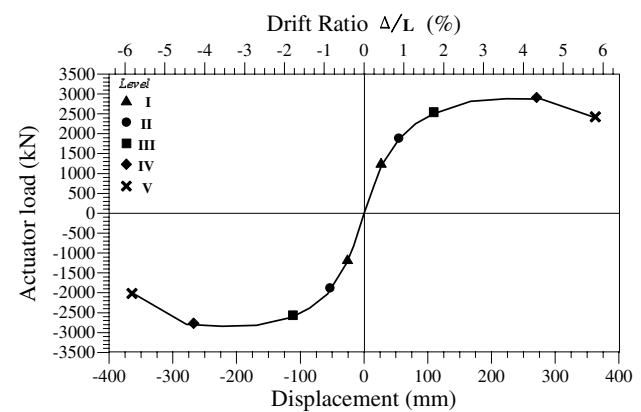
### Bridge Performance Assessment:

The first figure below shows the measured lateral force vs. displacement response of unit *SMV-II*. Up to displacement ductility 8, hysteresis behavior was symmetric and stable. At ductility 10, the lateral load capacity dropped 11% in the push direction and 12% in the pull direction between the first and second cycles coinciding with rupturing of the starter bars. Cycling at ductility 13 saw a reduction of the lateral load capacity of 16% in the push and 28% in the pull direction indicating strength degradation and consequent failure of the system. Failure was represented by full formation of a plastic hinge mechanism in the column end regions. The link beam effectively protected the cap beam by mitigating joint cracking and stabilizing pullout of the bottom cap beam reinforcement. Damage to the link beam was minimal. The lateral load capacity increased by 41% from phase I while the stiffness increased by 13%. The carbon fiber wraps were a successful retrofit for confinement of the columns to force ductile column response and damage to occur in the gap regions. Although jacket strains were recorded as high as 5000  $\mu\epsilon$ , damage to the jackets in the form of flexural cracks was typically minimal. The jackets effectively clamped the lap splice regions preventing slip between the column longitudinal reinforcement and starter bars and forcing failure as rupture of the starter bars. The column drift levels were measured as the average lateral displacement at mid-height of the link beam divided by the clear column height of 6.28m (20 feet, 7 inches). The second figure below presents the envelope response and the associated five damage levels. Since cracking previously occurred during phase I of the testing, Level I parameters are not reported. The performance/design parameters for unit *SMV-II* are shown below. Since the columns were the critical components in this phase of testing, only the steel and concrete strains for the columns are reported.

Force-Displacement Hysteresis/Envelope:



Force-Displacement Envelope/Symbols:



Bridge Performance/Design Parameters:

Level	$\epsilon_s$	$\epsilon_c$	$\mu_o$	$\theta_p$	$p_c, p_t$
I	--	--	--	--	--
II	0.0176	0.0035*	1.84	0.004	0.44
III	0.0347	0.0073*	3.66	0.012	0.6
IV	0.10*	0.025*	10.83	0.036	0.69
V	0.12*	0.037*	15.62	0.053	0.57
Level	% Drift	$\mu_\Delta$	RDI	$\xi_{eq}$	$n_k$
I	--	--	--	--	--
II	0.81	2	0.4	9.8%	0.76
III	1.65	4	1.45	13.4%	0.52
IV	4.29	10	6.1	21.2%	0.23
V	5.61	13	8.58	21.4%	0.15

## References

- FEMA 273. 1997. *NEHRP guidelines for the seismic rehabilitation of buildings*. FEMA 273. Washington, D.C.: Federal Emergency Management Agency. October.
- FEMA 274. 1997. *NEHRP commentary on the guidelines for the seismic rehabilitation of buildings*. FEMA 274. Washington, D.C.: Federal Emergency Management Agency. October.
- FEMA 306. 1999. *Evaluation of earthquake damaged concrete and masonry wall buildings: basic procedures manual*. FEMA 306. Washington, D.C.: Federal Emergency Management Agency. May.
- Hose, Y. D., P. F. Silva, and F. Seible. 1999. Development of a performance evaluation database for concrete bridge components and systems under simulated seismic loads. *Earthquake Spectra*. (Forthcoming).
- Kawashima, K., and S. Unjoh. 1997. The 1996 seismic design specifications of highway bridges. *Workshop on Earthquake Engineering Frontiers in Transportation Facilities*, 299–321. Buffalo, New York.
- Kowalsky, M. J. 1997. *Direct displacement-based design: A seismic design methodology and its application to concrete bridges*. Dissertation submitted in partial satisfaction of the Ph.D. requirements in Structural Engineering. University of California, San Diego. La Jolla, California.
- Krawinkler, H. 1995. New trends in seismic design methodology. *10th European Conference on Earthquake Engineering*: 2: 821–30. Rotterdam: A.A.Balkema.
- Kunnath, S. K., A. El-Bahy, A. W. Taylor, and W. C. Stone. 1997. Cumulative seismic damage of reinforced concrete bridge piers. *NISTIR 6075*. Gaithersburg, Md.: National Institute of Standards and Technology. October.
- NCHRP 12-49. 1999. *Comprehensive specification for the seismic design of bridges*. Draft, NCHRP 12-49. American Association of State Highway and Transportation Officials. October.
- Priestley, M. J. N., F. Seible, and G. M. Calvi. 1996. *Seismic Design and Retrofit of Bridges*. New York: John Wiley & Sons, Inc.
- SEAOC. 1996. Appendix B: Conceptual framework for performance-based seismic design. *Vision 2000*: 393–416. [Sacramento, Calif.]: Structural Engineers Association of California.
- University of California, San Diego. 1999. The UCSD/PEER Performance Library for Concrete Bridge Components, Sub-Assemblages, and Systems under Simulated Seismic Loads. <http://www.structures.ucsd.edu/PEER/peer.html>.
- University of Washington. 1999. The UW-PEER Reinforced Concrete Column Test Database. <http://www.ce.washington.edu/~peera1>.

## PEER REPORTS

PEER reports are available from the National Information Service for Earthquake Engineering (NISEE). To order PEER reports, please contact the Pacific Earthquake Engineering Research Center, 1301 South 46<sup>th</sup> Street, Richmond, California 94804-4698. Tel.: (510) 231-9468; Fax: (510) 231-9461.

- PEER 1999/11** *Performance Evaluation Database for Concrete Bridge Components and Systems under Simulated Seismic Loads.* Yael D. Hose and Frieder Seible. November 1999. \$20.00
- PEER 1999/07** *Documentation of Strengths and Weaknesses of Current Computer Analysis Methods for Seismic Performance of Reinforced Concrete Members.* William F. Cofer. November 1999. \$15.00
- PEER 1999/06** *Rocking Response and Overturning of Anchored Equipment under Seismic Excitations.* Nicos Makris and Jian Zhang. November 1999. \$15.00
- PEER 1999/05** *Seismic Evaluation of 550 kV Porcelain Transformer Bushings.* Amir S. Gilani, Andrew S. Whittaker, Gregory L. Fenves, Eric Fujisaki. October 1999. \$15.00
- PEER 1999/04** *Adoption and Enforcement of Earthquake Risk-Reduction Measures.* Peter J. May, Raymond J. Burby, T. Jens Feeley, and Robert Wood. \$15.00
- PEER 1999/03** *Task 3 Characterization of Site Response General Site Categories.* Adrian Rodriguez-Marek, Jonathan D. Bray, and Norman Abrahamson. February 1999. \$20.00
- PEER 1999/02** *Capacity-Demand-Diagram Methods for Estimating Seismic Deformation of Inelastic Structures: SDF Systems.* Anil K. Chopra and Rakesh Goel. April 1999. \$15.00
- PEER 1999/01** *Interaction in Interconnected Electrical Substation Equipment Subjected to Earthquake Ground Motions.* Armen Der Kiureghian, Jerome L. Sackman, and Kee-Jeung Hong. February 1999. \$20.00
- PEER 1998/08** *Behavior and Failure Analysis of a Multiple-Frame Highway Bridge in the 1994 Northridge Earthquake.* Gregory L. Fenves and Michael Ellery. December 1998. \$20.00
- PEER 1998/07** *Empirical Evaluation of Inertial Soil-Structure Interaction Effects.* Jonathan P. Stewart, Raymond B. Seed, and Gregory L. Fenves. November 1998. \$26.00
- PEER 1998/06** *Effect of Damping Mechanisms on the Response of Seismic Isolated Structures.* Nicos Makris and Shih-Po Chang. November 1998. \$15.00
- PEER 1998/05** *Rocking Response and Overturning of Equipment under Horizontal Pulse-Type Motions.* Nicos Makris and Yiannis Roussos. October 1998. \$15.00

- PEER 1998/04** *Pacific Earthquake Engineering Research Invitational Workshop Proceedings, May 14–15, 1998: Defining the Links between Planning, Policy Analysis, Economics and Earthquake Engineering.* Mary Comerio and Peter Gordon. September 1998. \$15.00
- PEER 1998/03** *Repair/Upgrade Procedures for Welded Beam to Column Connections.* James C. Anderson and Xiaojing Duan, May 1998. \$33.00
- PEER 1998/02** *Seismic Evaluation of 196 kV Porcelain Transformer Bushings.* Amir S. Gilani, Juan W. Chavez, Gregory L. Fenves, and Andrew S. Whittaker, May 1998. \$20.00
- PEER 1998/01** Unassigned.